THESIS

OXIDATION CATALYST DEGRADATION IN THE EXHAUST STREAM OF A LARGE BORE 2-STROKE NATURAL GAS ENGINE

Submitted by

Kristen Davis

Department of Mechanical Engineering

In partial fulfillment of the requirements

For the Degree of Master of Science

Colorado State University

Fort Collins, Colorado

Spring 2015

Master's Committee:

Advisor: Daniel Olsen

Troy Holland
Michael A. de Miranda

ABSTRACT

OXIDATION CATALYST DEGRADATION IN THE EXHAUST STREAM OF A LARGE BORE 2-STROKE NATURAL GAS ENGINE

Lean burn 2-stroke natural gas engines are commonly used for power generation and gas compression. These engines, however, contribute to air pollution primarily through emissions of carbon monoxide, volatile organic compounds and some unburned hydrocarbons. Oxidation catalysts aid in reducing these harmful emissions. Lubrication oil carryover to engine exhaust degrades the oxidation catalyst making it less effective at reducing emissions. This work combines laboratory and field testing of an oxidative catalyst designed for lean burn natural gas engines. Catalyst performance is tracked over the course of a year to examine the rate and cause of degradation. The oxidation catalyst was housed in a slipstream in the exhaust stream of a Copper-Bessemer GMVH12 large bore 2-stroke natural gas engine between one and two months at a time. The catalyst was periodically removed and returned to the laboratory for emissions and material testing. Emissions testing was completed by diverting exhaust gas from a Cummins QSK19 4-stroke stationary natural gas engine through a slipstream. A fourier transform infra-red spectrometer and a 5-Gas analyzer were used to determine the exhaust composition pre-catalyst and post-catalyst.

Lubrication oil carry over and poisoning decreases the oxidation catalysts ability to reduce emissions, materials testing was performed to determine the exact levels of the poisons, such as sulfur, phosphorous and zinc. A scanning electron microscope and X-Ray spectrometer were used to complete materials testing. The catalyst material initially showed a sharp increase

in sulfur poisoning, but it quickly leveled off around 3 atomic%. Phosphorous and zinc poison buildup, however, rose throughout the duration of this study. As the catalyst experienced increasing levels of poison buildup, the reduction efficiency of emissions decreased due to blocked active catalyst sites.

Laboratory emissions testing showed degradation of reduction efficiency for carbon monoxide, formaldehyde and volatile organic compounds. During each round of testing, a temperature sweep and a space velocity sweep were completed. The temperature sweeps were run between 300°F (149°C) and 800°F (827°C) at 150,000 hr^{-1} and the space velocity sweeps were run between approximately 20,000 hr^{-1} to 200,000 hr^{-1} at 550°F (287°C). Reduction efficiencies for carbon monoxide, formaldehyde, propylene, ethylene and volatile organic compounds decreased over the six tests. Carbon monoxide reduction efficiency remained high, above 90%, throughout all temperature sweep tests. Formaldehyde exhibited high reduction efficiency, over 70%, for all tests, and its reduction efficiency decreased by 19% at 450°F and 4% at 600°F during the temperature sweep tests. Propylene showed the highest level of degradation. Over six tests, the reduction efficiency for propylene dropped 36% at 450°F and 28% at 600°F during temperature sweeps. Like carbon monoxide, ethylene maintained a reduction efficiency above 90% for all tests during the temperature sweeps. Volatile organic compound reduction efficiency, on the other hand, did not exceed 80% for any temperature sweep tests. Methane, propane and ethane reduction efficiencies were low and erratic for both temperature and space velocity sweeps for all tests.

ACKNOWLEDGEMENTS

I would first like to thank my family especially my parents, Steve and Carol Davis, for providing encouraging words and unwavering support throughout my entire graduate school experience. Also, thank you to my friends who have stood by my side and encouraged me to pursue my dreams.

Thank you to Dr. Olsen and the Pipeline Research Council International for providing me this opportunity to further my education while pursuing my interests in engine research. To all the staff, particularly Kirk Evans and Phillip Bacon, at the Powerhouse Institute, I appreciate your help with emissions and field testing. Thank you to Dr. McCurdy for your help with materials testing. Finally, thanks to Marc Baumgardner for all your help with testing, construction, data analysis, thesis editing, and answering all my questions.

TABLE OF CONTENTS

LIST OF FIGURES

LIST OF TABLES

1. Introduction

1.1 Background Information and Motivation

Air pollution from engine exhaust can cause detrimental health effects. Large bore two stroke natural gas engines emit regulated air pollutants, including carbon monoxide, volatile organic compounds, formaldehyde, and NOx. Inhalation of these emissions can cause an increase in asthma and other upper respiratory illnesses. The Environmental Protection Agency (EPA) has, therefore, enforced stricter engine exhaust emission standards. In order to meet these new and stricter standards, engines needed to be outfitted with a system that reduced exhaust emissions. Introducing after-treatment systems into the engine's exhaust stream assists in reducing the output of harmful emissions into the atmosphere.

1.1.1 Exhaust After-Treatment

In recent years, the EPA has enforced stricter emissions standards for engines [1]. To adhere to these standards, engine manufactures have incorporated a variety of exhaust gas after-treatment systems as part of standard engine configurations for a variety of conditions. Secondary air-injection systems, exhaust gas recirculation, particulate filters, selective catalytic reducer, three-way catalytic converters, and oxidation catalysts are commons methods of exhaust after-treatment.

Secondary Air-Injection System

Secondary air-injection system injects air into the exhaust in order to oxidize hydrocarbons (HC) and carbon monoxide (CO). Primitive secondary air-injection systems injected air directly into the exhaust manifold [2]. Re-combustion of the exhaust, however, proved detrimental to the exhaust manifold and valves. Another early method consisted of injecting the air downstream of the manifold. This air/exhaust mixture would then flow through an oxidation catalyst. These two secondary air-injection systems proved inefficient at emission reduction, but led the way for the development of other, more effective systems.

Exhaust Gas Recirculation

For an exhaust gas recirculation (EGR) after-treatment system, exhaust is re-injected into the combustion chamber to complete combustion of the recirculated exhaust gas constituents. For spark ignited engines, 10-15% of exhaust is recirculated back into the combustion chamber [2]. Re-injection of exhaust causes an increase of specific heat of the mixture in the combustion chamber. It also decreases the adiabatic flame temperature within the chamber. Since the combustion temperature is reduced, the EGR system is ideal for nitrogen oxides (NOx) reduction since lower combustion temperatures favor lower NOx production. This system, however, results in decreased engine performance and the EGR valves clog due to buildup of particulate matter [2].

Particulate Filters

Particulate filters are commonly used in diesel engines. Diesel engines are prone to high particulate matter (PM) in the exhaust. Particulate filters trap and oxidize PM on the surface of the filter. These filters are typically made of ceramic monoliths, alumina coated wire mesh, ceramic fiber materials, and silica fiber ropes [2]. Eventually the filters will clog, causing an increase in exhaust pressure. In order to maintain the integrity of the particulate filter, it must be periodically regenerated, by burning off the PM.

Selective Catalytic Reducers

Selective catalyst reducers (SCR) convert NOx to nitrogen and water. A reductant—typically anhydrous or aqueous ammonia or urea—is injection into the exhaust to aid reduction. Urea is more commonly used since ammonia is toxic and difficult to store [2]. Urea is normally used as an aqueous solution which consequently leads to vaporization in the exhaust. When ammonia is used, however, it reduces NOx via the following equations:

$$4NO + 4NH_3 + O_2 \rightarrow 4N_2 + 6H_2O$$

$$4NO_2 + 4NH_3 + O_2 \rightarrow 3N_2 + 6H_2O$$

$$NO + NO_2 + 2NH_3 \rightarrow 2N_2 + 3H_2O$$

When urea is used, it first undergoes thermal decomposition and forms ammonia and carbon dioxide (CO_2) as a byproduct. The overall reaction involving urea is shown below:

$$4NO + 2(NH_2)_2CO + O_2 \rightarrow 4N_2 + 4H_2O + 2CO_2$$

The exhaust/reductant mixture flows through a catalyst which typically contains a ceramic substrate, such as titanium oxide, so it can tolerate high temperature [2]. Vanadium oxides, molybdenum oxide, tungsten oxide, and zeolites are examples of potential active catalyst materials for an SCR.

Three-Way Catalytic Converter

Three-way catalytic converters, also called non selective catalytic reduction (NSCR) catalysts, oxidize CO and HC and reduce NOx. When the air-fuel ratio is close to stoichiometric conditions, CO and HCs are oxidized and NOx reduction is achieved [2]. The air-fuel ratio range is very narrow for optimum performance. Feedback loops with oxygen sensors are commonly implemented into three-way catalytic converters to help achieve the required air-fuel ratio range. The efficiency of the converter is thus extremely dependent on the air-fuel ratio, but it also depends on the temperature and type of active catalyst material.

Oxidation Catalyst

Oxidation catalysts are comprised of three main components: substrate material, active catalyst materials, and a washcoat. The substrate material is the catalyst component that carries the active catalyst materials and the washcoat. Typically, it is comprised of ceramic or metallic materials and can be corrugated or honeycomb shaped. Precious metals such as platinum, rhodium, and palladium are common active catalyst materials [3]. These materials aid in oxidizing exhaust emissions, therefore the

active catalyst's surface area should be maximized [3]. Uniformity of metal distribution promotes efficient reduction of exhaust emissions [3]. To apply these active catalyst materials to the substrate, they must first be suspended in a porous oxide washcoat. This washcoat, and active catalyst material mixture, is then thinly applied to the substrate [3]. Figure 1.1 shows a microscopic view of the oxidation catalyst structure.

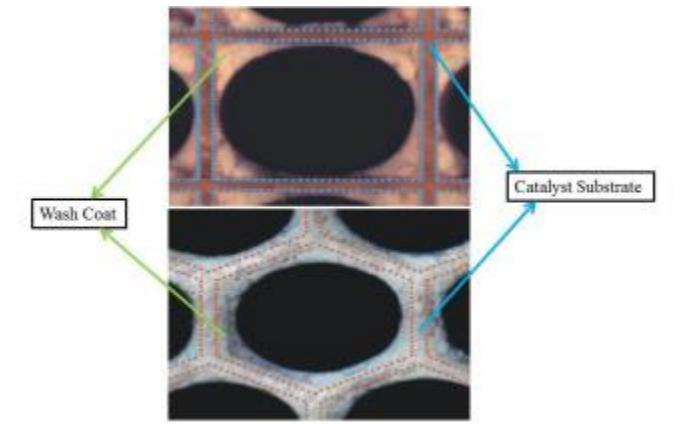

Figure 1.1: Oxidation catalyst structure for a honeycomb type catalyst [2]

Oxidation catalysts are generally used for engines that operate with very lean equivalence ratios (<0.8). Lean operation reduces engine-out NOx emissions and the addition of an oxidation catalyst reduces products of partial combustion, including HC and CO. Oxidation catalysts can also be used with stoichiometric or rich engines with air pumps, but this is not done with new engines.

1.1.2 Oxidation Catalyst Deactivation Modes

By definition, catalysts are "materials that increase the rate of a chemical reaction while not itself undergoing any permanent change" [3]. Essentially, exhaust flows through the catalyst, which promotes oxidation reactions, thus minimizing harmful emissions. HCs and CO, for example, are converted into water vapor and carbon dioxide as the exhaust passes through the catalyst [3]. While oxidation catalysts reduce emissions in engine exhaust, they unfortunately experience poisoning, fouling, and sintering from

fuel and lubricant components, as well as high exhaust gas temperatures [4]. Over time, these mechanisms degrade the oxidation catalyst's integrity and can even completely deactivate it.

Reduction Efficiency, Deactivation and Regeneration

Operating temperature, exhaust composition, and space velocity determine how efficiently the catalyst oxidizes the engine's exhaust [3]. How well the oxidation catalyst reduces exhaust emissions is known as the reduction efficiency. The reduction efficiency (η) for any single species (s) can be calculated from the incoming/exiting mass flows ($\dot{m}$) as follows [1]:

$$\eta_s = 1 - \frac{\dot{m}_{s,out}}{\dot{m}_{s,in}}$$

Over time, the reduction efficiency will deteriorate. Deactivation occurs when the catalyst has lost much of its initial activity [5]. The National Emissions Standards for Hazardous Air Pollutants (NESHAP) requires 2-stroke lean burn engines over 500 hp to reduce CO emissions by 58% or more OR a maximum of 12ppmv formaldehyde in the post-catalyst exhaust stream [6]. Once deactivation occurs, the catalyst will either need to be replaced or regenerated via chemical washing or heating [5]. Deactivation, however, is considered irreversible when highly stable catalyst poisons adhere to the surface of the catalyst and cannot be removed via regeneration [7].

After a catalyst has deactivated, it can be regenerated and used again. To regenerate a catalyst, the catalyst is immersed in a solvent such as tetrachloroethylene [8]. C.I Arapatsakos et. al. showed that washing the catalyst for 30 minutes significantly increases its ability to reduce emissions [8]. The exhaust from C.I. Arapatsakos' deactivated catalyst emitted 235 ppm HC and .56 vol% CO; however, after chemical regeneration exhaust emissions were reduced to only 170 ppm HC and .31 vol% CO [8]. Regeneration provides an economical method to prolong the catalyst's life.

Fouling

By definition, fouling is "the physical deposition of species from the fluid phase onto the catalyst surface which results in activity loss due to blockage of sites" [4]. Fouling leads to a retardation in reduction efficiency and ultimately catalyst deactivation. Basically, as exhaust flows through the catalyst, metals and other poisons from the fuel, lube oil, and odorants can deposit on the active catalyst materials, or sites, thus preventing the reducing reactions from occurring. An indication that fouling is occurring is an increase in pressure drop across the catalyst [4].

Lubrication Oil Fouling

Lubrication (lube) oil carry over severely deteriorates the catalyst's ability to reduce emissions and is the leading cause for fouling of oxidation catalysts [9]. Phosphorous (P), sulfur (S), calcium (Ca), and zinc (Zn) are the typical elements that induce catalyst fouling from lube oil carry over [7]. Lube oil carry over occurs when lube oil passes through the combustion chamber unburned and escapes into the exhaust. These compounds are added to engine oil for additional lubrication; however, when they are unburned in the exhaust, they can adhere to the catalyst surface. Once on the surface of the catalyst, these compounds block active catalyst material sites [9]. Since the active catalyst material facilitates oxidation, as these sites are blocked by the lube oil carry over, the reduction efficiency dwindles and eventually the catalyst is no longer effective.

Fuel Fouling

Along with lube oil carry over, the natural gas itself and fuel odorants cause fouling on the surface of an oxidation catalyst. Natural gas can contain hydrogen sulfide, and sulfur containing fuel odorants, such as tert-Butylthiol, tetrahydrothiophene, and ethanethiol , can also go unburned during the combustion process [10]. From here, the unburned sulfur travels through the exhaust system until it reaches the catalyst. Similar to lube oil carry over, the sulfur attaches itself to the catalyst surface, thus blocking active catalyst sites [11]. Hydrogen sulfide concentrations in natural gas are much larger than the

sulfur containing odorant compounds. The effects of both unburned hydrogen sulfide and odorant compounds fouling the catalyst are minor in comparison to lube oil carry over.

Relationship Between Elements and Fouling

Sulfur, unfortunately, causes significant decline of emissions reduction via oxidation catalysts. Unburned sulfur—from lube oil or fuel odorant—enters the catalyst and its highest level of accumulation is toward the entrance of the catalyst [10]. According to D.L. Mowery et al., over time, sulfur forms a layer over the entirety of the washcoat. This accumulation of sulfur physically blocks active catalyst sites, thus preventing oxidation [4]. C.H. Bartholomew et al. observed that a sulfur atom that strongly adsorbs to the catalyst surface, blocking at least one active catalyst site and up to four catalyst metal sites [4]. Figure 1.2 is adapted from C.H. Bartholomew and shows how sulfur (S) sits on the active catalyst sites (A) and metal sites (M) of the catalyst while also blocking its active sites [4]. Sulfur adsorbs so strongly to the metals which prevents adsorption of reactant molecules and ultimately leads to complete activity loss [4]. The carbon/hydrogen bonds are very strong in methane, thus making methane abatement difficult. As sulfur forms a layer of poison on the catalyst surface, methane oxidation becomes nearly impossible [12]. Non-methane hydrocarbons are similarly affected by the sulfur buildup on active sites [12]. If exhaust temperatures were to reach an excess of 500°C, sulfur poisoning would be limited since the sulfur would simply burn off [11].

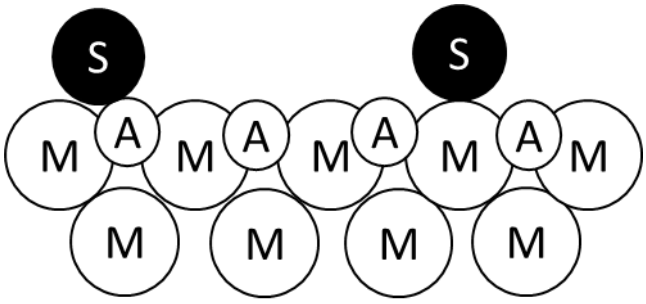

Figure 1.2: Blocking of Metal and Active Catalyst Sites

Phosphorous also fouls the catalyst and causes deactivation. Phosphorous originates from anti-wear and anti-oxidant additives in lube oil which causes fouling [13]. Similar to sulfur, it appears that phosphorous poisoning only initially affects the catalyst's entrance [10]; however, as time and fouling progress, phosphorous migrates throughout the rest of the washcoat [13]. Ultimately, the phosphorous forms a layer of highly stable aluminum phosphate on the washcoat, thus blocking active catalyst sites and preventing oxidation [10]. While phosphorous can foul the catalyst on its own, it appears that zinc cannot. Regions with zinc fouling contain phosphorous fouling as well [14] since both are found in lube oil wear additives such as zinc-dialkyldithiophosphates (ZDDP) [9].

Sintering

Along with fouling, sintering also degrades an oxidation catalyst's ability to reduce exhaust emissions. "Sintering is a thermal treatment for bonding particles into a coherent, predominantly solid structure via mass transport" [15]. Sintering happens at the atomic level [15] and results in a loss of catalyst surface area [13], as seen in Figure 1.3 which has been adapted from German's Sintering Theory and Practice [15].

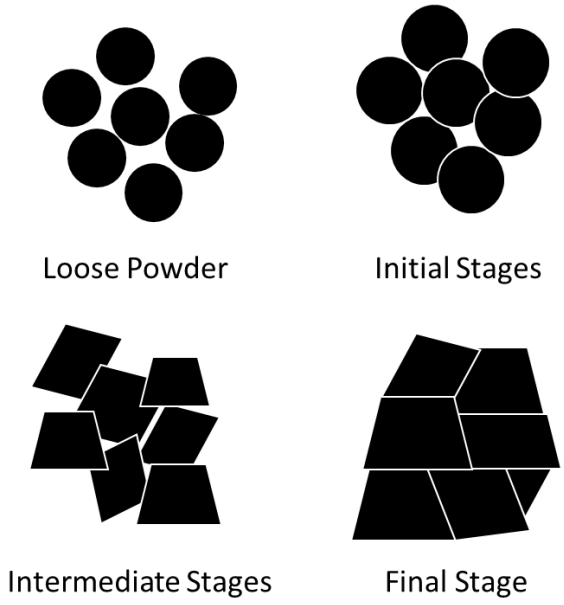

Figure 1.3: Stages of Sintering

During the loose powder stage, sintering has yet to occur and the active catalyst surface area, which is represented by the white space, is high [15]. Sintering causes the growth of contacts and during the initial stage there is a significant loss in active catalyst surface area. As sintering continues, distinct particles become less apparent, which starts occurring during the intermediate stages. Finally, the grains grow so large the formation is totally closed and the active catalyst surface area is significantly diminished.

Temperature, particle size, formation of a liquid phase, sintering time, heating rate, and process atoms all affect the rate of sintering [15]. High temperatures, for example, cause the atoms to move faster and stress directs the mass flow—also known as mobility—causing sintering [15]. Exhaust exiting the engine can be at temperatures high enough to result in high temperature sintering. High temperature sintering alters mass flow, resulting in particle bonding and eliminating surface curvature [15]. This results in a reduction in surface area [13] and an increase in density [15]. This reduction of surface area can ultimately lead to the collapse of the catalyst structure [9]. The combination of these two phenomena decrease the reduction efficiency of the catalyst [9]. High exhaust temperatures significantly increase sintering of precious metals and sintering of the washcoat [14].

Along with high temperatures, components in the exhaust can also increase the rate of sintering [4]. Water vapor and oxygen, for example, expedite the sintering process [4]. Since sintering results in the reduction of surface area, the number of active catalyst sites is also reduced [13]. Decline of active catalyst sites, in turn, lowers the catalyst's capability to oxidize exhaust constituents.

Catalyst Deactivation

While fouling and sintering both deactivate the catalyst, fouling drives the deactivation of oxidation catalysts. Adsorption of contaminates is due to chemisorption. Chemisorption is a chemical reaction between a surface and an adsorbate [4]. In catalysts, for example, chemisorption occurs between the catalyst washcoat, the active materials, and the exhaust. Chemisorption leads to fouling via

interactions with contaminates at the surface level and structure and contaminate adsorption [4]. Some species more readily foul due to their higher adsorption strength. When competing for an active catalyst site, the higher adsorption strength species wins over the lower adsorption strength species. Not only do poisons adhere to the catalyst surface, but they can also alter the electronic structure of the catalyst. Sulfur, for example, chemisorbs to the active catalyst sites and will bond with nearby reactant atoms. The bonding of these atoms hinders the reactant atoms' ability to dissociate [4]. Frequently this reaction occurs between sulfur and hydrogen, thus forming hydrogen sulfide (H_2S) on the catalyst surface. Finally, strongly adsorbed poisons form a layer on the catalyst surface, ultimately restructuring the catalyst [4]. This surface restructuring leads to changes in catalytic properties, especially for surface structure dependent reactions [4]. Strongly adsorbed contaminates hinder less strongly adsorbing contaminates from adhering and adsorbing onto the surface [5]. Unfortunately, species adsorption, electronic structure change, and catalyst surface structure change all result from contaminates chemisorbing on the catalyst surface, ultimately making it the foremost cause of catalyst deactivation.

1.1.3 Material Selection and Analysis

Reduction efficiency relies heavily on the active catalyst material, so choosing the correct active catalyst material is essential. Also, conducting material analysis on the catalyst ensures its integrity and assists in determining whether the catalyst has deactivated or not.

Active Catalyst Material Selection

Active catalyst material is the determining factor when choosing a catalyst. Rhodium, lanthanum, platinum, and palladium are a few examples of commonly used active catalyst material. Each one of these materials excels at reducing certain exhaust emissions. Therefore, determining which catalyst to purchase depends on the exhaust emission content. Methane is potentially one of the most difficult exhaust components to oxidize since the carbon/hydrogen bonds are so strong. In lean burn engines, methane abatement is crucial since lean burn engines produce high levels of unburned methane [10].

Palladium, for example, proves to be an ineffective active catalyst material for reducing methane emissions [10]. On the other hand, when lanthanum is mixed with a nickel alumina washcoat methane is effectively reduced [16]. Along with methane, lean burn engines produce high levels of non-methane hydrocarbons such as propane, ethylene, and formaldehyde [17]. Palladium catalysts initially show high non-methane hydrocarbon abatement; however, their effectivity rapidly declines [12]. Platinum-only catalysts ineffectively convert hydrocarbons [18]. Platinum particles are very susceptible to sintering, thus preventing hydrocarbon reduction. When platinum is coupled with rhodium, however, hydrocarbon reduction is drastically increased under stoichiometric conditions [18]. Rhodium-only catalysts, however, perform worse than palladium catalysts at hydrocarbon reductions [18].

In comparison to methane, carbon monoxide much more readily oxidizes. Tin (Sn), ceria (Ce) and gold are commonly used active catalyst materials for CO oxidation. Catalyst with an excess of Sn show higher CO oxidation than pure SnO_2 or CeO_2 catalysts [19]. When Sn and Ce are coupled in a 2:1 ratio, however, CO oxidation is the highest [19]. The incorporation of both lanthanum and yttrium into a Sn catalyst proves detrimental to CO oxidation [19]. Gold, on the other hand, proves as an excellent active catalyst material for CO oxidation. This is especially true when ceria and gold are coupled together as active catalyst material to oxidize CO [20]. Piotr Kaminski et. al. found that the highest CO conversion was achieved when using a CuAu/CeZrS (1:2) as the active catalyst material [20].

Nitrogen oxides (NOx) are also typically monitored exhaust emissions. Lean burn engines, however, do not produce significant levels of NOx unlike stoichiometric or rich burn engines. The reduction of NOx is not only structurally sensitive, but also thermodynamically sensitive [9, 21]. High oxygen levels and lower temperatures, however, favor NO converting to NO_2 [22]. In the presence of hydrogen, both palladium-lanthanum and palladium catalysts resist NOx reduction to N_2 [23]. Even without the presence of hydrogen, these catalysts are ineffective for NOx reduction. Both rhodium-only and palladium-only catalysts perform comparably for NOx conversion. According to R. G. Silver et al., rhodium catalysts with an alumina-ceria washcoat and palladium catalyst with an alumina-ceria washcoat

perform similarly for NOx reduction after aging for 100 hours [18]. Both the rhodium and palladium catalysts maintained around 55% NOx reduction [18]. Combining rhodium and palladium on an alumina-ceria washcoat, however, increased NOx reduction to 70% [18].

Adding modifiers to the washcoat can prevent premature deactivation. Platinum catalyst performance, for example, is increased by adding cerium to the washcoat. R. G. Silver et al. observed that a platinum catalyst without a cerium washcoat modifier would deactivate after 50 hours in a 450°C exhaust stream, under stoichiometric conditions [18]. Adding cerium washcoat prevents the platinum from sintering by leaving some of the platinum in a partially oxidized state [18]. Partially oxidized platinum is significantly harder to sinter than metallic platinum [18]. Given that sulfur alone can deactivate a catalyst, C.H. Bartholomew found that adding molybdenum or boron modifiers to the washcoat significantly decreased sulfur's ability to adsorb to nickel, cobalt or iron [4].

Material Analysis Techniques

Observing material changes on the catalyst assists in predicting deactivation. Scanning electron microscopes (SEM), energy dispersive x-ray spectroscopy (EDS), and x-ray photoelectron spectroscopy (XPS) are all destructive material analysis techniques. These techniques are considered destructive since, after analysis, the material cannot be reused for its original purpose. Time-resolved testing with these techniques shows buildup of poisons on the catalyst bed.

Energy Dispersive X-ray Spectrometer (EDS)

EDS machines are beneficial in determining gradual catalyst deactivation due to accumulation of poisons. EDS separates characteristic x-rays of different elements into an energy spectrum [24]. From here, the EDS software analyzes the data and determines the relative quantities of elements in the sample [24]. Figure 1.4 shows a sample of an output graph from EDS analysis showing X, Y, Z peaks.

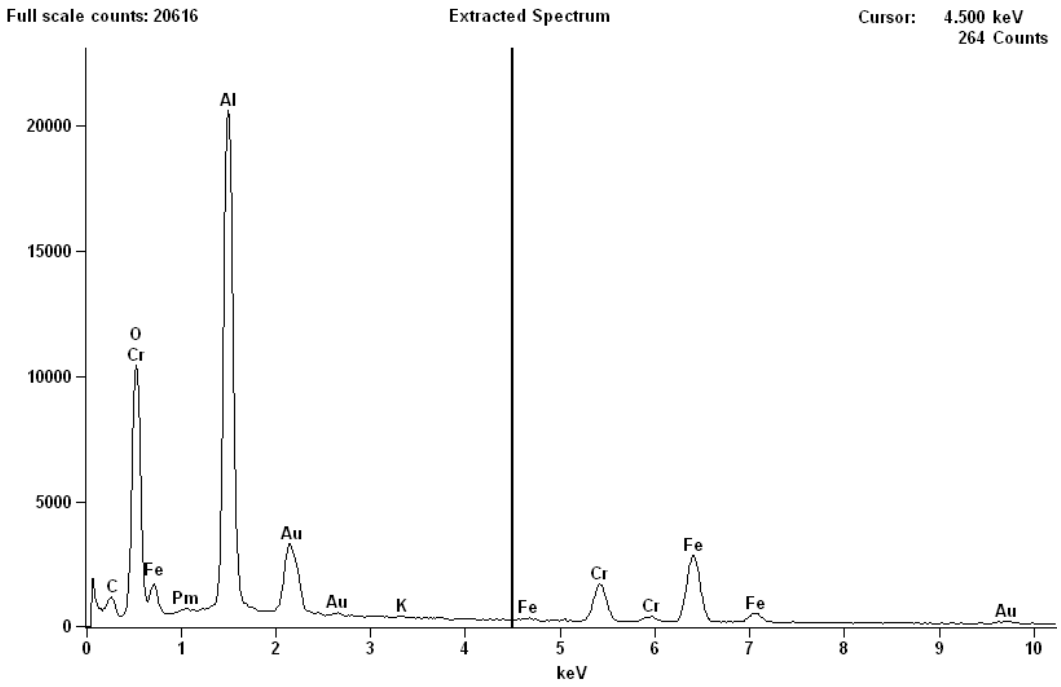

Figure 1.4: Energy Dispersive X-ray Spectroscopy Sample Graph [24]

Scanning Electron Microscopes (SEM)

The SEM completes a raster scan, using a beam of high energy electrons focused on the material, in order to determine external morphology [25]. SEM machines magnify from 20X up to 30,000X to show high resolution images of the shapes of the objects [25]. Typically, SEM machines are coupled with EDS machines, shown in Figure 1.5. Running SEM materials testing on the catalyst material determines if the catalyst has sintered or not. Sintering produces a larger crystallite size on the surface of the catalyst which can be seen via SEM [16]. SEM also provides qualitative information on where species such as sulfur and phosphorous deposit on the catalyst's surface.

Figure 1.5: Scanning Electron Microscope with Energy Dispersive X-ray Spectroscopy Detector.

X-Ray Spectrometer (XPS)

XPS is another commonly used surface analysis technique for determining catalyst poison buildup. In order to determine the concentration of elements or chemical states, the sample must be flooded with mono-energetic x-rays. The material then emits photoelectrons from which a binding energy and intensity can be determined. XPS data is only valid for materials between the atomic masses of lithium and uranium [26]. Figure 1.6 shows a typical XPS machine. XPS analysis provides quantitative species data, but SEM and EDS shows where the species deposit. SEM and EDS also looks deeper into the catalyst surface than XPS. These destructive material analysis techniques can be used to monitor poison accumulation on the catalyst bed and assist in determining a deactivation point for the catalyst.

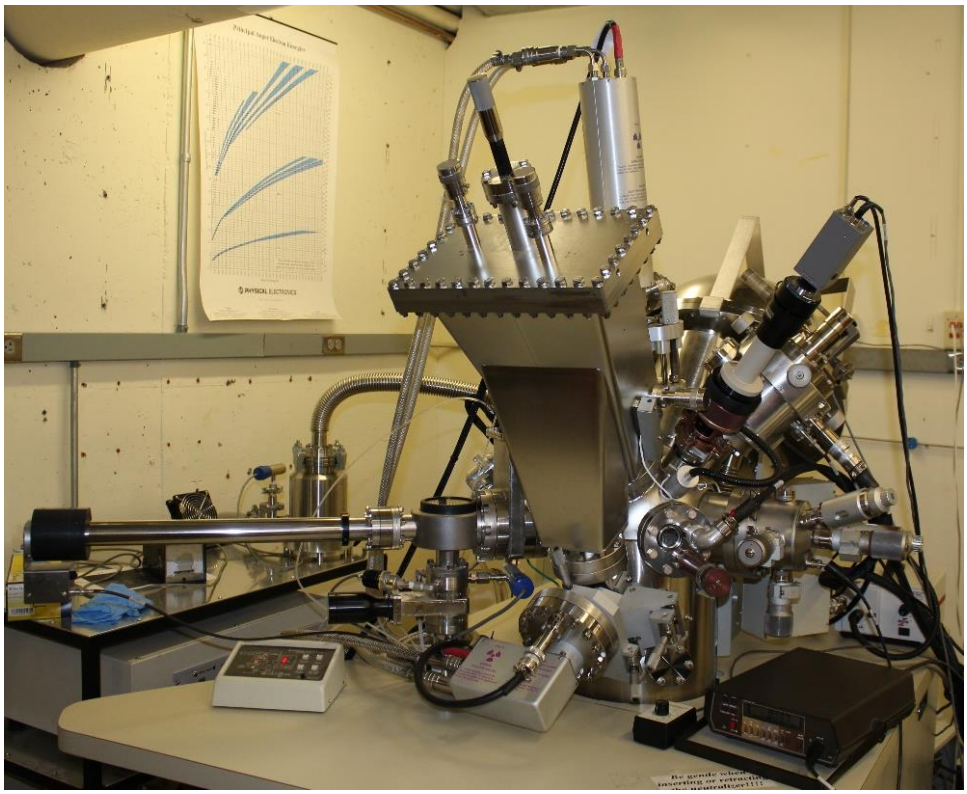

Figure 1.6: X-Ray Spectrometer

2. Experimental Materials and Methods

2.1 Field and Laboratory Experimental Set Up

Catalyst degradation is time sensitive in that for degradation to occur, a catalyst must sit in an exhaust stream for an extended period of time. Running an engine continuously to achieve catalyst degradation in a laboratory setting is not practical. As such, an outside facility was used to house and age the catalyst. The site runs large bore 2-stroke natural gas engines virtually all day and every day.

The laboratory setting, however, still plays a vital role for monitoring and quantifying catalyst degradation. The typical protocol was to age the catalyst in the field between one and two months. The catalyst was then removed and brought back to the laboratory for emissions testing. After laboratory testing was completed, the catalyst returned to the field and the cycle began again.

2.1.1 Engine Description

In order to both age the catalyst and quantify how much the catalyst has aged two separate engines were required. The laboratory engine was responsible for quantifying how much the catalyst had degraded by conducting emissions testing. The field engine was responsible for physically aging the catalyst.

Laboratory Engine

A Cummins QSK19 is a 4-stroke stationary natural gas engine. It has six cylinders and is turbocharged with a total displacement of 1159 in^3 (19 L). Figure 2.1 shows the laboratory engine set up. Both the bore and the stroke are 6.25" (159 mm). The Cummins QSK19G produces power at 470 hp (351 kW) at 1800 rpm and 450 hp (336 kW) at 1500 rpm. A summary of the engine specifications can be seen in the Table 1. The engine specification sheet and an averaged engine parameter table can be found in Appendix A.

Field Engine

A Cooper Bessemer GMVH-12 2-stroke large bore stationary natural gas engine was used for the field experiments. This turbocharged 12 cylinder engine has displacement of 2135 in^3 (35 L) per cylinder. Figure 2.2 shows one bank of the field engine. The Cooper Bessemer bore and stroke are 14" (355 mm). Its rated power is 2700 hp (2013 kW) at 330 rpm. Table 2 provides the Cooper Bessemer engine specifications and average observed engine specifications can be found in Appendix A.

Figure 2.1: Laboratory Cummins QSK19G Engine

Table 2.1: Laboratory Cummins QSK19G Engine Specifications

Engine Specifications	
Manufacturer and Model	Cummins QSK19G
Displacement	1159 in^3 (19 L)
Bore	6.25” (159 mm)
Stroke	6.25” (159 mm)
Rated Power	470 hp (351 kW) at 1800 rpm
	450 hp (336 kW) at 1500 rpm
Fuel	Pipeline Natural Gas

Figure 2.2: Field Cooper Bessemer GMVH-12 Engine

Table 2.2: Field Cooper Bessemer GMVH-12 Engine Specifications

Engine Specifications	
Manufacturer and Model	Cooper Bessemer GMVH-12
Displacement	2135 in^3 (35 L) per cylinder
Bore	14” (355 mm)
Stroke	14” (355 mm)
Rated Power	2700 hp (2013 kW) at 330 rpm

2.1.2 Laboratory and Field Catalyst Slipstreams

In order to age and degrade a catalyst exhaust must flow through the catalyst. For both the laboratory and the field setups, a slipstream was installed. Essentially a slipstream diverts exhaust from the engine and through the catalyst. The catalysts used were small in comparison to the quantity of exhaust output from the engine. Using a slipstream assembly allows for the appropriate amount of exhaust to flow through the catalyst.

Laboratory Slipstream Assembly

The laboratory slipstream assembly diverts exhaust from the engine allowing it to flow through the catalyst and provides independent control over the operating parameters. A liquid-gas heat exchanger and control valve allow for both temperature and space velocity control. Residence time—the amount of time the exhaust spend in the catalyst—is the inverse of space velocity. Figures 2.3 and 2.4 show the slipstream assembly in the laboratory and a schematized model of the slipstream assembly, respectfully.

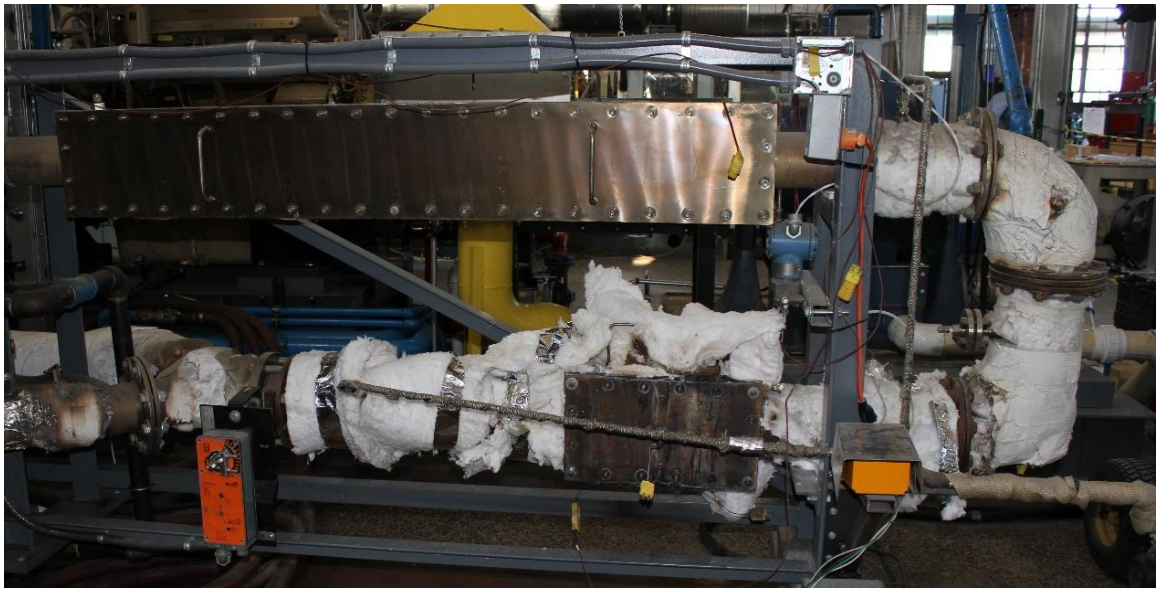

Figure 2.3: Laboratory Slipstream Assembly

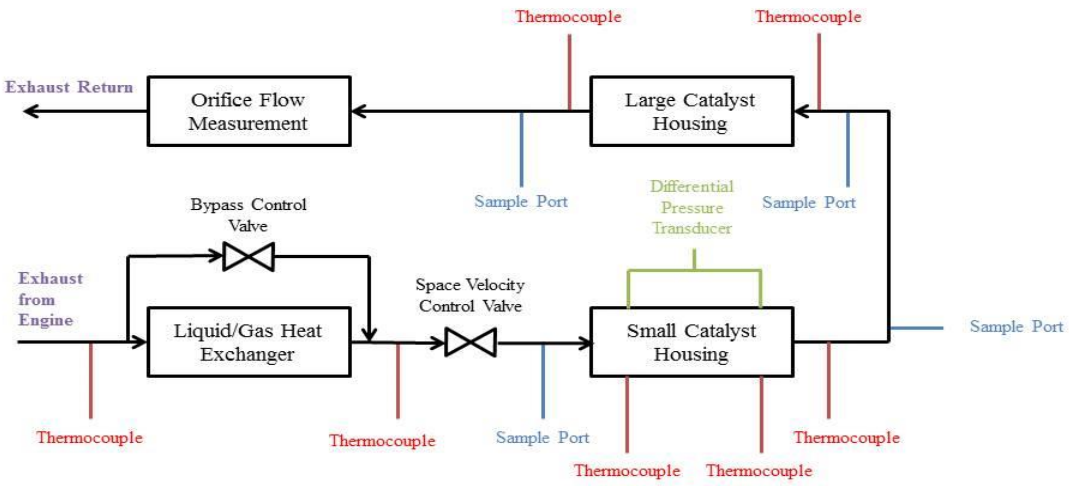

Figure 2.4: Schematic of Laboratory Slipstream

The slipstream is connected to the engine's exhaust stream via insulated stainless steel flexible tubing. Engine exhaust is diverted through the slipstream as seen in the bottom half of the model and bypass control valves set the flow rate through the heat exchanger to control temperature via LabView. Engine coolant is pumped through the liquid side of the heat exchanger. Another control valve, which controls the space velocity, is located downstream of the heat exchanger. Like the temperature control, the space velocity is controlled by a program in LabView. For a more in-depth discussion on the laboratory slipstream assembly please refer to Koushik Badrinarayanan's thesis [2].

Field Slipstream Assembly

Prior to the installation of the field slipstream assembly, the exhaust from the engine would flow through piping, up through a silencer and out into the surroundings. In order to flow exhaust through the catalyst, a separate apparatus was constructed and installed onto the existing exhaust stream structure. The field catalyst slipstream tapped into the existing exhaust stream structure. This set up allowed for the engine exhaust to travel up the field slipstream's 4" piping, through the catalyst and out the top. The field slipstream assembly is shown in Figure 2.5.

Figure 2.5: Initial Field Catalyst Slipstream Assembly

While the catalyst resided in the field, pressure differential across the catalyst and pre and post catalyst temperature measurements were recorded. The two temperature probes were Omega K-type and are 3/8" in diameter. The pressure differential was measured via a 4-20 mA Emerson Rosemount 3051 Pressure Differential Transmitter. Both the temperature and the pressure differential measurements were recorded via Dataq USB loggers. The differential pressure was recorded by an EL-USB-4 4-20 mA current loop data logger. The temperature loggers are EL-USB-TC K-type thermocouples rated from 32°F (0°C) to 752 °F (400°C).

The exhaust flow can be computed from catalyst differential pressure data; however, high variability in this measurement made it difficult to accurately calculate exhaust flow. To achieve more

accurate measurements a pitot tube was installed to measure exhaust velocity directly. Exhaust velocity is used to compute space velocity. Figure 2.6 shows the pitot tube configuration on the field slipstream.

The pitot tube has two output tubes running to a Testo 6381 differential pressure transmitter. The Testo transmitter converts total and static pressure measurements from the pitot tube to velocity, which is recorded by another Dataq El-USB-4 data logger.

The velocity data showed that not enough exhaust flowed through the field slipstream. In order to draw more exhaust through the field slipstream a blower was installed on top of the existing structure. The blower was a Tjernlund model HS2 Power Venter. This 1 hp motor was predicted to increase velocity flow by a factor of two, which was close to the actual increase of 1.7x. Figure 2.7 and 2.8 show the blower set up and a schematized model of the final structure, respectively.

Figure 2.6: Field Catalyst Slipstream Assembly with Pitot Tube

Figure 2.7: Final Catalyst Slipstream Assembly with Blower and Pitot Tube

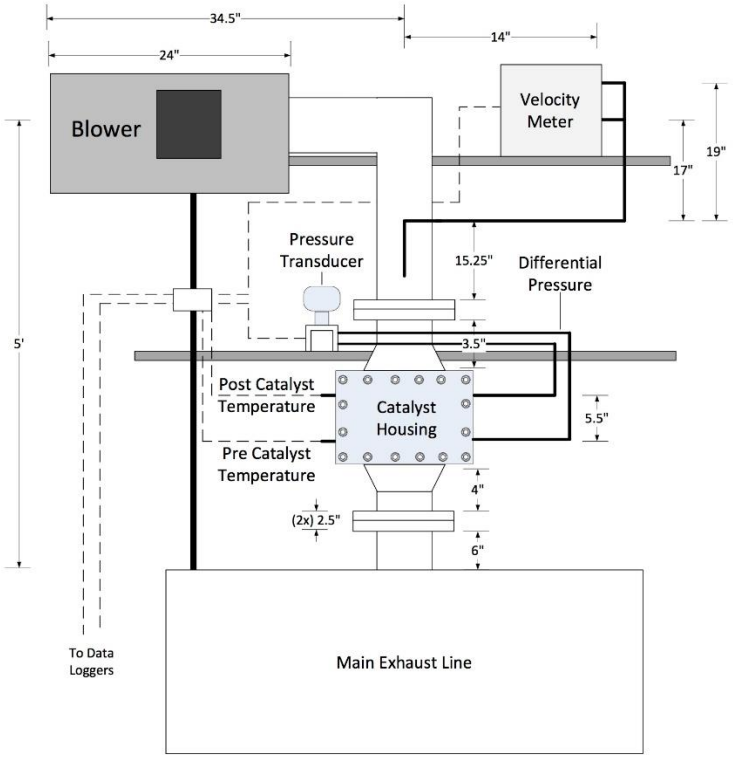

Figure 2.8: Schematic of Final Field Catalyst Slipstream Assembly

2.1.3 Laboratory Analyzers

Emissions and material testing plays a vital role in detecting and monitoring catalyst degradation. In the laboratory, several different instruments were used to monitor the catalyst's degradation. Those instruments are a 5-gas analyzer, Fourier transform infra-red spectrometer, gas chromatograph, scanning electron microscope and x-ray spectrometer.

5-Gas Analyzer

A Rosemount 5-gas measurement bench measures five different emission species which are CO, CO_2, NOx, THC and O_2. Dry emission samples must be used for these measurements. To obtain dry samples, the exhaust flows through a peltier type condenser which removes water from the exhaust. Infra-red radiation is then used to excite certain emissions such as CO and CO_2. The concentrations of CO and CO_2 are quantified by using the radiation adsorption profile.

The THC concentration is found by using a Flame Ionization Detector (FID). A hydrogen-air flame decomposes the hydrocarbons in the exhaust sample which produces positively charged ions and electrons. An electrode with a potential difference attracts the ions to its surface resulting in current flow. The ion current is measured and used to quantify the THC concentration.

The NOx concentration is found using chemiluminecense. Chemiluminecense is used to measure the NOx concentration via the following equations:

$$NO_2 \rightarrow NO + \tfrac{1}{2} O_2$$

$$NO + O_3 \rightarrow NO_2^* + O_2$$

$$NO_2^* \rightarrow NO_2 + \text{photon}$$

As exhaust passes through the oxidation catalyst, NOx species are reduced to NO. The NO passes through a chamber containing ozone which forms NO_2 in an excited state. Then the excited NO_2

molecules release a photon thus returning it back to its neutral state. The quantification of the emitted light is measured by a photo diode.

Diatomic oxygen maintains a higher magnetic susceptibility compared to the other exhaust gases. Oxygen concentration can, therefore, be measured by utilizing its magnetic susceptibility. During testing the 5-gas analyzer shows real time exhaust measurements. These measurements are then saved via a LabView program. The laboratory 5-gas analyzer can be seen in Figure 2.9.

Figure 2.9: Laboratory 5-Gas Analyzer

Fourier Transform Infra-Red Spectrometer

Hazardous Air Pollutants (HAPs) such as formaldehyde, acetaldehyde and acrolein are analyzed using the Fourier Transform Infra-Red Spectroscopy (FTIR). The FTIR utilizes infra-red radiation adsorption to detect HAPs. The exhaust samples are scanned using varying wavelengths of infra-red

radiation. The FTIR determines the species concentrations by comparing exhaust absorption spectra with species absorption spectra from calibration standards.

Heated sample lines are vital to FTIR measurements. Some of the emission species are water soluble so heated lines allows for wet measurements but prevents certain species from adsorbing into water by maintaining the water in a vapor state. The FTIR analyzer can be seen below in Figure 2.10.

Figure 2.10: Laboratory Fourier Transform Infra-Red Spectrometer

Scanning Electron Microscope

The scanning electron microscope (SEM) used was a JEOL JSM-6500F at the Central Instrument Facility at Colorado State University [27]. The SEM rasters a 10 to 30 kV electron beam over the specimen. When an electron beam strikes the material's surface, core electrons can be knocked out of orbitals of atoms inner shells. When an electron from a higher energy orbital falls into this vacated orbital an x-ray can be given off. This x-ray's energy is quantized and can be measured to determine the element it came from. The output data for the SEM is only semi-quantitive and should not be used to quantify atomic percentages on the surface unless certain specifications are met, such as having standards and the surface being smooth. The SEM used for this project can be seen in Figure 2.11.

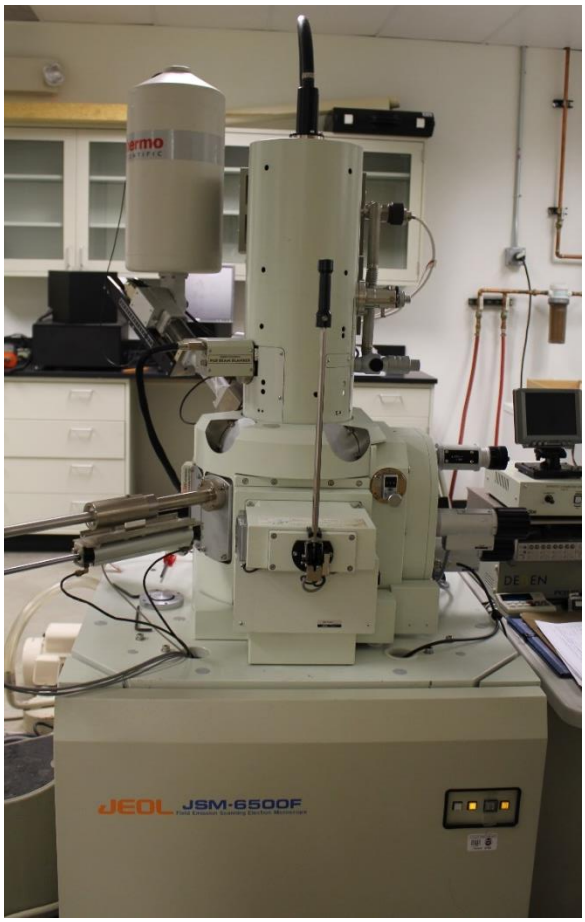

Figure 2.11: Laboratory Scanning Electron Microscope

X-ray Spectrometer

X-ray Spectroscopy (XPS) helps quantify elemental species on the surface of a material. The XPS uses an Al K_α x-ray source at 350 kW and 15 kV with a photoelectron take off angle of 45° to flood the material specimen with x-rays. The x-rays hit the material specimen and electrons can be ejected to be collected by a hemispherical analyzer. XPS Peak v4.1 software was used to interpret the electron data collected and quantifies the elements of the surface of the material. At the Central Instrument Facility at Colorado State University [27], a Physical Electronics PHI-5800 ESCA/AES, XPS machine was used to collect the data and can be seen in Figure 2.12. Survey spectra were taken at a pass energy of 186.5 eV and a step size of 1.6 eV. High resolution scans were taken at a pass energy of 23.5 eV and a step size of 0.1 eV.

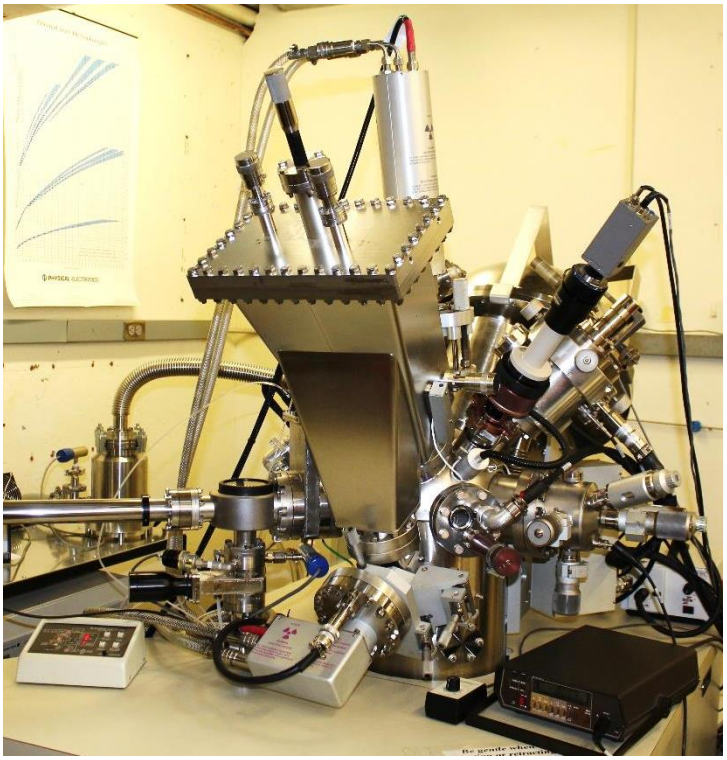

Figure 2.12: Laboratory X-ray Spectrometer

2.1.4 Field Analyzers

One of the main causes of catalyst deactivation is catalyst poisoning from lube oil carryover in the exhaust. Previous work has shown that lube oil carryover can be detected in the exhaust using a mass based particulate matter (PM) measurement technique utilizing a dilution tunnel [28]. It is assumed that the majority of the PM in the exhaust is lube oil carry over.

Dilution Tunnel

The dilution tunnel was set up to measure PM pre-catalyst. Sample tubes—fabricated in accordance to EPA Method I guidelines [29]—were inserted pre and post catalyst (post catalyst tubes were used for the portable emissions analyzer described below). These sample tubes allowed exhaust to be captured and travel through heated sample lines to the filter. Again, heated sample lines are imperative to

this process since they prevent water condensation in the sample lines which also prevents emission adsorption into the condensed water.

PM samples were taken pre-catalyst every 30 minutes. For 30 minutes, PM accumulates on the filter from pre-catalyst emissions. After 30 minutes this filter is removed, weighed and replaced with a new filter. For a more in-depth analysis please see Roshan Joseph Kochuparampil's thesis [30]. Figure 2.13 below shows the field site dilution tunnel set up.

Figure 2.13: Field Dilution Tunnel Set Up

Portable Emissions Analyzer

ECOM America model J2KN-IND, shown in Figure 2.14, portable emissions analyzer was used to measure CO (low range), CO (high range), NO, NO_2 and methane (CH_4) in field. An internal pump in the ECOM America draws the emissions gas through heated lines to the analyzer. Emission samples were drawn from pre-catalyst tubes, described above, for 10 minutes. The internal pump was then

bypassed to allow for a 10 minute air purge. Then the emissions analysis switched, via a three way valve, to post-catalyst for 10 minutes.

Figure 2.14: ECOM Portable Emissions Analyzer used in Field

2.2. Test Procedure

Degradation and deactivation of catalysts is time sensitive. Initially the catalyst stayed in field for approximately a month at a time. About once a month it was brought back to the laboratory for emissions and materials testing. After approximately one year of monthly tests it was observed that the catalyst was not aging as quickly as was hoped. It was then decided to install the blower and begin leaving the catalyst in field for roughly two months at a time.

2.2.1 Oxidation Catalyst Preparation

Prior to placing the catalyst in the field slipstream assembly, it was degreened. Degreening is a baking process that initially sinters the catalyst causing the active catalyst material to attach to the washcoat material. The amount of sintering is assumed to be comparable to what occurs in the field during initial aging. This eliminates this degradation mechanism from subsequent aging, effectively decoupling sintering and chemical deactivation mechanisms. The catalyst was baked at 1200°F (649°C) for 24 hours in a kiln at the laboratory.

2.2.2 Laboratory Testing Procedure

Over time oxidation catalysts become ineffective at reducing exhaust emissions. In order to determine the life of this catalyst, it was removed periodically from the field and installed into the slipstream for emissions testing. Both space velocity and temperature sweep tests were run on the catalyst at different stages of its lifetime.

The proper catalyst temperature is critical for sufficiently reducing exhaust emissions. The temperature sweeps are run between 300°F (149°C) and 800°F (827°C). To determine the reduction efficiency of the catalyst, emissions data was collected every two seconds for five minutes post-catalyst and then every two seconds for one minute pre-catalyst. An automated valve continuously toggle the exhaust flow from pre to post catalyst using this timing sequence. This allows catalyst efficiency to be accurately computed throughout the sweep, even if engine conditions drift and cause a small shift in pre catalyst emissions. During the temperature sweeps the space velocity remained constant at 150,000 hr^{-1}.

Residence time is how long the exhaust spends inside the catalyst. Typically residence time is shown in the form of space velocity which is the inverse of residence time. During the space velocity sweeps, the temperature is held constant at 550°F (287°C) while the space velocity varies from approximately 20,000 hr^{-1} to 200,000 hr^{-1}. Like the temperature sweeps, emission points were taken every two seconds for one minute pre-catalyst and for five minutes post-catalyst.

2.2.3 Material Testing Procedure

Poison build up on the catalyst bed degrades its ability to reduce exhaust emissions. Monitoring the poison build up can help determine the cause of catalyst deactivation.

Material Preparation

Of the two catalysts aged in field, one catalyst's sole purpose was materials testing. Each time the catalysts were removed from the field, the top of one catalyst block was removed and a sheet of the catalyst material was extracted for materials testing. Figure 2.15 shows the partially disassembled on the right.

Figure 2.15: Catalyst modules. Emissions Module on Left and Material Sampling Module on Right (partially disassembled).

After the top of the materials catalyst is removed, the first sheet of the catalyst material is removed for materials testing. The sheet is then cut into six smaller pieces; three pieces cut from the front right and three cut from the back left. The remainder of the catalyst sheet is then discarded and the top is welded back on the catalyst housing. Six pieces were cut from the catalyst material to see if the amount of buildup varied with position. The specimen positions permit comparisons between leading and trailing edges of the catalyst and from the center to the edge of the flow. Figure 2.16 shows a diagram specimen locations.

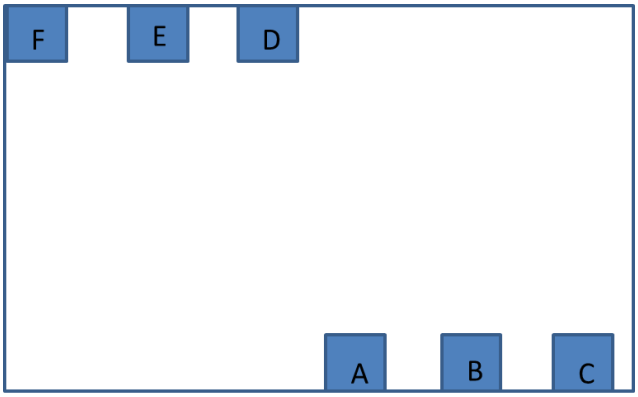

Figure 2.16: Catalyst Specimen Material Cutting Diagram

For the first three tests, a sheet of catalyst material was removed, cut into pieces and then material analysis, XPS and SEM, was immediately preformed. After the third test an excess of carbon built up on the catalyst bed preventing accurate poison readings. To remove the excess carbon a bake-out method was implemented. To find the appropriate bake-out test procedure, Test 3 material was used to ensure the same amount of poisons could be detected pre/post baking. This was done since the carbon buildup on the Test 3 was low enough that pre and post baking measurements could be taken. Ideally the bake time and temperature should burn off the excess carbon without removing any poisons such as sulfur. After trial and error, 860°F (460°C) for 1 hour resulted in complete carbon burn off with negligible poison burn off. This temperature was in line with that observed from the literature [31]. Post bake out, the six pieces of catalyst material underwent materials analysis.

SEM Procedure

The six pieces initially from the catalyst were too large to fit in the SEM, so before testing smaller pieces were cut from the original six pieces. For each test a piece of catalyst material was fixed to a standard SEM stub with double sided copper tape. It was then placed in the SEM and X-rays were collected from a 20 keV electron beam hitting the specimen using a Noran System Six energy dispersive spectroscopy system. The EDS is able to measure energy of the X-rays and provide semi-qualitative elemental data.

XPS Procedure

The XPS was used to quantify how much poison had adhered on the catalyst surface. For each of the six samples, an Al K_α X-ray source was used at 350 kW and 15 kV. A pass energy of 186.5 eV and 23.5 eV were used to collect electrons knocked out of their orbitals by the K-a X-rays for survey and high resolution electrons respectively. Each of the five tests underwent XPS analysis to determine the buildup of poisons on the surface of the catalyst material.

3. Catalyst Materials Analysis

Poison buildup on the catalyst washcoat and active sites is the main mode of catalyst deactivation after initial thermal deactivation (sintering). Quantifying how much poison has built up can aid in pinpointing when critical catalyst deactivation will occur. The National Emissions Standards for Hazardous Air Pollutants (NESHAP) regulations dictate minimum emissions levels post-catalyst. Once an excess of poison has accumulated and prevents one of the minimum emissions levels to be met the catalyst is considered deactivated.

3.1 Space Velocity and Catalyst Exchange Calculations

Understanding how much exhaust flows through the catalyst is imperative to comprehending the poisoning patterns. Space velocity is the inverse of the residence time or the amount of time exhaust spends in the catalyst. Space velocity (SV) is not a measured parameter, but it can be calculated via the following equations.

$$Q_{act} = U*A$$

$$A = \frac{\pi}{4} d^2$$

$$Q_{std} = Q_{act} \frac{T_0}{T} \frac{P}{P_0}$$

$$SV = \frac{Q_{std}}{V_{cat}}$$

Where U is the exhaust velocity, d is the pipe diameter, T_o and P_o are standard temperature and pressure respectively and V_{cat} is the volume of the catalyst. Plotting the calculated space velocity against recorded horsepower provides a line of best fit which helps estimate the space velocity for a given horsepower. Figures 3.1 and 3.2 show the plots that determined space velocity equation pre and post blower installation, respectively. The line of best fit for both scenarios results in a horsepower dependent equation to solve for the space velocity.

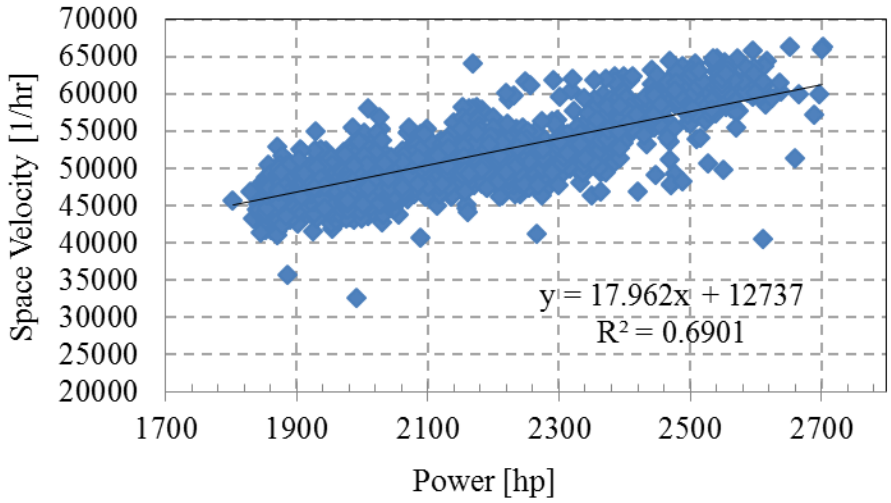

Figure 3.1: Pre-Blower Installation Space Velocity Calculation

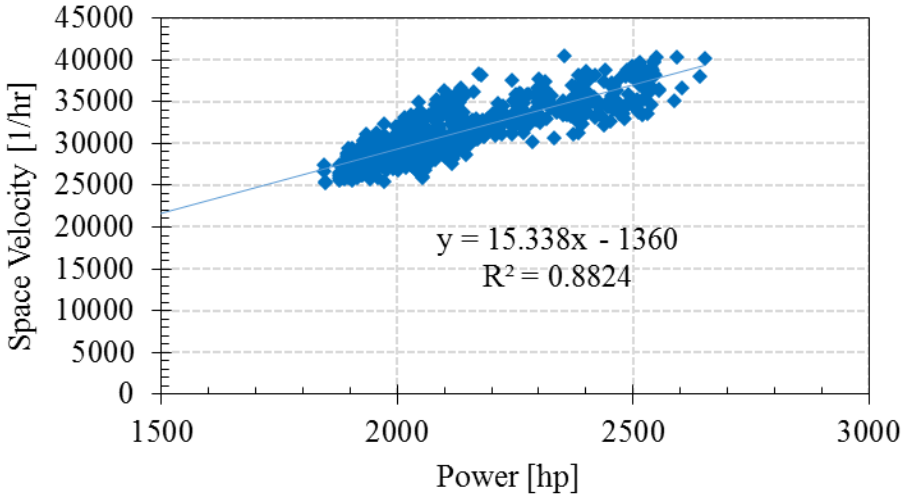

Figure 3.2: Post-Blower Installation Space Velocity Calculation

Catalyst exchanges is a unit-less measure which quantifies how many times exhaust has entered and cleared the catalyst. Every time exhaust enters and leaves the catalyst, the exhaust can poison the catalyst. Knowing this value helps understand how much of the poison is deposited per catalyst exchange which can be used to predict future poison buildup. Catalyst exchanges are calculated via the following equation.

$$\text{Catalyst Exchanges} = SV * \Delta t$$

3.2 Field Particulate Matter and Lube Oil Results

Lube oil carry over is suspected to be the primary contributor to oxidation catalyst degradation and ultimately deactivation. Being able to quantify how much unburned lube oil escapes the power cylinder and travels through the catalyst could help estimate the life of the catalyst. Knowing the exact amount of lube oil carry over was not possible for this experimental set up. However, taking PM measurements coupled with lube oil supplied to the cylinder provides a range for lube oil carry over since it is assumed that the majority of PM detected will result from lube oil in the exhaust. PM measured from dilution tunnel testing can be seen in Figure 3.3 which has been adapted from Olsen et al.[28].

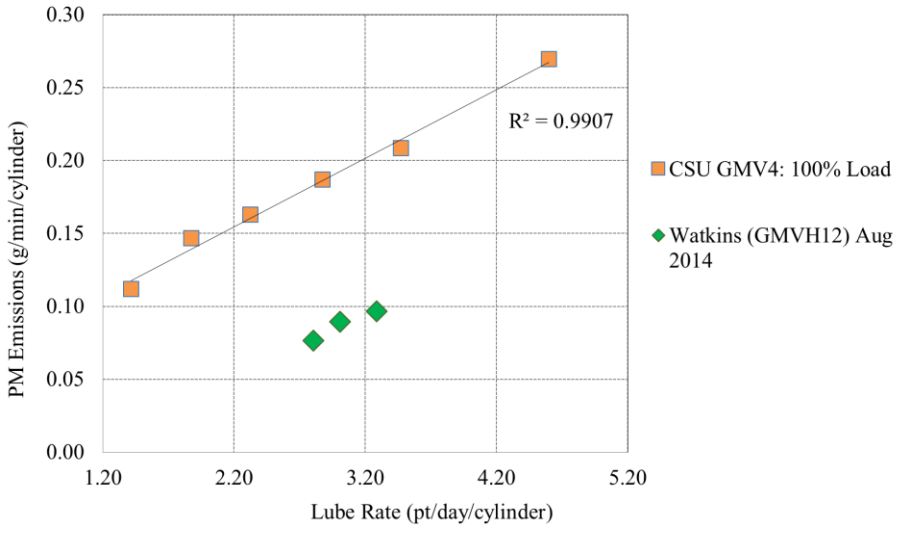

Figure 3.3: Particulate Matter Emissions vs Lubrication Rate

The field engine is equipped with a lube oil meter which records how much lube oil is supplied to the power cylinders; this value was reported on an hourly basis. Operators for the field engine also track the amount of fresh oil supplied to the engine daily – both values were reported to CSU for the dates the catalyst was in the field. A schematic of this system is seen in Figure 3.4**,** where the general path of engine oil can be seen. Some of the fresh oil makes it to the power cylinders; however, much of it is diverted to engine bearings and to the turbocharger or is lost via leaks. Taking the data from the lube oil meters and the PM data, a range of potential lube oil carry over is quantified in Figure 3.5.

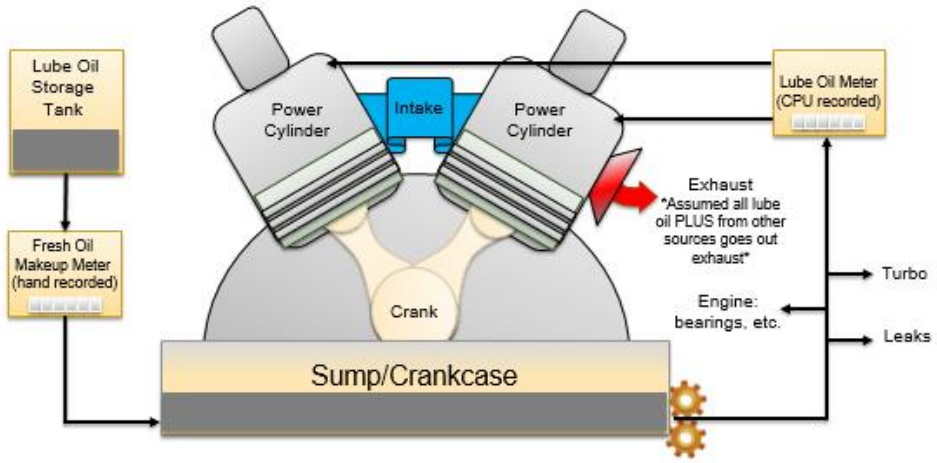

Figure 3.4: Lubrication Oil Schematic

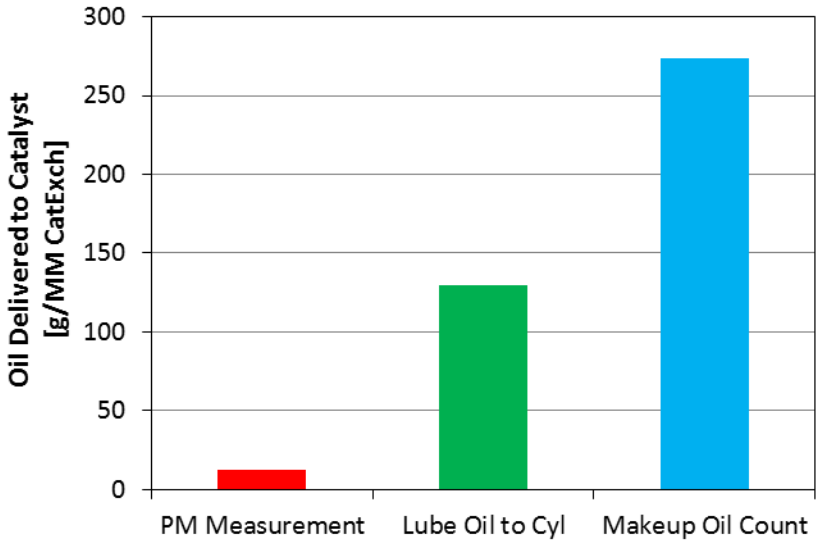

Figure 3.5: Potential Lubrication Oil Delivered to the Catalyst

Lube oil contains sulfur, zinc and phosphorous in addition to other elements and metals to aid in wear reduction. When unburned lube oil escapes the engine's power cylinders it travels to the exhaust and then to the catalyst, causing fouling. New oil was removed from the engine and was tested for these contaminates by PEAK Testing [32] and SOS Fuels Lab Testing [33] services. The results can be seen in Table 3.1 and the specification sheets can be found in Appendix B**.**

Table 3.1: Lubrication Oil Contaminates

Fresh Lube Oil Testing	S [ppm]	Zn [ppm]	P [ppm]	Ca [ppm]	Pb [ppm]
PEAK Testing	5080	451	359	n/a	n/a
SOS Fuels Lab Testing	n/a	424	442	25	1

3.3 Scanning Electron Microscope Results

The scanning electron microscope provides semi-quantitative poison buildup data. Figure 3.6 shows SEM results for sulfur on the Test 1 section 'A' specimen. Sulfur deposits are represented by the green dots spread through the image. After one month in field, the sample shows sulfur poisoning dispersed throughout the sample. The concentration of the sulfur deposits, however, is higher on the left side of the image, which is the valley of the corrugated catalyst material. The peak, on the right side, rubs against the layer above it, thus making poison deposition difficult.

As the catalyst ages in field, it is expected that sulfur will continue to deposit on the active catalyst sites until they are totally covered [10]. Visually inspecting Test 4 specimen 'A', in Figure 3.7, and comparing it to Test 1, it appears that the Test 4 specimen has more sulfur spread throughout than Test 1. Test 1 sulfur poisoning was just starting to cover the washcoat surface, whereas Test 4 shows more of an even coat of sulfur. As in Test 1, this specimen shows significantly more sulfur in the valley on the left and right sides. The SEM data provides insight into the location of poison deposition; however, it does not quantify the amount of poison deposited.

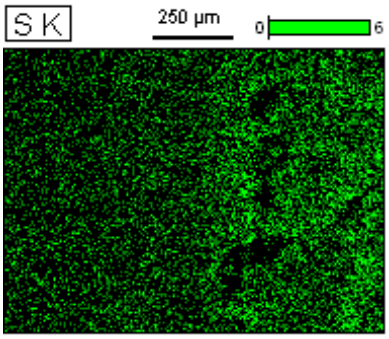

Figure 3.6: Test 1 Specimen ‘A’ SEM Sulfur Poisoning Map

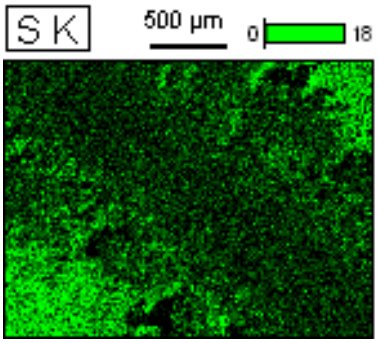

Figure 3.7: Test 4 Specimen ‘A’ SEM Sulfur Poisoning Map

Phosphorous deposits directly onto the washcoat from anti-wear and anti-oxidant additives [10, 13]. The phosphorous deposits are represented by blue dots in Figure 3.8. The left side shows significantly more deposited phosphorous than the right side. Again this indicates a valley in the catalyst material. Phosphorous tends to poison the front of the catalyst first and before poisoning the rest of the catalyst [10]. Figure 3.8 shows heavy poisoning in the front of the catalyst, thus confirming this finding.

As the catalyst continues to age and degrade, the phosphorous levels are expected to rise until the entire washcoat is covered [13]. Figure 3.9 shows more poisoning on the left and ride sides. These two regions are valleys in the catalyst material and it is much easier for poisoning to occur in these regions. Comparing Figures 3.8 and 3.9, more concentrated phosphorous poison has built up in the valleys of the later tests. Still little poison occurs on the peaks of the catalyst. The increase in phosphorous poisoning confirms Dairene Uy et. al. findings [13].

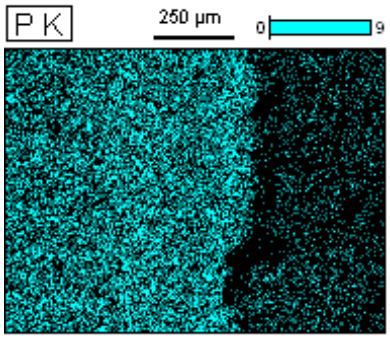

Figure 3.8: Test 1 Specimen ‘A’ SEM Phosphorous Poisoning Map

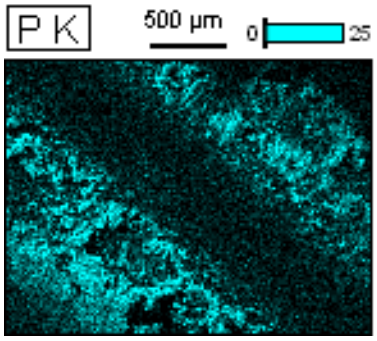

Figure 3.9: Test 4 Specimen ‘A’ SEM Phosphorus Poisoning Map

Zinc also contributes to catalyst poisoning and deactivation. Test 1, however, zinc was not tested for during SEM testing. Test 4 does show evenly distributed zinc shown in Figure 3.10. Like phosphorous, zinc adheres to the washcoat and eventually forms a thin layer over the entire washcoat. Test 4 shows zinc poisoning throughout the catalyst and confirms the literature findings.

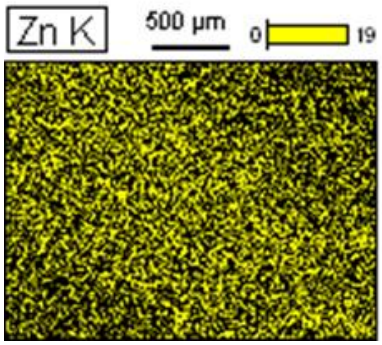

Figure 3.10: Test 4 Specimen ‘A’ SEM Zinc Poisoning Map

3.4 Material Poisoning Results

Figures 3.11 and 3.12 show species build up vs. catalyst exchanges and the total poison build up vs. catalyst exchanges, respectively. This data was gathered using X-Ray Spectroscopy (XPS), which gathers elemental data from the surface. Since the poisons deposit on the surface of the catalyst, XPS provides adequate information for poison buildup. For each species buildup test points, the six XPS results were averaged to form one cohesive point. The total poison buildup points however are the sum of zinc, phosphorous and sulfur atomic percent from each test.

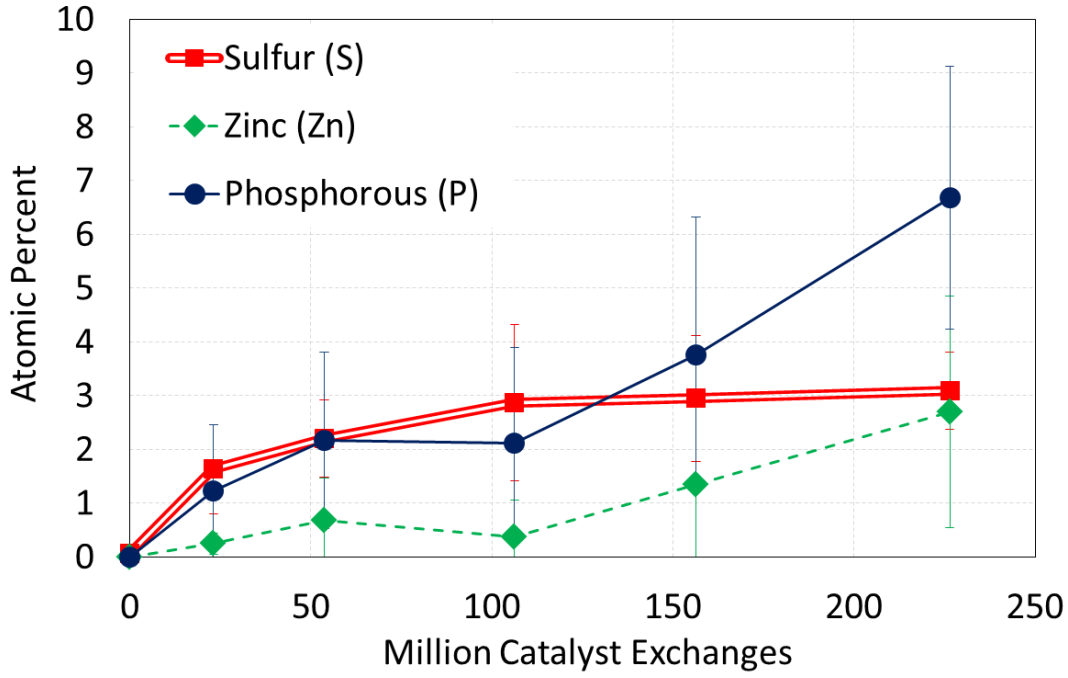

Figure 3.11: Poison Species Buildup per Catalyst Exchange

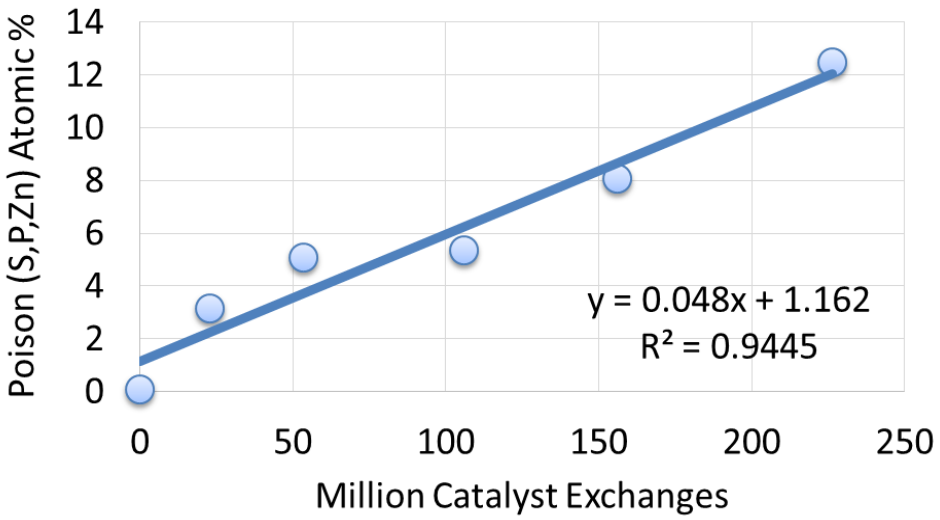

Figure 3.12: Total Poison Buildup on the Catalyst

Unburned sulfur enters the catalyst and adheres to the active metal sites [4]. Above in Table 3.1, new oil enters the engine containing 5080 ppm of sulfur. When the oil goes unburned it flows through the catalysts causing poisoning. The graph, shown in Figure 3.11, shows a sharp increase of sulfur deposition during the first 25 million catalyst exchanges. Prior to being in the field slipstream the catalyst experienced no sulfur poisoning. Incoming sulfur, therefore, initially had a plethora of active sites to which it could adhere. After this point, the sulfur poisoning rate levels off. Sulfur eventually forms a layer of poison on the catalyst surface [12]. Leveling off of sulfur poison deposition could indicate a layer of sulfur has already adhered to the catalyst surface, making it difficult for new sulfur molecules to find active catalyst metal.

Zinc poisoning with phosphorous is mutually inclusive since both are observed in lube oil wear additives such as zinc-dialkyldithiophosphates (ZDDP) [9], though some phosphorus-oxygenate species have been shown to deposit without the presence of zinc. Overtime both phosphorous and zinc poisoning increases at similar rates with phosphorous at a higher magnitude. The oil used in the field contained 359 ppm phosphorous and 451 ppm zinc; although, no tests yielding the speciation of the Zn and P compounds were done. Therefore, it is presently unclear how much of the phosphorus is tied up in ZDDP-

type compounds as opposed to in the form of free phosphorus or other phosphorus compounds. While the quantity of zinc in the oil is higher, zinc cannot poison the catalyst on its own, but phosphorous can [14]. Consequently, phosphorous has more opportunities to adhere to the washcoat.

Sulfur, zinc and phosphorous will eventually coat the catalyst. Even though the sulfur deposition rate has leveled off (implying it has adhered to as many active catalyst sites as possible), both phosphorous and zinc are still rising thus causing the total poison count to also rise. Since the washcoat surface area is much larger than the active catalyst surface area, phosphorous and zinc poisons coating the entire washcoat will take more time. Once these two poisons have covered the washcoat the total poisons should level off and be constant.

3.5 Poison Distribution Results

It is suggested by Deborah L. Mowery et. al.[10] that sulfur poisoning initially occurs solely at the front of the catalyst, but over time the sulfur poisoning will disperse throughout the entire catalyst. The Baseline Test, which the catalyst had just experienced degreening, shows a negligible amount of sulfur in the front specimen average, shown in Figure 3.13. The front specimen average for Tests 1 through 5, though, are lower in atomic percent than the back specimen average.

Test 1 shows a sharp spike in sulfur poisoning in both the front and the back. This occurrence is inconsistent with the literature findings. During the initial stages of aging, it is suggested that sulfur solely poisons the front of the catalyst. This is not observed in the test data. As the catalyst ages and encounters more sulfur poisoning, sulfur begins poisoning the entirety of the catalyst. Tests 3-5 front to back specimen averages are within 1 atomic percent of each other. This suggests that the sulfur has migrated throughout the washcoat as D.L. Mowery found [10].

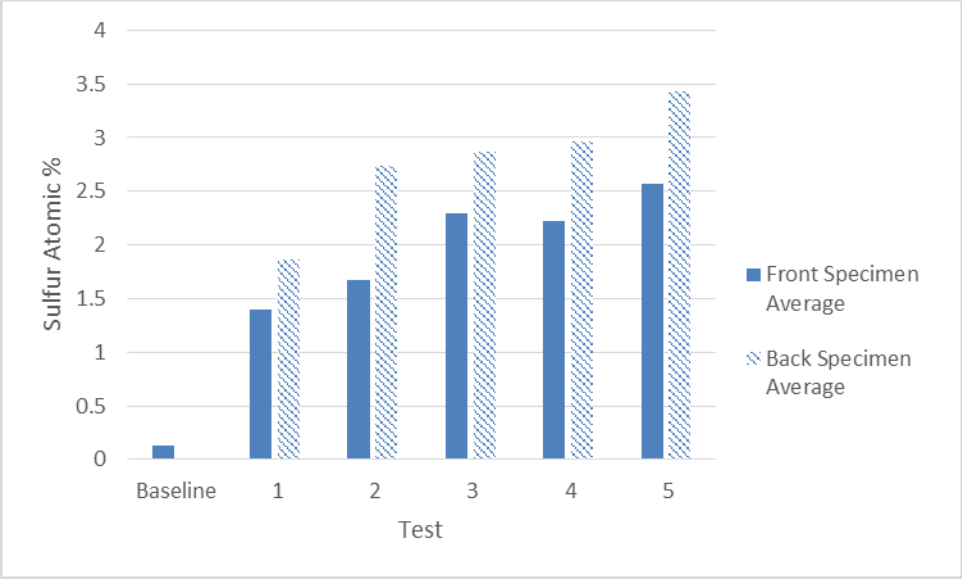

Figure 3.13: Front and Back Specimen Averages for Sulfur Poisoning

Initially both the front and back specimen average for phosphorous exhibits no poisoning. Tests 1 and 2 show more phosphorous poisoning in the back specimens than the front. Test 3, however, shows the front and back specimen average as equal. Once the blower was installed, for Tests 4 and 5, the front specimen average is substantially higher than the back specimen average. The front and back specimen averages for phosphorous poisoning are shown in Figure 3.14.

The first four tests show that the magnitude of the front versus the magnitude of the back poisoning is relatively close. Therefore, these tests neither confirm nor deny the literature findings. Once the catalyst experienced higher volume of catalyst exchanges, post blower installation, the front specimen phosphorous poisoning increased drastically. Similar to sulfur, the literature suggests that phosphorous initially poisons the front of the catalyst, but then the poisoning evenly coats the catalyst [10, 13]. Tests 4 and 5 are support this trend. As time progresses it is expected that the phosphorous will cover the entire catalyst. Phosphorous and zinc deposition continuously increase whereas sulfur poisoning levels off. The continuous buildup of phosphorous on the front of the catalyst could prohibit sulfur from depositing there, thus causing the sulfur to find other locations, such as the back of the catalyst, to deposit.

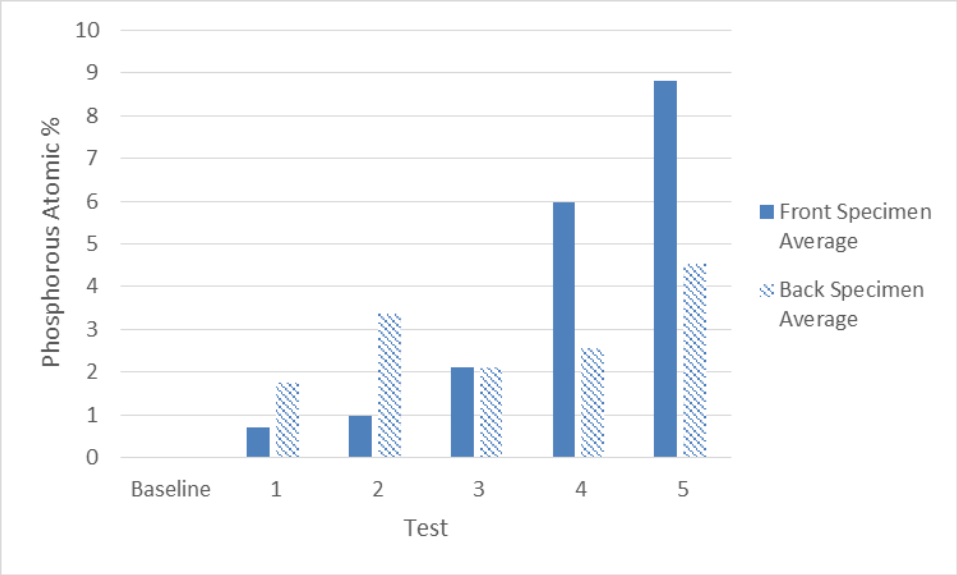

Figure 3.14: Front and Back Specimen Averages for Phosphorous Poisoning

Of the three monitored poisons, zinc displays the most similar trends to phosphorous. The Baseline Test shows no zinc poisoning for either the front or the back. Test 1 favors zinc poisoning in the front; however, Test 2 and 3 show higher levels of poisoning in the back specimens than the front specimens. Then Tests 4 and 5 show significantly higher levels of zinc poisoning in the front specimens than the back specimens. These trends are shown in Figure 3.15.

Zinc poisoning is dependent on phosphorous poisoning [14]. So it is expected that both phosphorous and zinc would maintain similar poisoning trends from front to back. Like phosphorous poisoning, the first four tests do not show a significant difference in magnitude from front to back poisoning. Tests 4 and 5, however, indicates a large increase in poisoning on the front of the catalyst. Like phosphorous, this is indicative of initial poisoning of the catalyst. The catalyst needs to age more to determine if zinc poisoning will spread throughout the catalyst.

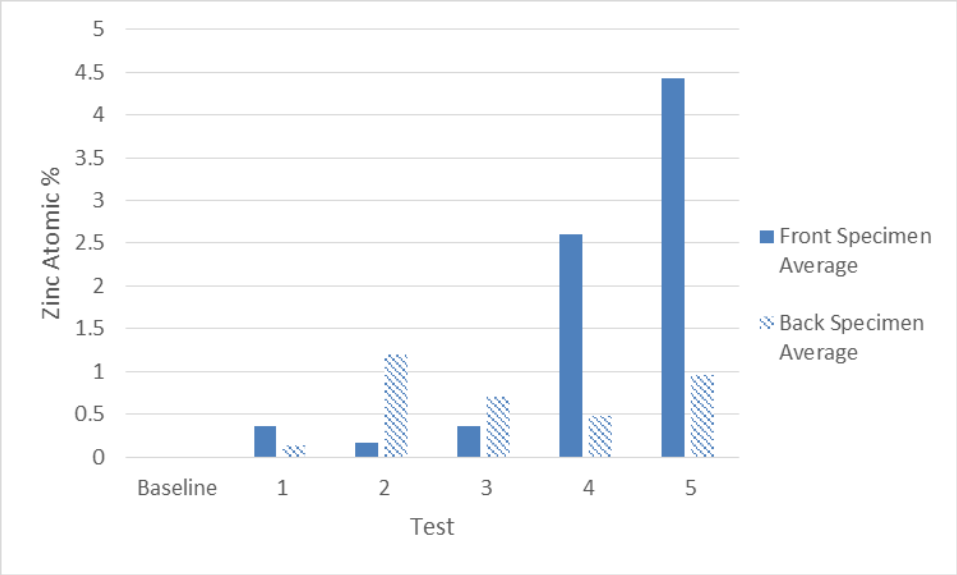

Figure 3.15: Front and Back Specimen Averages for Zinc Poisoning

4. Catalyst Emissions Analysis

Catalyst degradation is best monitored through emissions testing. As the catalyst is poisoned its ability to reduce emissions dwindles. The main parameters tracked are the catalyst light off temperatures, reduction efficiencies, and absolute reduction for each species of interest.

4.1 Emissions Data

Reduction efficiency measures how well the catalyst reduces or oxidizes emissions. To calculate reduction efficiency emissions data must be gathered for both pre-catalyst and post-catalyst locations. With the current setup at the EECL, gathering pre and post-catalyst emissions is done by toggling between the two locations. If the catalyst is effective this toggling results in alternating high and low levels of a given emission, corresponding to the pre and post-catalyst locations, respectively. The highest points, in Figure 4.1, represent the pre-catalyst emissions data, and the low points are the post-catalyst emissions data for CO. The tails between the high and low points are emissions measured during the toggle process. These data points represent the time it takes for the exhaust to travel through the sampling lines and does not reveal information about either of the two sampling locations, but rather just the

transition period of switching. These data points are, therefore, removed during post-processing of the data and only the line-out portions of the data are kept, shown in Figure 4.2. For this test temperature, shown on both plots, transitions from high to low. As the temperature is reduced pre-catalyst and post-catalyst values move closer together, indicating lower catalyst reduction efficiency.

During testing a calibration error occurred with the FTIR data for some of the species during Tests 4 and 5. While this calibration error does not affect the reduction efficiency data, it does affect the reported pre-catalyst ppm data. A correction factor has been applied to methane, propane and ethylene. The average correction factor magnitude is 80%. The other emission species measured by the FTIR, however, are uncorrected.

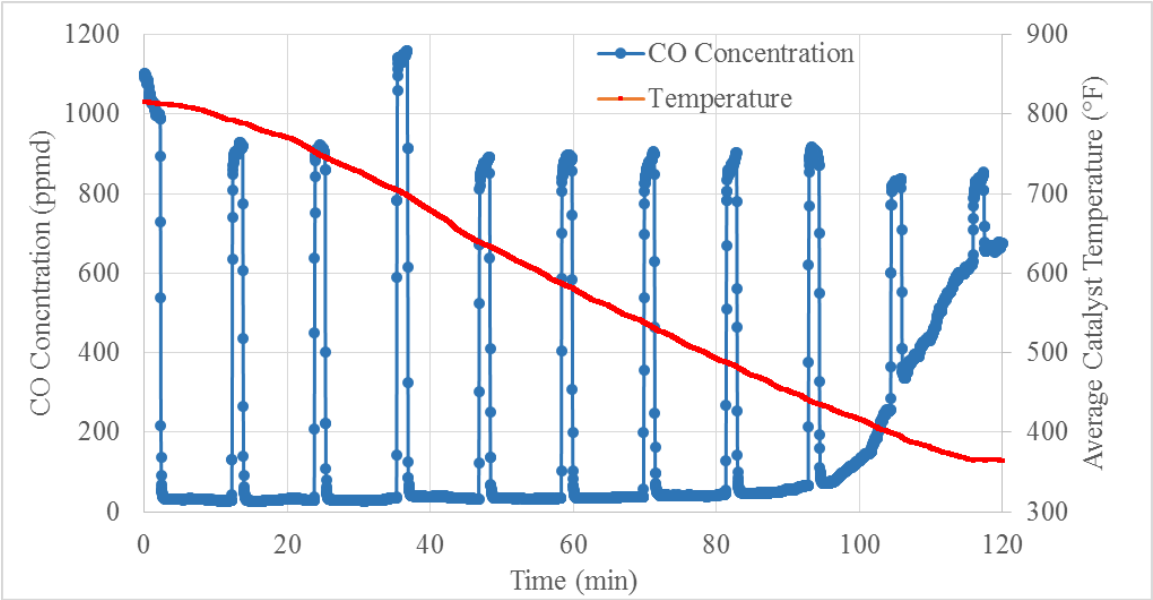

Figure 4.1: Raw Emissions Data for Carbon Monoxide

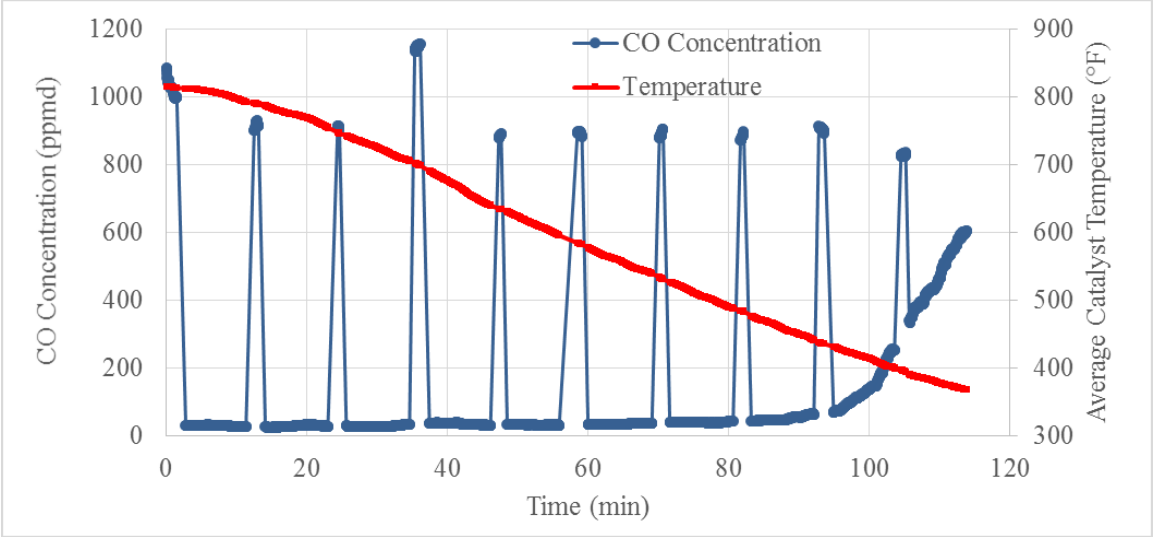

Figure 4.2: Processed Emissions Data for Carbon Monoxide

4.2 Light Off Temperature

Light off temperature is the corresponding temperature when the post-catalyst value of a given incoming species reaches 50% of the pre-catalyst value. As poisons build up and block active catalyst sites, it becomes increasingly difficult for emission species to oxidize. The oxidation reactions that govern the emission destruction processes are sensitive to temperature, and the rate constants for these reactions increase exponentially as temperature increases. Therefore as fouling progresses and active catalyst sites are covered or occupied, the catalyst temperature must be raised to achieve a desired level of reduction efficiency. The light off temperature represents the temperature at which the catalyst transitions between low and high efficiency and thus can be used to track the overall level catalyst health. As catalyst ages, the light off temperature must increase to maintain activity - Figure 4.3 shows how light off temperature has increased with time for the field-aged catalyst.

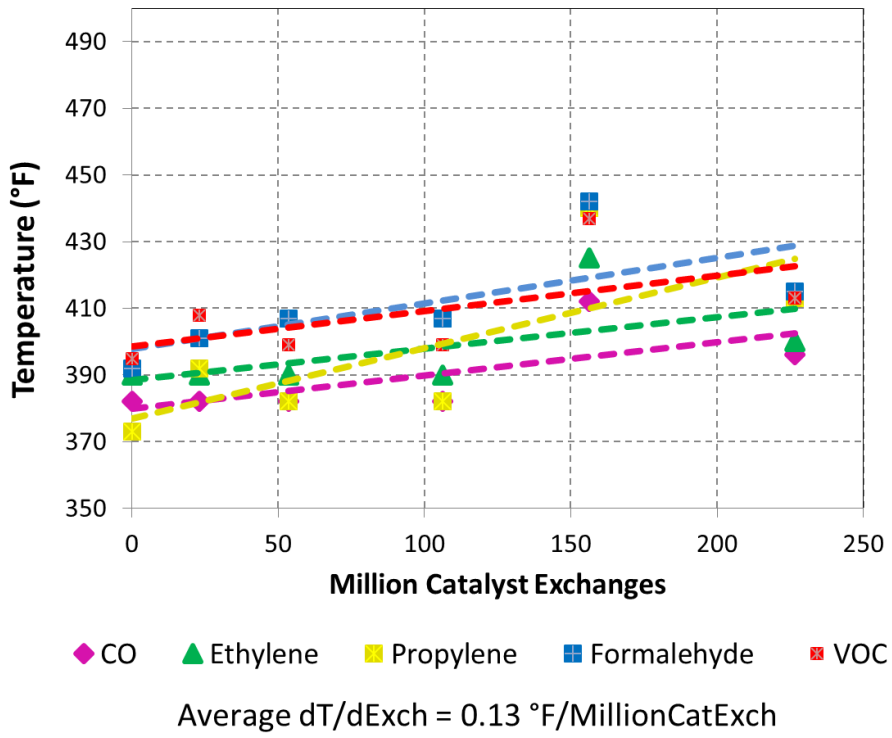

Figure 4.3: Light Off Temperature

Apart from test 4, which had higher than normal olefin levels, the light off temperature trend is fairly linear. Olefins can be representative of a gas composition which is more difficult to oxidize. Comparing the total poisons data in Figure 3.12—which is also linear—to the light off temperature, it can be determined that rate of poisoning and light off temperature directly correlate to one another. Exhaust flows through the field slipstream at a constant velocity, which implies a steady, linear buildup of poisons. Since poison deposition and light off temperature are directly related, a linear increase of light off temperature makes sense. The rise in average light off temperature (dT) can be estimated using the following:

dT = .13°F/million catalyst exchanges * million catalyst exchanges

After a million catalyst exchanges the average light off temperature increases 0.13°F. Total poison buildup is quantified via a linear equation where x is millions of catalyst exchanges and y and total poison in atomic percent.

$$y = .048x + 1.16$$

After 1 million catalyst exchanges the total atomic percent of poison buildup will be 1.2. This means for every 0.13°F increase in light off temperature, the total poison also increases by 1.2 atomic percent.

4.3 Carbon Monoxide Reduction

CO conversion throughout the five tests is relatively high and shows little signs of degradation for both the temperature sweeps and the space velocity sweeps. The temperature sweep data, shown in Figure 4.4, shows a sharp increase in reduction efficiency between 350°F and 450°F; however, after 450°F the trend becomes linear with almost a zero slope. All tests exhibit high reduction efficiency with the Baseline Test achieving a maximum efficiency of 97% and Test 5 achieving maximum efficiency at 95%.

Like the temperature sweep data the space velocity data, Figure 4.5, shows high reduction efficiency for all tests. Both the Baseline Test and Test 5 achieve a maximum efficiency of 99%. As space velocity increases, however, reduction efficiency decreases in all tests. Larger space velocities represent smaller catalyst residence times, which reduces oxidation reaction time. The Baseline Test has a minimum reduction efficiency of 94% at 164,000 hr^{-1}. Test 5, however, has a minimum reduction efficiency of 87.7% at a space velocity of 187,000 hr^{-1}. The temperature at 50% reduction efficiency, however, is migrating toward the right to higher temperatures, which is indicative of higher light off temperature requirements as seen above in Figure 4.3 (light off temp graph).

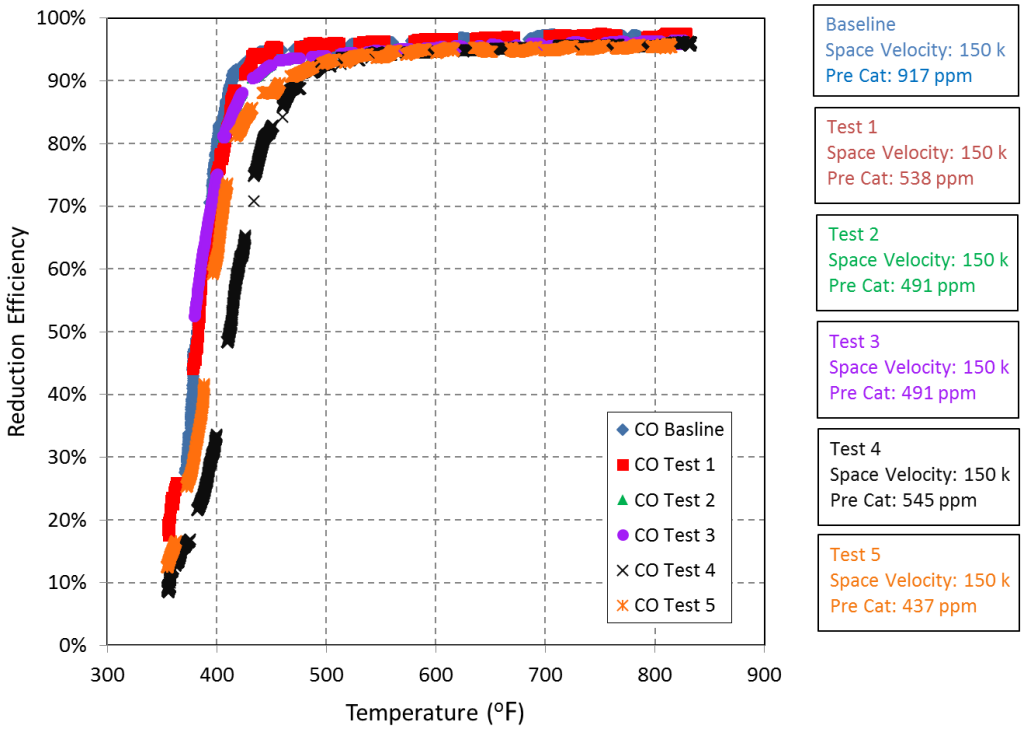

Figure 4.4: Carbon Monoxide Temperature Sweeps

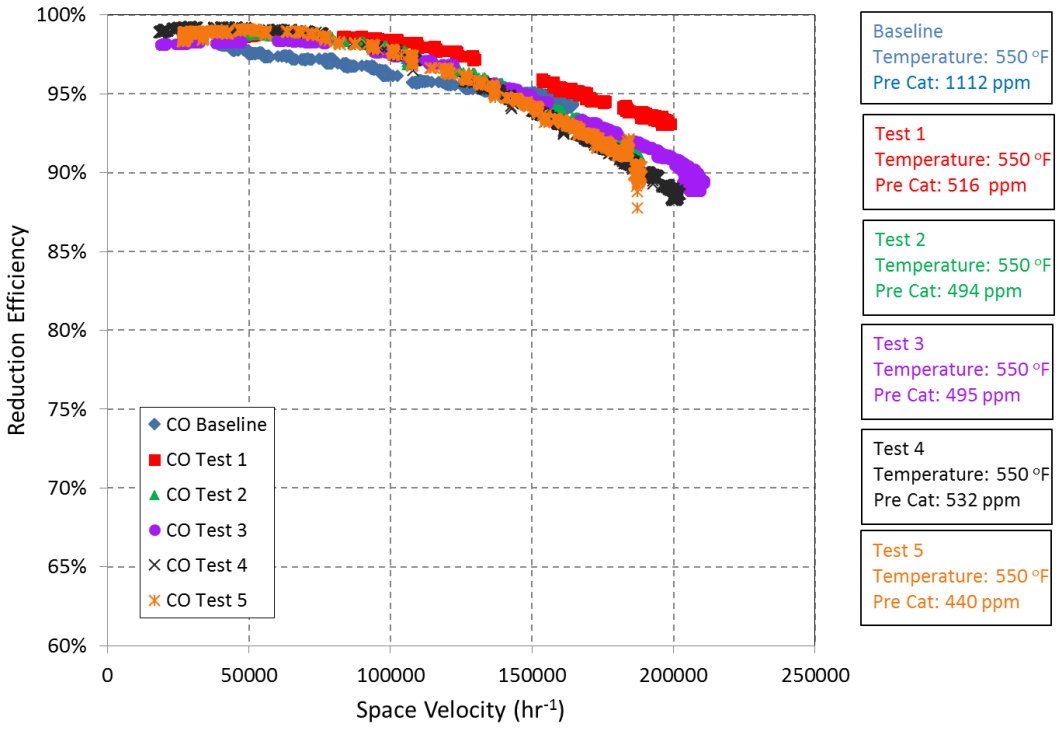

Figure 4.5: Carbon Monoxide Space Velocity Sweeps

Like the temperature sweep the reduction efficiency is fairly high for the five tests. Looking at 150,000hr^{-1} and above, there's a slight downward trend in efficiency especially when comparing tests 1, 3 and 5. As poison builds up it is harder for the emissions to oxidize via the active catalyst material, which is exacerbated at higher space velocities since there is comparatively less time for oxidation reactions to take place.

4.4 Formaldehyde Emissions Results

The reduction efficiency for all tests exceeded a maximum of 80%. Although, initially the catalyst reduced formaldehyde emissions by 90.6%. After ageing in field for a year and half, the catalyst could only reduce formaldehyde emissions by 83.4%. Again, all these tests experienced an exponential ramp up period for the reduction efficiency as temperature is increased. The Baseline Test, Test 1 and Test 2 ramp up rapidly and peak just before 90% efficiency. Tests 3, 4 and 5 still experience a sharp increase initially, but not nearly as steep as the first two tests. All test runs except for Test 4 show a shift down and to the right for reduction efficiency during the temperature sweeps, shown in Figure 4.6. As the catalyst ages the light off temperature increases. The light off trend for formaldehyde is also shown in Figure 4.3. This means that over time, light off of formaldehyde will require higher and higher temperatures and as poison levels increase the reduction efficiency trend will continue to shift down and to the right.

Space velocity tests 1, 2, 3, 4 and 5 shows steady decline of formaldehyde oxidation, shown in Figure 4.7. In all tests, except for the Baseline Test, the reduction efficiency exceeds 95% for low space velocity. As space velocity increases, though, the reduction efficiency decreases at a fairly linear rate. The minimum efficiency ranges from 83% at 197,658 hr^{-1} for Test 1 and 71.6% at 187,911 hr^{-1} for Test 5. Formaldehyde results are similar to other emissions in that reduction efficiency decreases with increasing space velocity. Note that Test 1 efficiencies are relatively higher than all other tests; the exact cause for this shift is unclear but could be due to a slightly lower pre-catalyst formaldehyde value than was seen in other test sweeps.

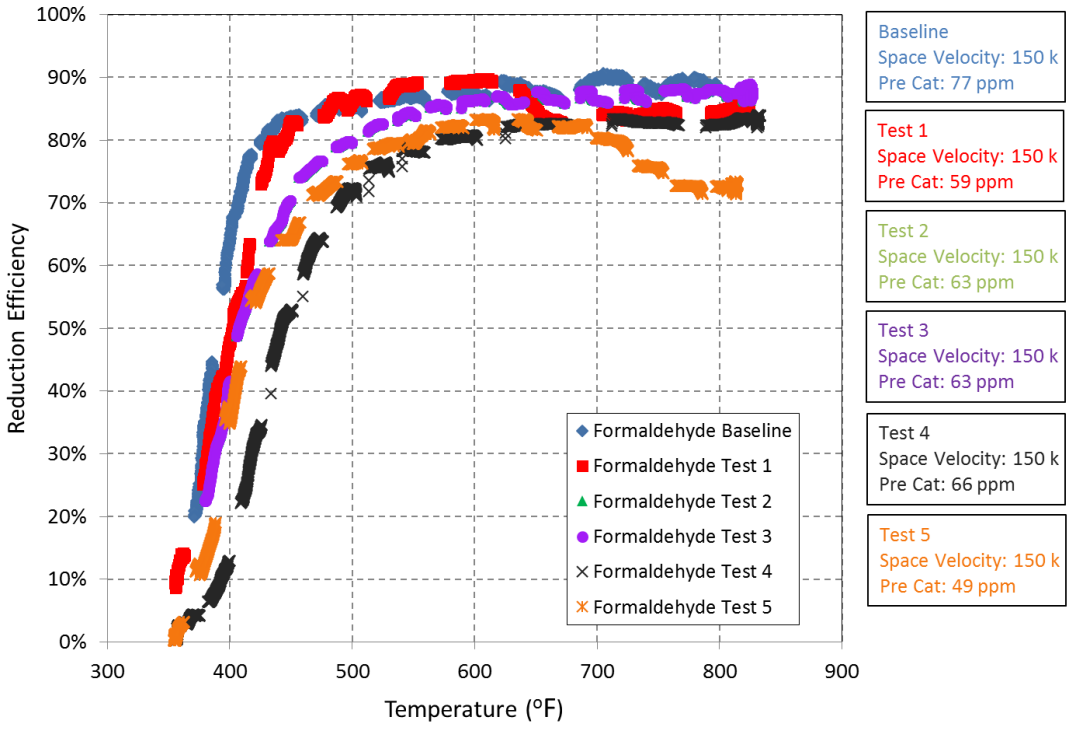

Figure 4.6: Formaldehyde Temperature Sweeps

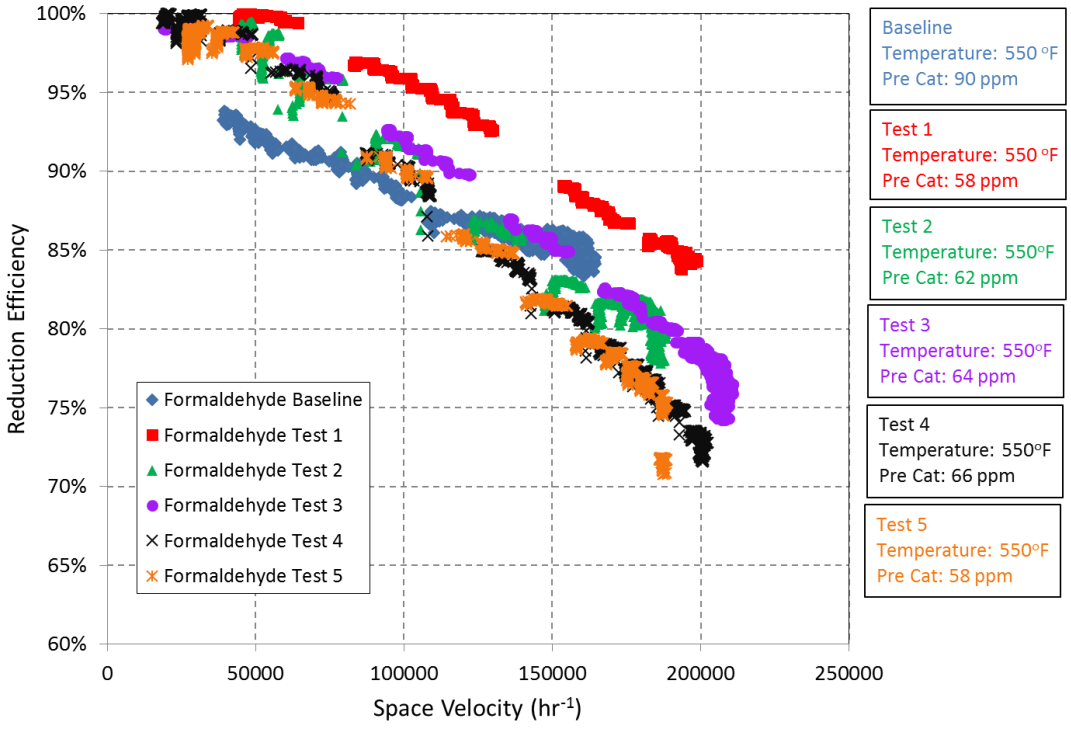

Figure 4.7: Formaldehyde Space Velocity Sweeps

4.5 Propylene Emissions Reduction

Propylene temperature sweeps show significant degradation, shown in Figure 4.8. Similar to CO tests, propylene reduction efficiency drastically increases between 350°F and 450°F, but after that the trend levels off and becomes linear. The Baseline Test achieves a maximum reduction efficiency of 100%, but after aging Test 5 only reaches a maximum efficiency of 76.6%. Between tests 3 and 4 propylene's maximum reduction efficiency significantly dropped**.** Referencing the poison build up graph (Figure 3.11), between tests 3 and 4 both phosphorous and zinc experienced a sharp increase in deposition. Poisons adhering to the wash coat, like phosphorous and zinc, contribute to lower reduction efficiencies. Additionally, there was a shift in the lab exhaust propylene content between Test 3 and 4. Note that Test 1 also had relatively high propylene content, but at this early stage of poison deposition catalyst activity did not yet appear to be negatively affected.

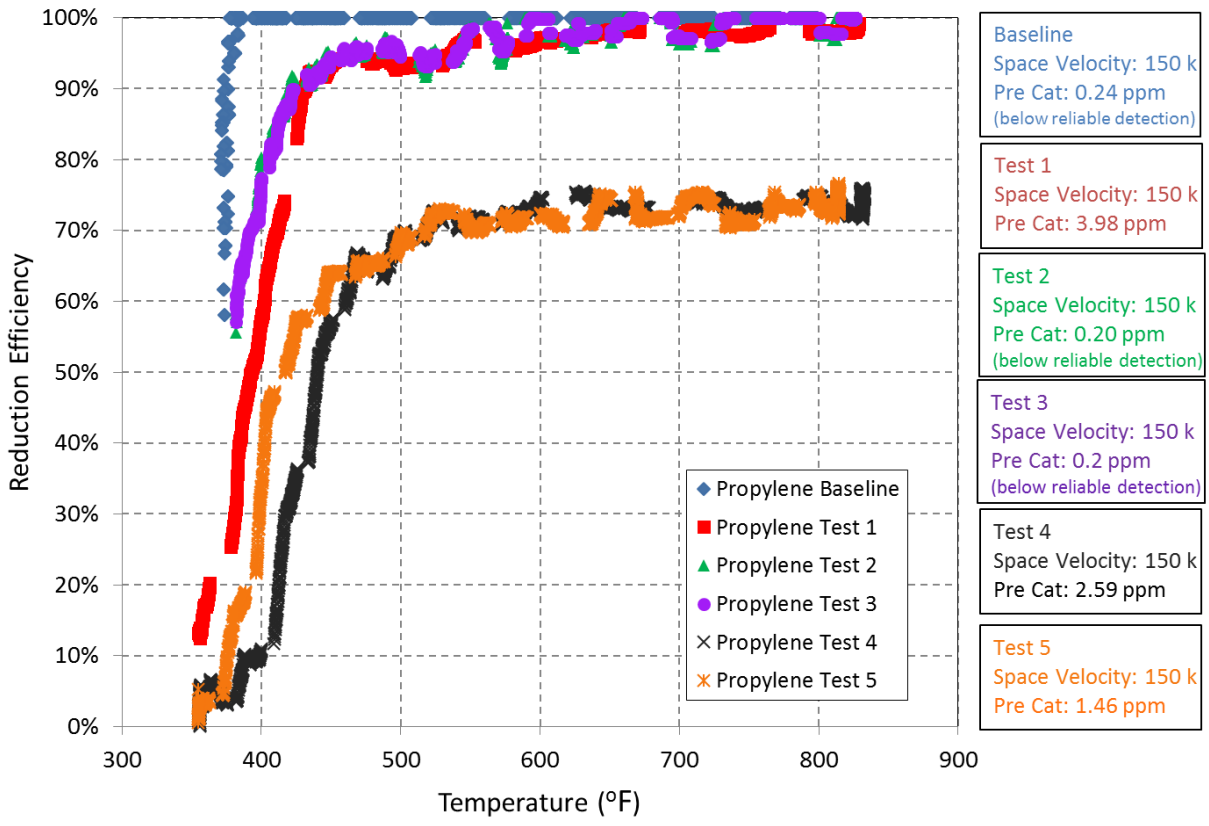

Figure 4.8: Propylene Temperature Sweeps

Like the temperature sweeps, the space velocity sweeps also show degradation of reduction efficiency as seen in Figure 4.9. Again similar to the propylene temperature sweeps, the Baseline Test reached a maximum reduction efficiency of 100%. Test 5, however, shows a drop in reduction efficiency and only reaches a maximum reduction efficiency of 76%. There is a significant dip in reduction efficiency between tests 2, 3 and 4. Interestingly there was a significant drop between the Test 3 Temperature and Space Velocity Sweeps. Note that the propylene content of the exhaust increased from 0.2 ppm during the Temperature Sweep up to 3.76 ppm for the Space Velocity Sweep. As a result of this increase the reduction efficiency dropped from a peak value of over 95% during the Temperature Sweeps to below 90% during the Space Velocity Sweeps. This is indicative of the dramatic affect that exhaust gas composition can have on the overall reduction efficiency.

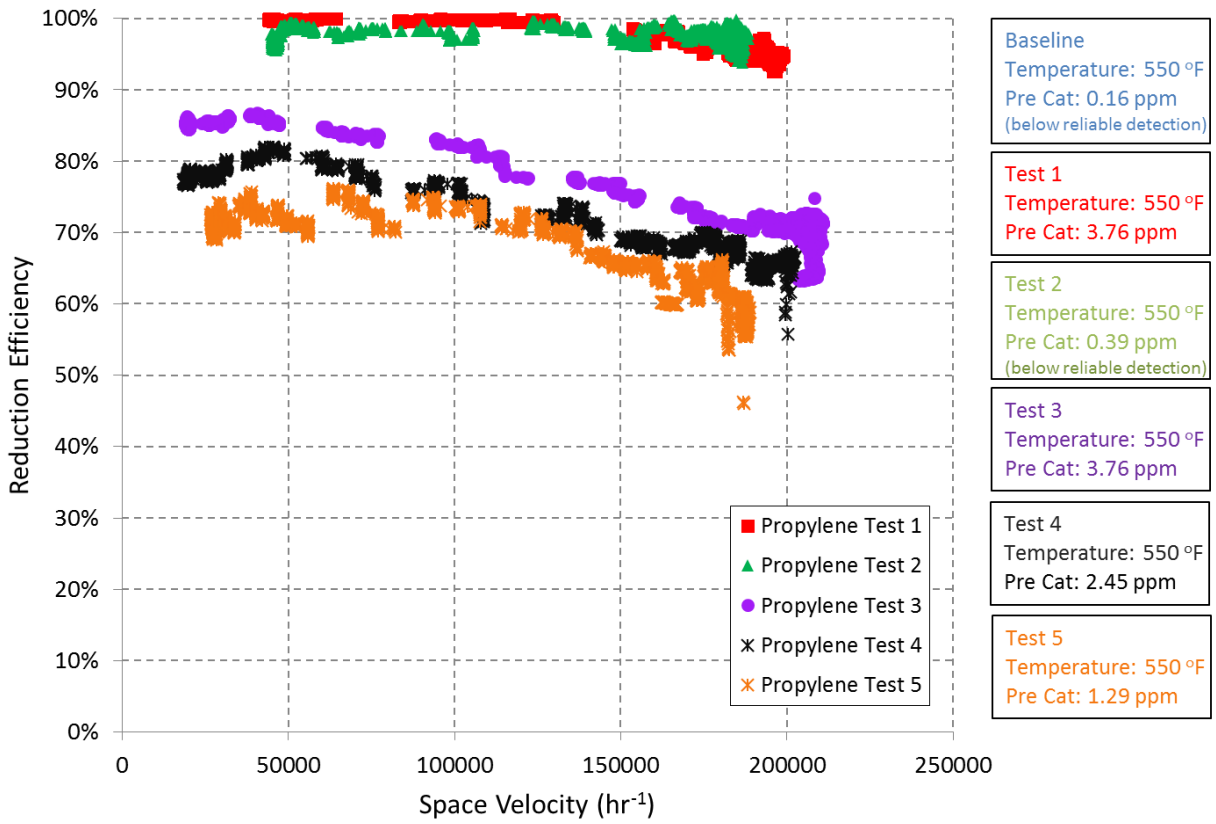

Figure 4.9: Propylene Space Velocity Sweeps

4.6 Ethylene Emissions Reduction

Similar to CO and propylene, the temperature sweep for ethylene shows high reduction efficiency and slight degradation over time, shown in Figure 4.10. As the temperature increases from 350°F to 450°F the reduction efficiency rises exponentially, but then levels off. The Baseline Test reaches a maximum of 95% reduction efficiency. Over time the maximum declines and for the last test, Test 5, the catalyst is only capable of reducing ethylene by a maximum of 91.5%. During temperature ramp up, Test 4 migrated further to the right (higher temperature) than the rest of the tests. Comparing the pre-catalyst concentration of ethylene from Test 3 and 5 to Test 4, there is considerably more ethylene concentration pre-catalyst in Test 4. Test 4 had the poorest feed quality of all the tests since it contained higher levels of olefins. Compounding elevated olefin level with poisoning could cause a decrease in reduction efficiency at lower temperatures.

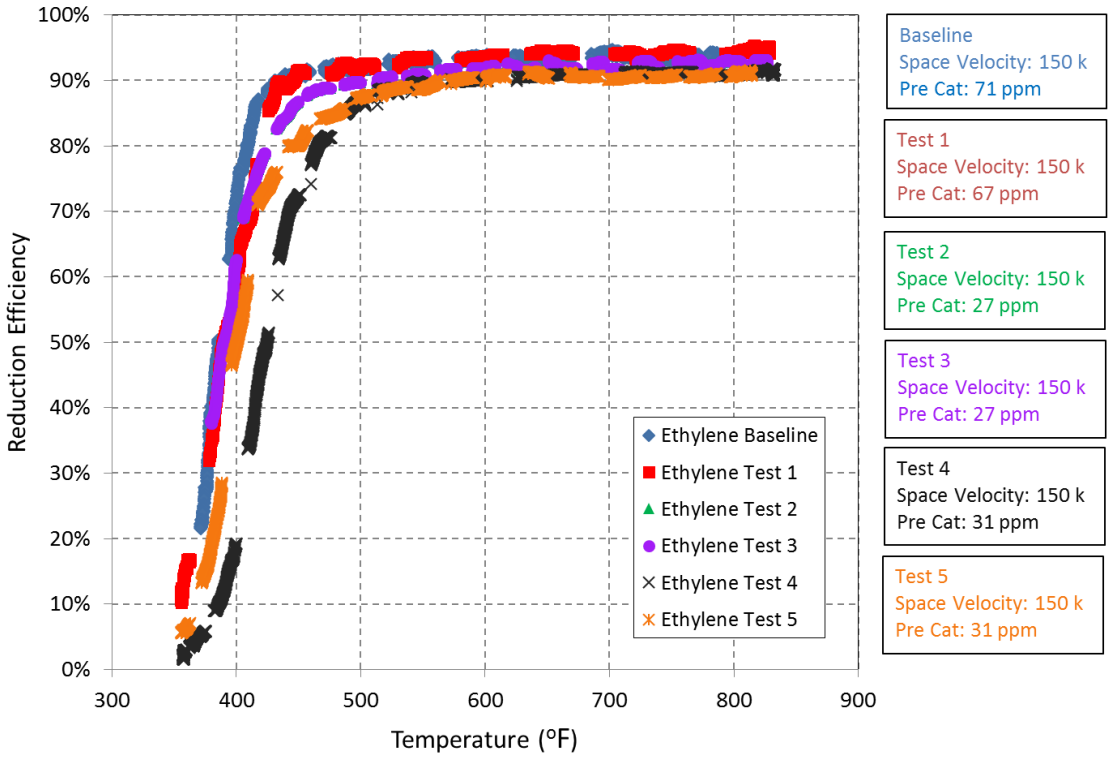

Figure 4.10: Ethylene Temperature Sweeps

Slight degradation in the catalyst's reduction efficiency of ethylene is seen via the space velocity plot in Figure 4.11. At lower space velocity, or high residence time, the reduction efficiency reaches well into the high 90% range for most tests with the initial test, the Baseline Test, 99.6% efficiency. As space velocity increases, though, the efficiency dwindles. Higher space velocity means the exhaust spends less time traveling through the catalyst. As time progresses and poisons build up on the catalyst, oxidation becomes increasingly difficult. The combination of high space velocity and poison build up hinders oxidation.

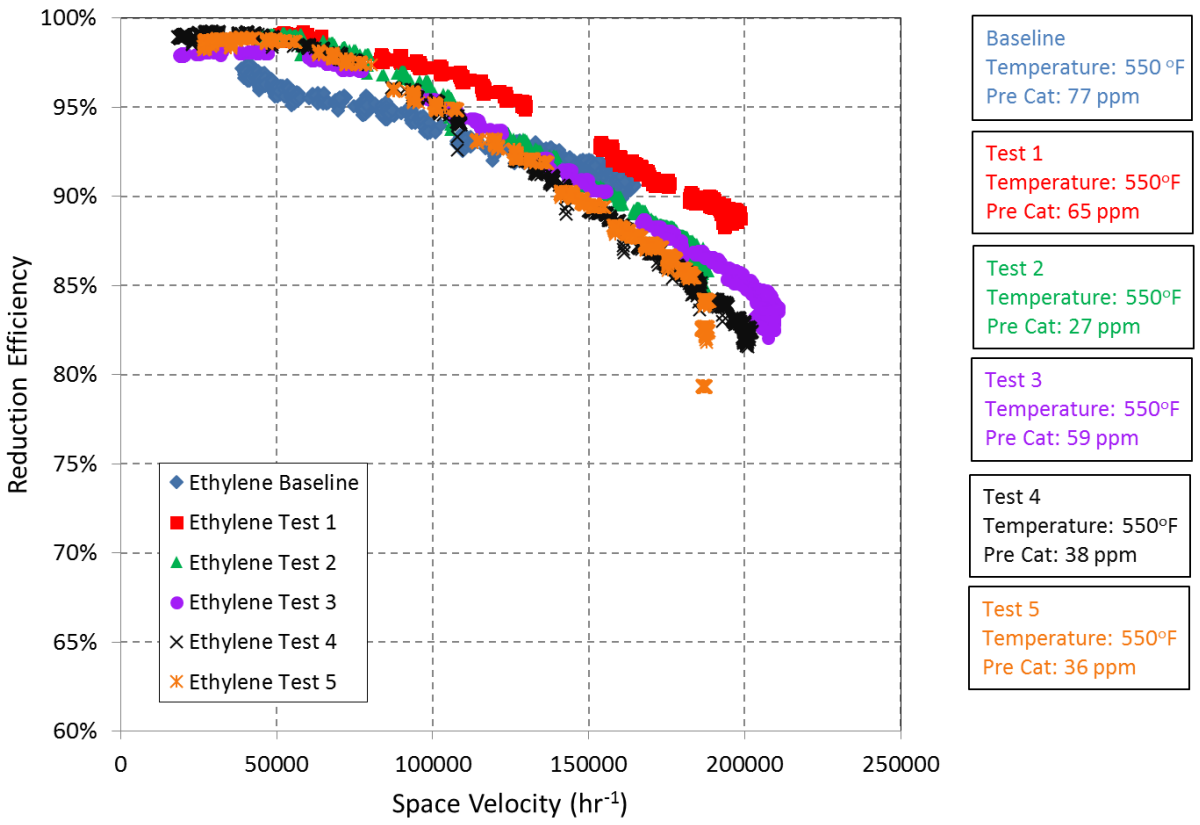

Figure 4.11: Ethylene Space Velocity Sweeps

4.7 Volatile Organic Compound Emissions Reduction

Volatile organic compound (VOCs) emissions are non-methane, non-ethane hydrocarbons, excluding formaldehyde. In this case it is the sum of propylene, propane and ethylene emissions. For the temperature sweep data, shown in Figure 4.12, none of the tests consistently exceed 80% efficiency. The efficiency rises exponentially between 350°F and 400°F and becomes linear between 400°F and 850°F. Except for Test 4, which had higher levels of olefins than other tests, the exponential rise migrates to the right and indicates an increase in light off temperature. The linear region, after 450°F, also shows a decrease in maximum efficiency. Test 1 maximum reduction efficiency is 76% whereas Test 5 maximum reduction efficiency is 73%. While this is only a decrease in 3% efficiency it certainly indicates catalyst degradation.

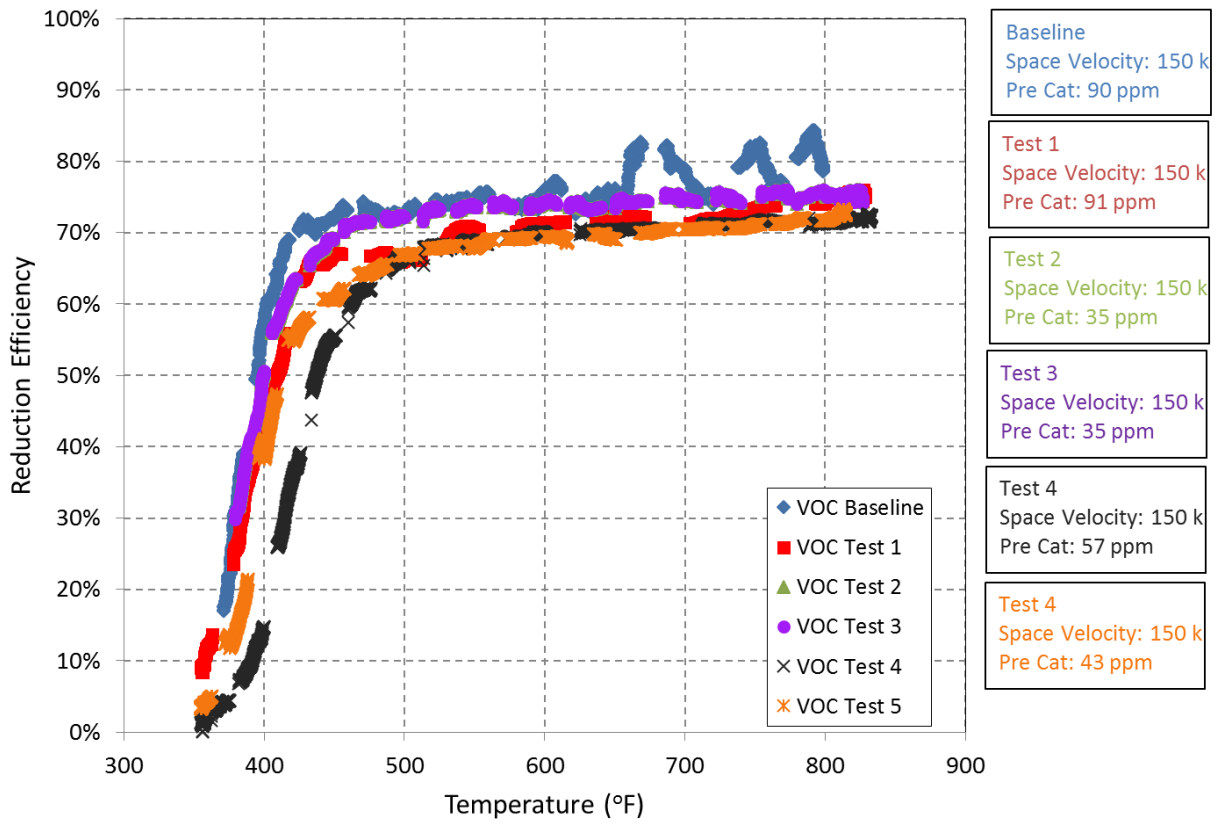

Figure 4.12: Temperature Sweep for Formaldehyde

The space velocity sweeps for VOCs, shown in Figure 4.13, do not show consistent degradation trends like the temperature sweeps. The lowest reduction efficiency for an entire test is Test 3, and Test 5 reduction efficiency resides in the middle. Test 3 only reaches a maximum reduction efficiency of 75%, but Test 5 achieves a maximum reduction efficiency of 78%. As the catalyst ages and collects poisons, the reduction efficiency should decrease over time. Since VOCs are the sum of propylene, propane and ethylene emissions, this peculiar trend can be explained by propane's observed erratic oxidation tendencies. Propane data are shown in Appendix D.

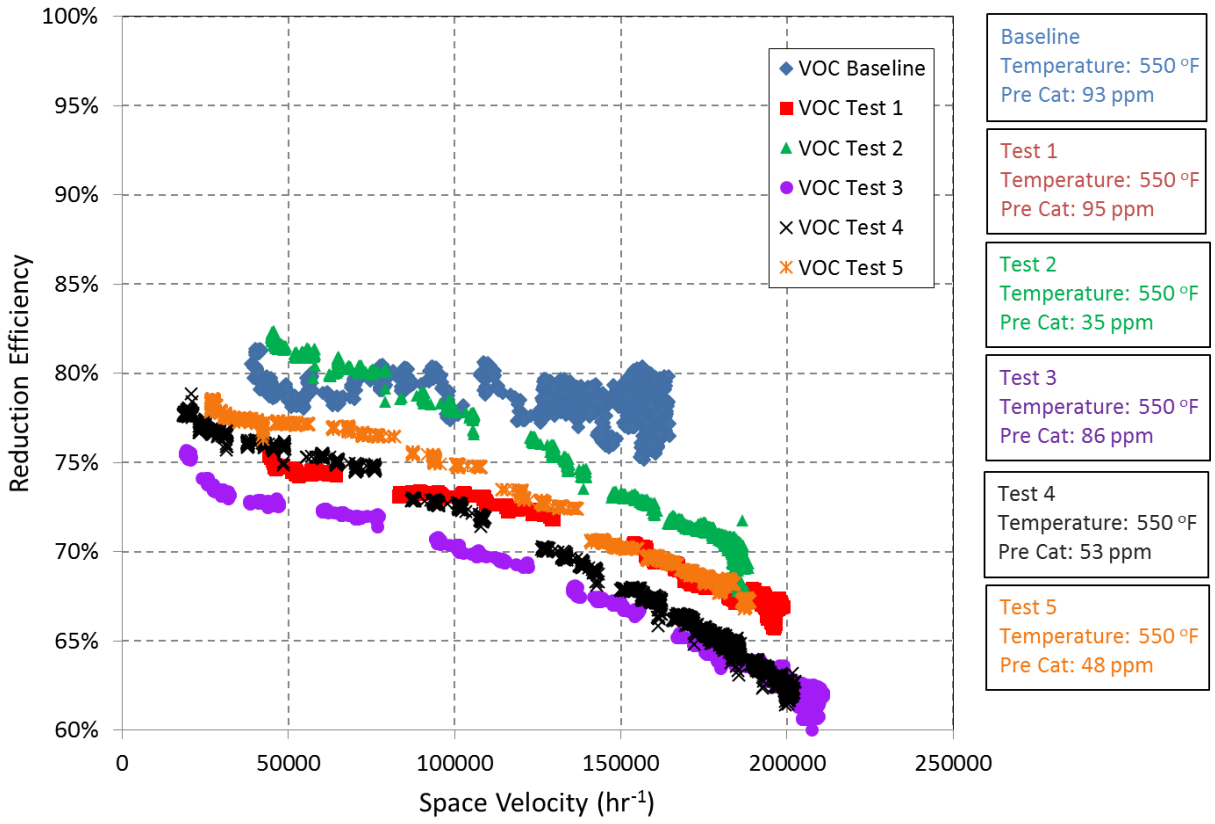

Figure 4.13: VOC Space Velocity Sweeps

4.8 Methane, Propane and Ethane Emissions Reduction

Methane is one of the harder emissions to oxidize due to its high carbon-hydrogen bond strength. As shown in both Figures 4.14 and 4.15, methane oxidation only occurred at very low percentages and remained at those levels for the duration of all the tests.

Ethane and propane performed similarly throughout all the tests. Oxidation catalysts cannot effectively oxidize methane, ethane or propane at the temperatures tested causing low and erratic reduction efficiencies. Both the temperature and the space velocity sweeps for ethane and propane may be viewed in Appendix D.

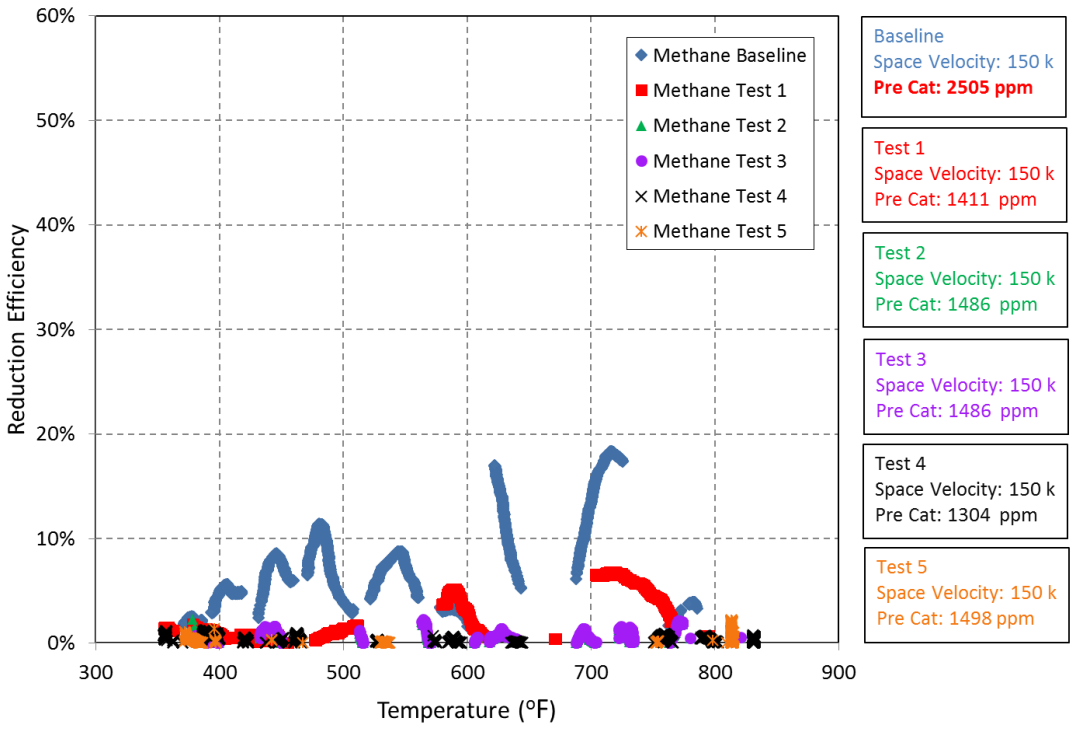

Figure 4.14: Methane Temperature Sweeps

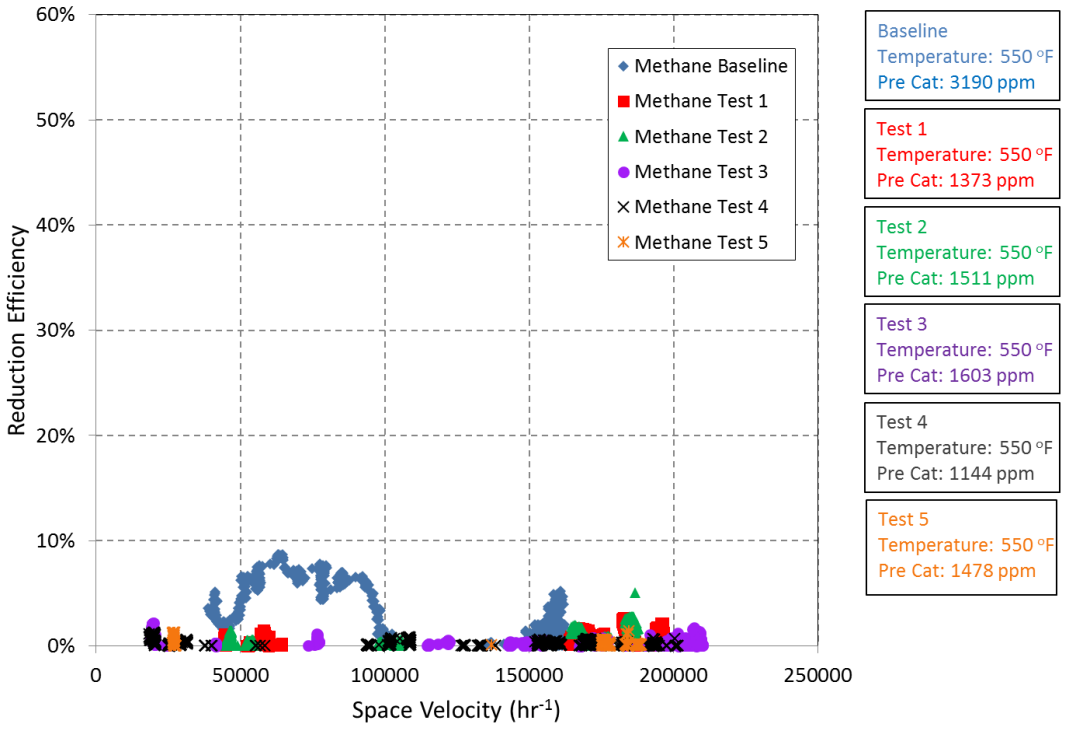

Figure 4.15: Methane Space Velocity Sweeps

4.9 Catalyst Deactivation and Reduction Efficiency Drop

Catalyst deactivation guidelines typically differ from site-to-site, but ultimately most sites reportedly adhere to some version of the EPA's ruling covering the national emission standards for hazardous air pollutants (NESHAP) [32]. The NESHAP guidelines set emissions limits for large and small bore stationary internal combustion engines. Typically engine operators run their catalysts until they fail to meet their respective NESHAP regulations. For the field engine used in this study the applicable NESHAP guideline covers two stroke, large bore stationary engines over 500hp and sets limits of a 58% reduction in CO emissions OR a maximum of 12ppmv formaldehyde in the post-catalyst exhaust stream [32]. The collected formaldehyde ppm values must be converted to dry values at 15% oxygen which is calculated via the following:

Formaldehyde ppm * ((20.9-15)/(20.9-%O2 measured)) * 100/(100-%H2O measured)

Figures 4.16 and 4.17 show the NESHAP limits for both formaldehyde and CO at both 450°F and 600°F, respectively. The NESHAP rule does not specify an operating temperature. The temperatures evaluated here cover the typical range of two-stroke lean burn engines. Measured oxidation catalyst temperatures during catalyst aging average 429 +/- 39° F. At 450°F, CO reduction efficiency is always well above the minimum 58%. Formaldehyde at the same temperature, however, crosses over the 12ppmv threshold at Test 4, but it retreats just under the requirement for Test 5. Again at 600°F, CO reduction efficiency does not cross the minimum 58%, and in fact stays above 90% for all six tests. Formaldehyde also does not exceed the NESHAP guidelines at 600°F. Test 4 shows a spike in formaldehyde ppmv, but it is not as drastic as the spike at 450°F. Even with this spike at 600°F, formaldehyde stays below the NESHAP limit of 12ppmv.

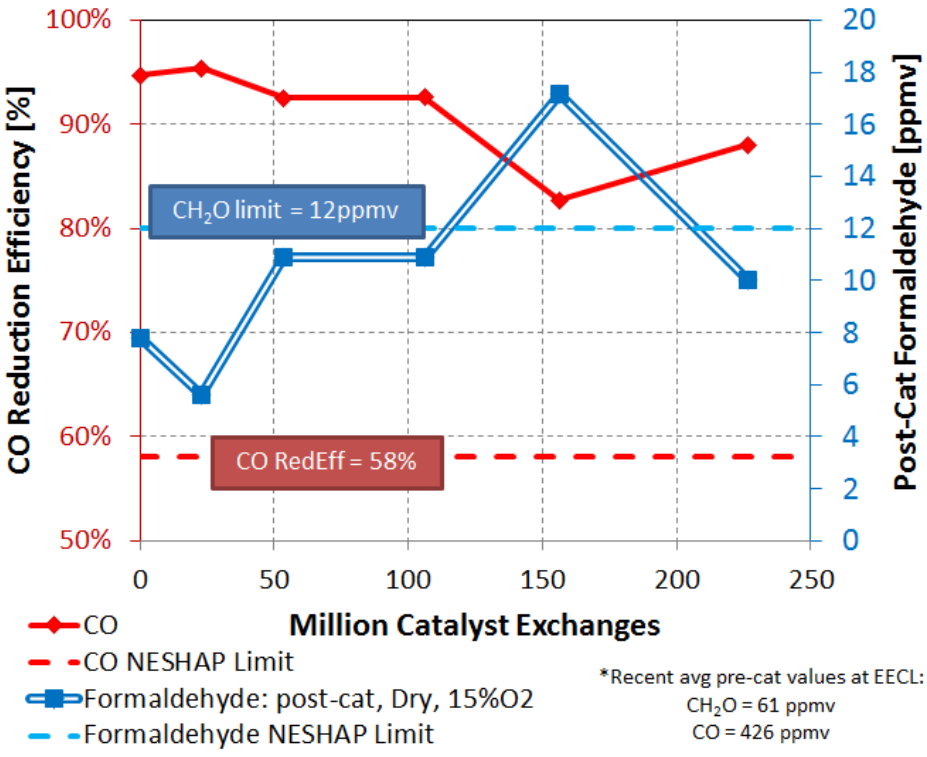

Figure 4.16: NESHAP Limits at 450°F

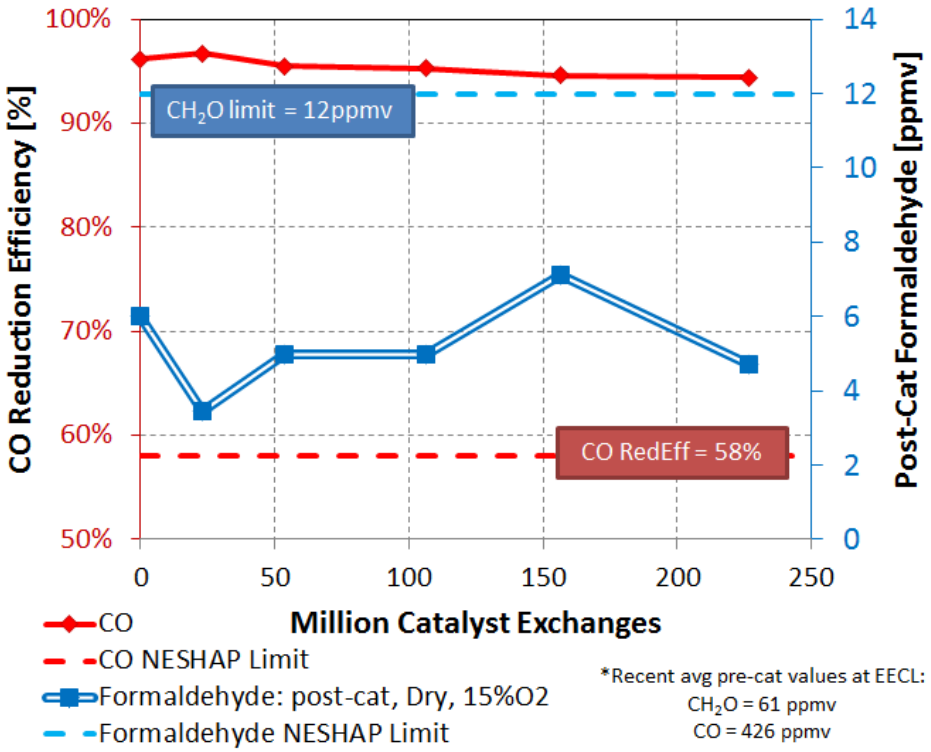

Figure 4.17: NESHAP Limits at 600°F

Reduction efficiency at both 450°F and 600°F, seen in Figures 4.18 and 4.19, respectively, declines for the Baseline Test and Tests 1-3. Test 4 shows a large dip in reduction efficiency especially at 450°F, which is due to the higher levels of olefins pre-catalyst. Test 5 reduction efficiency increases slightly since the pre-catalyst olefin levels are not as high as Test 4. Comparing reduction efficiency at 450°F and 600°F for similar species, the 600°F reduction efficiency is higher for each test. Higher temperatures more readily promote breaking of chemical bonds and oxidation reactions, which reduce post-catalyst emissions.

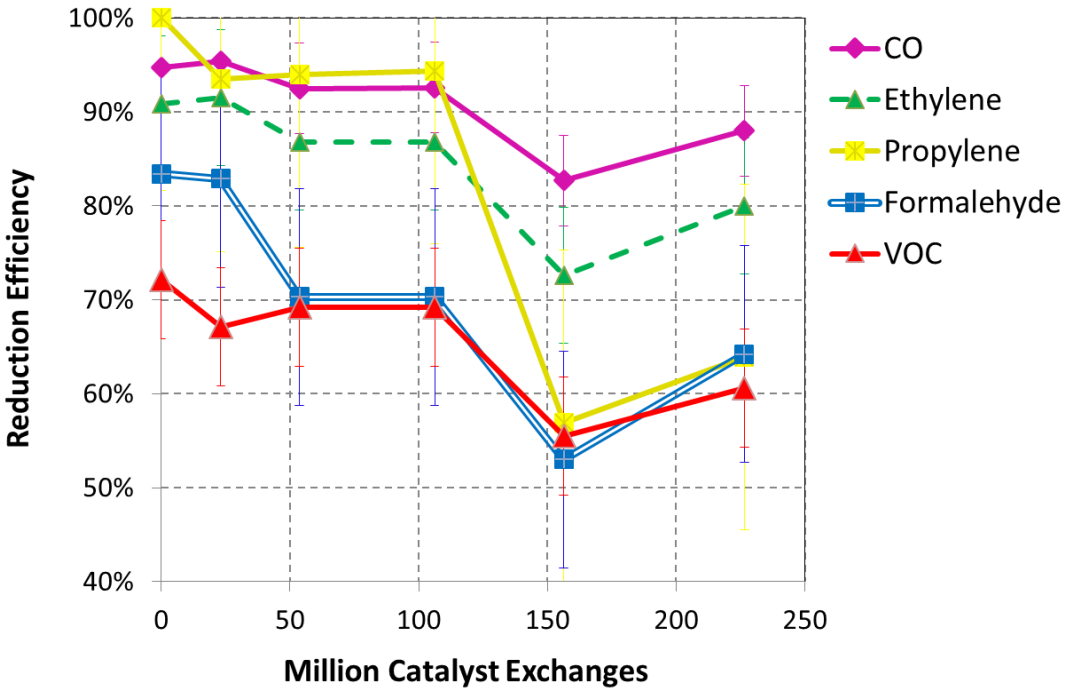

Figure 4.18: Reduction Efficiency of Specific Exhaust Contaminants at 450°F

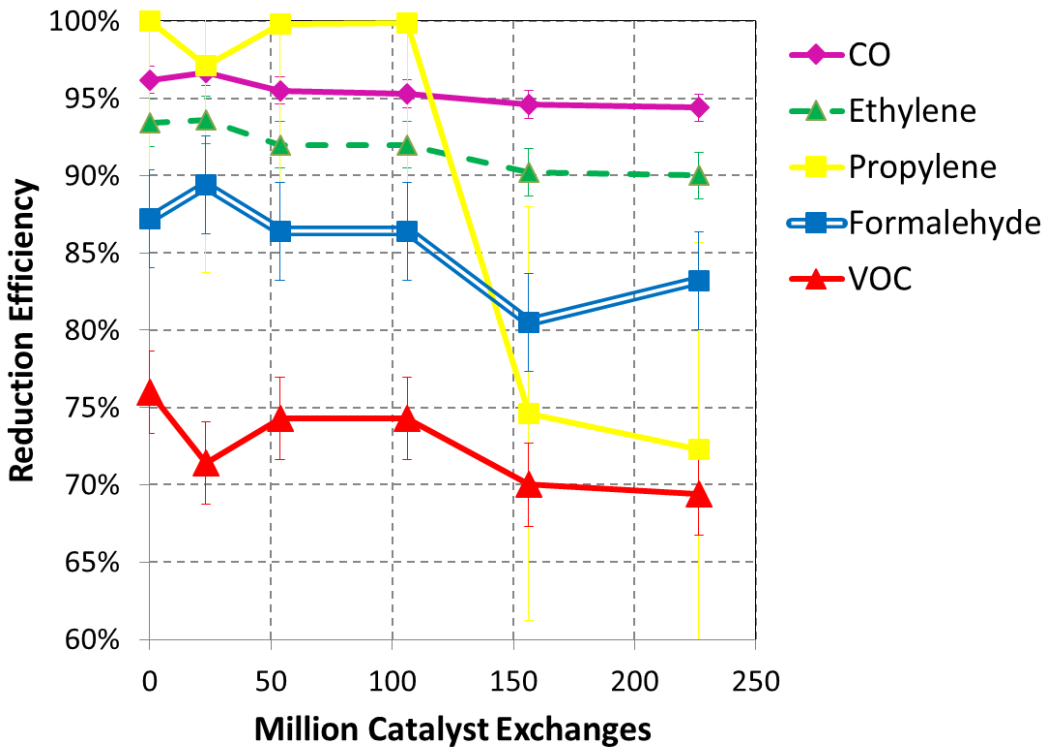

Figure 4.19: Reduction Efficiency of Specific Exhaust Contaminants at 600°F

Formaldehyde emissions at 450°F indicate that the NESHAP limit is close to being exceeded under these conditions. However, more data is needed to establish this due to the inconsistent Test 4 and 5 results. Carbon monoxide, on the other hand, clearly shows that the catalyst is not deactivated. CO experienced a 6.7% drop in reduction efficiency (η_{tot}) at 450°F in 226.5 million catalyst exchanges (millioncatexch). This relationship is illustrated with the equation below.

$$\frac{\eta_{tot}}{\text{millioncatexch}} = \frac{6.7\%}{226.5\ \text{millioncatexch}} = .03\ {}^{\%}/_{\text{millioncatexch}}$$

The reduction efficiency of CO drops .03% for every 1 million catalyst exchanges. The reduction efficiency drop per million catalyst exchanges for all species are shown in Table 4.1.

Table 4.1: Reduction Efficiency per Million Catalyst Exchange for each Species

Species	Reduction Efficiency per Million Catalyst Exchanges (%) at 450°F	Reduction Efficiency per Million Catalyst Exchanges (%) at 600°F
CO	.03	.008
Formaldehyde	.08	.02
Propylene	.16	.12
Ethylene	.02	.008
VOCs	.05	.03

NESHAP states the CO emissions must be reduced by 58%. If the catalyst continues aging at its current rate it will be deactivated in 1933 million catalyst exchanges with an exhaust temperature of 450°F and 7298 million catalyst exchanges with an exhaust temperature of 600°F. The calculation below show how many catalyst exchanges must occur to consider the catalyst deactivated at 450°F.

$$\frac{1}{\eta_{tot}/_{\text{millioncatexch}}} * 58\% = \frac{1}{.03\ {}^{\%}/_{\text{millioncatexch}}} * 58\% = 1933.3\ \text{millioncatexch}$$

5. Conclusions

5.1 Summary

Over the span of a year and a half, the oxidation catalyst was aged in the field and tested six times at the laboratory. During each laboratory test, both material analysis and emissions analysis was completed on the oxidation catalyst. The materials testing showed an increase of poisons on the catalyst surface overtime. Reduction efficiency also showed signs of degradation during emissions testing.

The field slipstream underwent several design iterations. Initially the slipstream simply housed the catalysts and measured differential pressure and temperature. The catalyst, however, was not exposed to enough exhaust flow, so a pitot tube was installed to determine more precisely how much exhaust was flowing through the slipstream. As predicted, more exhaust needed to be pulled extracted from the main engine exhaust stream. In order to achieve this a blower was installed on top of the slipstream. This apparatus increased exhaust flow by 1.7x.

The catalyst experienced 226.5 million catalyst exchanges causing both poison buildup and degradation in emissions reduction efficiency. Sulfur, phosphorous and zinc poisoned the catalyst most significantly. Initially, sulfur poisoned the catalyst rapidly, but then the sulfur deposition rate leveled off. Phosphorous and zinc, however, exhibited continuously increasing poison deposition trends. Poison build up effected the catalyst's ability to reduce emissions. The reduction efficiency for all emissions species was impacted. Propylene, however, experienced the highest level of reduction efficiency degradation.

5.2 Conclusions

After analyzing the laboratory acquired data, emissions data and materials data, the following conclusions can be drawn:

- Poison buildup on the catalyst increases light off temperature of emission species.
    - Sulfur poisoning increased rapidly and then leveled off around 3 atomic%.

- Phosphorus and zinc continuously increased at the same rate, but the magnitude of phosphorous poisoning is always higher.
- Estimating the total poison buildup can be done via the following:
  - $y = 0.048x + 1.16$
  - where x is the number of million catalyst exchanges and y is the poison atomic percent.
  - This means that for every 1 million catalyst exchanges the total poison atomic percent will increase by 0.05.
- On average the light off temperature increased at a rate of 0.13 °F/million catalyst exchanges.
  - For every 1 million catalyst exchanges the light off temperature will increase by 0.13°F and an additional 0.05 atomic percent of poison will be added to the catalyst.

- Poison buildup on the catalyst decreases reduction efficiency of emission species.
  - Catalyst poisoning increased by 12.0 atomic percent over 226.5 million catalyst exchanges.
  - As the poison builds up reduction efficiency degrades
    - Carbon Monoxide maximum reduction efficiency decreased by 2.0% from 97% to 95% over a year and a half of aging as shown during the temperature sweep testing. At 450°F, carbon monoxide reduction efficiency reduces by 6.7% and at 600°F reduction efficiency decreases by 1.8%.
    - Formaldehyde maximum reduction efficiency decreased by 7.2% from 91% to 83% during the six temperature sweep tests. Reduction efficiency also dropped by 19% at 450°F and 4% at 600°F over the six temperature sweep tests.

- Propylene maximum reduction efficiency decreased by 23% from 100% to 76% over the six temperature sweep tests. At 450°F propylene reduction efficiency decreases by 36% and by 28% at 600°F during the six temperature sweep tests.
- Ethylene maximum reduction efficiency decreased by 3.5% from 95% to 92% from the Baseline Test to Test 5 of the temperature sweeps. Reduction efficiency dropped 11% at 450°F and 3.4% at 600°F during the six temperature sweep tests.
- VOCs maximum reduction efficiency decreased by 11% from 84% to 73% from the Baseline Test to Test 5 during the temperature sweep tests. VOC reduction efficiency decreased by 12% at 450°F and 6.6% at 600°F during the six temperature sweep tests.

o Each emissions species was affected by catalyst poisoning; however, they were not all effected at the same rate.

- Carbon Monoxide, for example, reduction efficiency decreased at a rate of 0.03% per million catalyst exchanges at 450°F and 0.008% per million catalyst exchanges at 600°F. Which also relates to a decrease in reduction efficiency of 0.652% for every 1 atomic percent buildup of poison at 450°F and 0.16% for every 1 atomic percent buildup of poison at 600°F.
- For every million catalyst exchanges, formaldehyde's reduction efficiency decreased by 0.08% at 450°F and 0.02% at 600°F. Formaldehyde reduction efficiency also decreases by 1.6% for every 1 atomic percent of poison accumulation at 450°F. At 600°F formaldehyde reduction efficiency decreased by 0.42% for every 1 atomic percent of poison buildup.
- Propylene reduction efficiency decreased at a rate of 0.16% per million catalyst exchanges at 450°F or a decrease in reduction efficiency of 3.3% for every 1 atomic percent buildup of poison at 450°F. At 600°F, propylene reduction

efficiency dropped at a rate of 0.12% per million catalyst exchanges or a decrease in reduction efficiency of 2.5% per every 1 atomic percent buildup of poison.

- Ethylene reduction efficiency decreased at a rate of 0.02% per million catalyst exchanges at 450°F or reduction efficiency decrease of 0.16% for every 1 atomic percent of poison buildup. Ethylene reduction efficiency decreased at a rate of 0.008% per million catalyst exchanges at 450°F or reduction efficiency decrease of 0.42% for every 1 atomic percent of poison buildup.
- VOC reduction efficiency decreased by 0.05% per million catalyst exchanges at 450°F or by 1.04% per every 1 atomic percent buildup of poison. At 600°F, VOC reduction efficiency dropped at a rate of 0.03% per million catalyst exchanges or a decrease in reduction efficiency of .625% per every 1 atomic percent buildup of poison.

5.3 Future Works

Unfortunately, this project did not see complete deactivation of the oxidation catalyst. For future works, it is recommended to age the oxidation catalyst until it completely deactivates while continuing to monitor the poison buildup and the emissions reduction. This could potentially be accomplished through higher catalyst space velocities than were seen herein for the duration of a given test. After a catalyst has deactivated, it can be potentially regenerated ("washed") and used again, though regeneration depends on the type and level of poison deposition. Also, testing different regeneration techniques, such as chemical or burn off regeneration, and how it effects the catalyst's ability to reduce emissions, would be an interesting future project. The exact quantity of lube oil carry over could not be measured for this project. Being able to determine the amount of lube oil traveling to and fouling the catalyst would be helpful in determining a deactivation timeline for a given catalyst size and engine size. Installing a device to measure the lube oil carry over would help determine this in the future.

6. References

1- EPA United States Environmental Protection Agency, http://www.epa.gov/otaq/standards/nonroad/

2- Koushik Badrinarayanan, "Performance evaluation of multiple oxidation catalysts on a lean burn natural gas engine", Master's Thesis. Colorado State University

3- Heywood, J. B., & Sher, E. "The Two-Stroke Cycle Engine." Philadelphia: Taylor & Francis. (1999) 317-324.

4- Calvin H Bartholomew, "Mechanisms of catalyst deactivation", Applied Catalysis A: General 212 (2001) 17-60.

5- J.A. Moulijin et. al., "Catalyst deactivation: is it predictable? What to do?" Applied Catalysis A: General 212 (2001) 3-16

6- Brittany Smith, "Summary of RICE NESHAP Rule," Ohio EPA. (2010) 1-18.

7- Jonas Andersson et. al., "Deactivation of diesel oxidation catalysts: vehicle- and synthetic aging correlation", Applied Catalysis B: Environmental 72 (2007) 71-81.

8- C.I. Arapatsakos and P.D. Sparis, "Catalyst regeneration via chemical treatment and emission tests at idle speeds," Journal of Automobile Engineering. 213 (1999) 359-364.

9- Alexander Winkler et. al., "The influence of chemical and thermal aging on the catalytic activity of a monolithic diesel oxidation catalyst" Applied Catalysis B: Environmental 93 (2009) 177-184.

10- Deborah L. Mowery et. al., "Deactivation of PdO–Al2O3 oxidation catalyst in lean-burn natural gas engine exhaust: aged catalyst characterization and studies of poisoning by H2O and SO2", Applied Catalysis B: Environmental 21 (1999) 157–169.

11- J.A.Z. Pieterse et. al., “Selective catalytic reduction of NOx in real exhaust gas of gas engines using unburned gas: Catalyst deactivation and advances toward long-term stability”, Chemical Engineering Journal 120 (2006) 17-23.

12- Jordan K. Lampert et. al., “Palladium catalyst performance for methane emissions abatement from lean burn natural gas vehicles”, Applied Catalysis B: Environmental 14 (1997) 211-223.

13- Dairene Uy et. al., “Raman Studies of Automotive Catalyst Deactivation”, SAE Technical papers 2006 SAE World Congresses.

14- Alexander Winkler et. al., “Influence of aging effects on the conversion efficiency of automotive exhaust gas catalysts”, Catalysis Today 155 (2010) 140-146.

15- Randall M German, “Sintering Theory and Practice”, New York: Wiley, 1996.

16- Sang-Hoon Song et. al., “Enhancing effects on the catalytic performance during the preparation of nickel supported lanthanum-alumina catalyst for the catalytic carbon dioxide dry reforming of methane”, Reaction kinetics, mechanisms and catalysis 108 (2013) 161-171.

17- Robert L. McCormick et. al., “Rapid Deactivation of Lean burn Natural Gas Engine Exhaust Oxidation Catalyst”, Sensors and Actuators, 1996, Vol. 1206, 63-77.

18- R.G. Silver et. al., “Design and Performance Evaluation of Automotive Emission Control Catalyts”, Catalysis and Automotive Pollution Control II, (1991) 167-180.

19- Xianglan Xu et. al., “Effects of La, Ce and Y oxides on SnO_2 catalysts for CO and CH_4 Oxidation,” ChemCatChem. 5 (2013) 2025-2036.

20- Piotr Kaminski et. al., “FTIR spectroscopic study of CO oxidation on bimetallic catalysts,” Catalyst Today. 243 (2015) 218-227.

21- Erik M. Holmgreen et. al, “Dual-catalyst aftertreatment of lean-burn natural gas engine exhaust”, Applied Catalysis B: Environmental 74 (2007) 73-82

22- Daniel B. Olsen et. al., “Impact of Oxidation Catalysts on Exhaust NO_2/NO_x Ratio from Lean-Burn Natural Gas Engines”, Journal of the Air and Waste Management Association 60 (2010) 867-874.

23- Hikeaki Muraki et. al., “Palladium-lanthanum catalysts for automotive emission control”, Industrial and Engineering Chemistry Research, 25 (1986) 202-208.

24- John Goodge. “Energy-Dispersive X-Ray Spectroscopy (EDS)”, University of Minnesota-Duluth, http://serc.carleton.edu/research_education/geochemsheets/eds.html

25- Susan Swapp. “Scanning Electron Microscopy”, University of Wyoming, http://serc.carleton.edu/research_education/geochemsheets/techniques/SEM.html

26- Mark Engelhard. “X-Ray Photoelectron Spectroscopy XPS”, ESML, http://www.emsl.pnl.gov/emslweb/sites/default/files/engelhard_xps.pdf

27- http://cif.colostate.edu/

28- Daniel Olsen, et. al., “Development and Testing of a Timed Power Cylinder Lube Oil Injection System,” 2014 Gas Machinery Conference. (2014) 1-11.

29- “Method 1- Sample and Velocity Traverses for Stationary Systems,” http://www.epa.gov/ttnemc01/promgate/m-01.pdf

30- Kochuparampil, Roshan Joseph. Performance Evaluation of an Advanced Air-fuel Ratio Controller On a Stationary, Rich-burn Natural Gas Engine. MS thesis Colorado State U, 2013. Colorado State University Digital Repository. <http://hdl.handle.net/10217/80256>

31- Eaton, S., Bunting, B., Toops, T., and Nguyen, K., "The Roles of Phosphorus and Soot on the Deactivation of Diesel Oxidation Catalysts," SAE Technical Paper 2009-01-0628, 2009.

32- Peak- Petroleum Testing Services, http://www.peakpetrotesting.com/

33- Empire Cat, “S.O.S Fluids Lab and Condition Monitoring” http://www.empire-cat.com/fluidslab/

Appendix A: Engine Specifications

Engine Performance Data Cummins Inc Columbus, Indiana 47202-3005 http://www.cummins.com	Power Generation **QSK19G** **FR 4562**	450 hp (336 kWm) @ 1500 rpm 1576 lb-ft (2137 N-m) @ 1500 rpm		
		Configuration **D483002GX03**	CPL Code **2112**	Revision **27-May-11**

Compression Ratio:	**11.0:1**	Displacement:	**1150 in³ (18.8 L)**
Fuel System:	**Natural Gas**	Cylinders:	**6**
Combustion:	**Lean Burn**	Bore x Stroke:	**6.25 x 6.25 in (159 x 159 mm)**
Emission Certification:	**500 mg/nm3 NOx (1 TALuft) Capable**	Aspiration:	**Turbocharged and Aftercooled**

Engine Rating:

Engine Speed	Continuous Power	
rpm	hp	kWm
1,500	450	336

Engine Fuel Consumption @ 1500 rpm

Output Power			Fuel Consumption	
%	hp	kWm	BTU/hp-hr	MJ/kWm-hr
Continuous Power				
100	450	336	7232	10.2
75	338	252	7548	10.7
50	225	168	7979	11.3
25	113	84	N/A	N/A

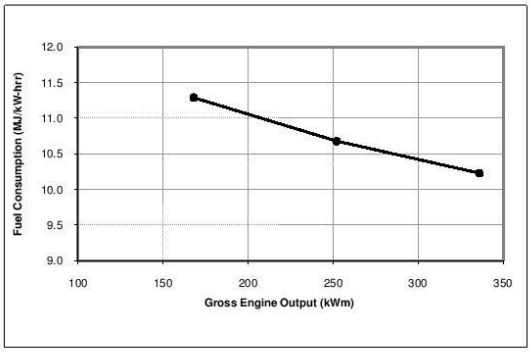

These guidelines have been formulated to ensure proper application of generator drive engines in A.C. generator set installations.

~~STANDBY POWER RATING: Applicable for supplying emergency power for the duration of the utility power outage. No overload capability is available for this rating. Under no condition is an engine allowed to operate in parallel with the public utility at the Standby Power rating. This rating should be applied where reliable utility power is available. A Standby rated engine should be used for a maximum of an 80% average load factor and 200 hours of operation per year. This includes less than 25 hours per year at the Standby Power rating. Standby ratings should never be applied except in true emergency power outages. Negotiated power outages contracted with a utility company are not considered an emergency.~~

~~PRIME POWER RATING: Applicable for supplying electric power in lieu of commercially purchased power. Prime Power applications must be in the form of one of the following two categories:~~

~~UNLIMITED TIME RUNNING PRIME POWER: Prime Power is available for an unlimited number of hours per year in a variable load application. Variable load should not exceed a 70% average of the Prime Power rating during any operating period of 250 hours. The total operating time at 100% Prime Power shall not exceed 500 hours per year. A 10% overload capability is available for a period of 1 hour within a 12 hour period of operation. Total operating time at the 10% overload power shall not exceed 25 hours per year.~~

~~LIMITED TIME RUNNING PRIME POWER: Limited Time Prime Power is available for a limited number of hours in a non-variable load application. It is intended for use in situations where power outages are contracted or in other utility power curtailment. Engines may be operated in parallel to the public utility up to 750 hours per year at power levels never to exceed the Prime Power rating. The customer should be aware, however, that the life of any engine will be reduced by this constant high load operation. Any operation exceeding 750 hours per year at the Prime Power rating should use the Continuous Power rating.~~

CONTINUOUS POWER RATING: Applicable for supplying utility power at a constant 100% load for an unlimited number of hours per year. No overload capability is available for this rating.

Reference AEB 10.47 for determining Electrical Output.

Data shown above represents gross engine performance capabilities obtained and corrected in accordance with reference conditions of 99.51 kPa (29.39 in Hg) barometric pressure, 152 m (500 ft) altitude, 25 °C (77 °F) air inlet temperature, and relative humidity of 50% using dry processed gas natural gas fuel with 48 Mega Joules per Kilogram lower heating value. Derates shown are based on 15 in H_2O air intake restriction and 2 in Hg exhaust back pressure.

Power output curves are based on the engine operating with fuel system, water pump and lubricating oil pump; not included are battery charging alternator, fan, optional equipment and driven components.

Data Status:Final-(Measured data)

Data Tolerance: +/- 5%

CHIEF ENGINEER: Alfred S Weber

Figure A.1: Cummins QSK19G Engine Specifications at 1500rpm

Engine Performance Data Cummins Inc Columbus, Indiana 47202-3005 http://www.cummins.com	Power Generation **QSK19G** **FR 4560**	471 hp (351 kWm) @ 1800 rpm 1374 lb-ft (1863 N-m) @ 1800 rpm		
		Configuration **D483002GX03**	CPL Code **2113**	Revision **27-May-11**

Compression Ratio:	**11.0:1**	Displacement:	**1150 in³ (18.8 L)**
Fuel System:	**Natural Gas**	Cylinders:	**6**
Combustion:	**Lean Burn**	Bore x Stroke:	**6.25 x 6.25 in (159 x 159 mm)**
Emission Certification:	**1 g/hp-hr NOx EPA NSPS Compliant Capable**	Aspiration:	**Turbocharged and Aftercooled**

Engine Rating:

Engine Speed	Continuous Power	
rpm	hp	kWm
1,800	471	351

Engine Fuel Consumption @ 1800 rpm

Output Power			Fuel Consumption	
%	hp	kWm	BTU/hp-hr	MJ/kWm-hr
Continuous Power				
100	471	351	7720	10.9
75	353	263	7998	11.3
50	236	176	8683	12.3
25	118	88	N/A	N/A

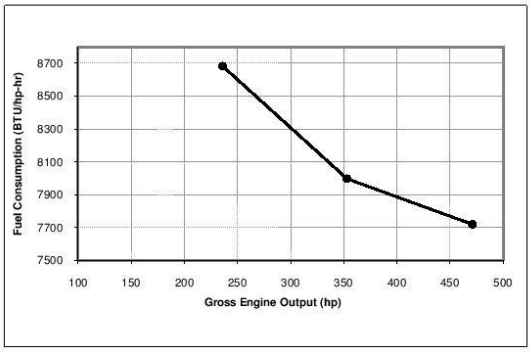

These guidelines have been formulated to ensure proper application of generator drive engines in A.C. generator set installations.

~~STANDBY POWER RATING: Applicable for supplying emergency power for the duration of the utility power outage. No overload capability is available for this rating. Under no condition is an engine allowed to operate in parallel with the public utility as the Standby Power rating. This rating should be applied where reliable utility power is available. A Standby rated engine should be sized for a maximum of an 80% average load factor and 200 hours of operation per year. This includes less than 25 hours per year at the Standby Power rating. Standby ratings should never be applied except in true emergency power outages. Negotiated power outages contracted with a utility company are not considered an emergency.~~

~~PRIME POWER RATING: Applicable for supplying electric power in lieu of commercially purchased power. Prime Power applications must be in the form of one of the following two categories:~~

~~UNLIMITED TIME RUNNING PRIME POWER: Prime Power is available for an unlimited number of hours per year in a variable load application. Variable load should not exceed a 70% average of the Prime Power rating during any operating period of 250 hours. The total operating time at 100% Prime Power shall not exceed 500 hours per year. A 10% overload capability is available for a period of 1 hour within a 12 hour period of operation. Total operating time at the 10% overload power shall not exceed 25 hours per year.~~

~~LIMITED TIME RUNNING PRIME POWER: Limited Time Prime Power is available for a limited number of hours in a non-variable load application. It is intended for use in situations where power outages are scheduled, such as in utility power curtailment. Engines may be operated in parallel with a public utility up to 750 hours per year at power levels never to exceed the Prime Power rating. The customer should be aware, however, that the life of any engine will be reduced by this constant high load operation. Any operation exceeding 750 hours per year at the Prime Power rating should use the Continuous Power rating.~~

CONTINUOUS POWER RATING: Applicable for supplying utility power at a constant 100% load for an unlimited number of hours per year. No overload capability is available for this rating.

Reference AEB 10.47 for determining Electrical Output.

Data shown above represents gross engine performance capabilities obtained and corrected in accordance with reference conditions of 99.51 kPa (29.39 in-Hg) barometric pressure, 152 m (500 ft) altitude, 25 °C (77 °F) air inlet temperature, and relative humidity of 50% using dry processed gas natural gas fuel with 48 Mega Joules per Kilogram lower heating value. Derates shown are based on 15 in-H_2O air intake restriction and 2 in-Hg exhaust back pressure.

Power output curves are based on the engine operating with fuel system, water pump and lubricating oil pump; not included are battery charging alternator, fan, optional equipment and driven components.

Data Status:Preliminary, Pending Final Review

Data Tolerance: +/- 5%

CHIEF ENGINEER: Alfred S Weber

Figure A.2: Cummins QSK19G Engine Specifications at 1800 rpm

Table A.1: Example Cummins QSK19G Average Engine Parameters

	Baseline Test	Test 1
Engine Speed (RPM)	1800	1800
Power[hp]	354	354
Torque[ft-lb]	1033	1033
Fuel Flow[#ph]	156.8	140
Fuel Pressure[psig]	5.6	5.5
Fuel Temp[F]	90.2	83.9
Inlet Air Pres[inHg]	5	5
IMAP[psia]	32.5	29.2
Boost Pressure[psig]	31.1	30.1
Inlet Air Temperature[F]	92.8	84.1
Intake Manifold Temp[F]	126.2	135.4
Boost Temp[F]	342.9	319.9
Inlet Air RH[%]	22.8	35.13
Exhaust Back Pres[inHg]	5	5
EMAP[psia]	41.2	37.16
Exhaust Temp[F]	1013.6	1000
Turbine In Temp[F]	1246.6	1214.8
Exh Port 1[F]	1132.31	1129.2
Exh Port 2[F]	1125.5	1113.7
Exh Port 3[F]	1138.9	1120.2
Exh Port 4[F]	1147.8	1130.5
Exh Port 5[F]	1144.2	1146.1
Exh Port 6[F]	1115.3	1103.13
JW In Temp[F]	170.5	171
JW Out Temp[F]	180	180
ACW In Temp[F]	109.3	123
ACW Out Temp[F]	120.4	132.15
Dyno In Temp[F]	99	98.3
Dyno Out Temp[F]	124.5	122.6
Oil Sump Temp[F]	207.4	208.9
Oil Rifle Temp[F]	198.75	200.5
Oil Pressure[psig]	7607	75.6
THC[ppm dry]	3748.73	2062.3
O2[%dry]	9.46	6.5
NOx[ppm dry]	17.1	42.7
NO[ppm dry]	11.5	0
NO2[ppm dry]	5.6	0
CO2[% dry]	6.2	6.7

	Baseline Test	Test 1
CO[ppm dry]	414.5	183.7
ICW CV Pos.	46.6	47.14
Exh Back Pres CV	64.5	69.65
JW Temp Valve Pos.	57.6	60
Jacket Water Flow [gpm]	218.52	232.6
Intercooler Flow [gpm]	136.7	161.8
Dyno Water Flow [gpm]	83.3	90.7
Boiler Return Temp [C]	81.3	78.1
Boiler Supply Temp [C]	80.8	78.1
BMEP[psi]	134.36	134.3
Ambient Pressure[psia]	12.3	12.3
Propane Flow[lb/hr]	0.008	1.86
Blowby Flow[acfm]	7.5	7.05
BlowbyPressure [inH2O]	7.4	6.7
Blowby Temp [F]	157.7	150.9

Table A.2: Example Cooper Bessemer GMVH-12 Raw Engine Parameters

Engine Speed (rpm)	275	300	330
Turbo Speed (rpm)	12888	14326.7	14950
Air Maifold Pressure (psi)	9.6	12.4	13.8
Air Maifold Temperature (°F)	105	110	115
Brake Horsepower (hp)	1880	2241	2460
Brake Specific Fuel Consumption	7309	7488	7507
Engine Oil Pressure (psi)	31.2	34.6	36.6
Air Fuel Ratio	41.5	41.6	42
Power Cycliner Lube Rate (pints)	0.04	0.05	0.05
Exhaust Velocity (m/s)	10.2	13.02	13.68
Catalyst Temperature (°F)	447	441	438
PM Emissions (μg/min)	29	22	14
O2 (ppm)	15.5	15.3	14.67
CO (ppm)	98.3	98.24	107.46
NO (ppm)	125.6	140.85	140.16
NOx (ppm)	153.9	169.78	171.9
HC (ppm)	132.5	109.6	95.6
CO2 (ppm)	3.09	3.27	3.55
Methane (mol%)	99.6	96.4	88.76
Ethane (mol%)	0	0	7.79
Propane (mol%)	0	0	1.14
Iso-Butane (mol%)	0	0	0.072
Iso-Pentane (mol%)	0	0	0.014
Normal Butane (mol%)	0	0	0.12
Normal Pentane (mol%)	0	2.22	0.012
N2 (mol%)	0.388	0	0.63
Hexane (mol%)	0.009	1.35	0.03
Carbon Dioxide (mol%)	0	0	1.4

Appendix B: Oil Contaminate Specification Sheets

Figure B.1: CAT Oil Contaminates Specification Sheet

COLORADO STATE UNIVERSITY
ROBERT KILLIAN

FAX:
PHONE:
SAMPLE TYPE: OIL
SAMPLE SHIP TIME (days): 7

COMPANY NAME: COLORADO STATE UNIVERSITY
CUSTOMER EQUIP NUM: GMVH12
COMPARTMENT NAME: NEW OIL
SERIAL NUMBER: GMVH12
MANUFACTURER: OTHER
MODEL: UNKNOWN
JOB SITE:
EXT WARR NUMBER:

SHOP JOB NUM:
COMP SERIAL NUM:
COMPARTMENT MODEL:
COMP MANUFACTURER:
SAMPLE LABEL NUM:
FLUID BRAND/WEIGHT: PEGASUS805/40
FLUID TYPE:
EXT WARR EXPIRE DATE:
FUEL CONSUMED:

WAGNER CAT

SOS Services Laboratory
18000 E SMITH RD
AURORA, CO 80011-3511
1 (303) 739-3165
www.wagnerequipment.com

LAB CONTROL NUMBER	SAMPLE DATE	PROCESS DATE	EQUIPMENT METER	METER ON FLUID	FLUID CHANGED	MAKE UP FLUID	MAKE UP FLUID UNITS	FILTER CHANGED
E250-44160-8001	6/2/14	6/9/14	0	0	Unknown			

Monitor Compartment

FIRST SAMPLE/NO TREND ESTABLISHED. ALL READINGS ARE NORMAL FOR OIL BLENDED FOR CAT NATURAL GAS ENGINES. HOWEVER, PARTICLE COUNT IS SOMEWHAT HIGH. ADVISE KIDNEY-LOOPING TO IMPROVE FLUID CLEANLINESS AND RESAMPLING IN 6 MONTHS

Wear Metals (ppm)	Cu	Fe	Cr	Al	Pb	Sn	Si	Na	K	B	Mo	Ni	Ag	Ca	Mg	Zn	P
E250-44160-8001	0	0	0	0	1	1	3	0	1	0	2	0	0	25	1	424	442

Oil Condition / Particle Count (ct/ml)	ST	OXI	NIT	SUL	W	A	F	V100	ISO	4µ	6µ	10µ	14µ	18µ	21µ	38µ	50µ
E250-44160-8001	0	11	4	16	N	N	N	14.1	22/20/15	25232	5800	958	222	70	34	4	1

Ag = Silver, Al = Aluminum, B = Boron, Ca = Calcium, Cr = Chromium, Cu = Copper, Fe = Iron, P = Phosphorus, K = Potassium, Mg = Magnesium, Mo = Molybdenum, Na = Sodium, Ni = Nickel, Pb = Lead, Si = Silicon, Sn = Tin, V = Vanadium, Zn = Zinc, A = Antifreeze, F = Fuel, W = Water, P = Positive, N = Negative, T = Trace, E = Excessive, NIT = Nitration, OXI = Oxidation, ST = Soot, SUL = Sulfation, ISO = ISO Rating, PFC = Percent Fuel Content, PQI = Particle Quantifying index, NaW = Salt Water, FL Pt = Flash Point, TAN = Total Acid Number, TBN = Total Base Number, H2O = Karl Fisher result, V100 = Viscosity@100C, V40 = Viscosity@40C

Notice: This analysis is intended as an aid in predicting mechanical wear. No guarantee, expressed or implied, is made against failure of this piece of equipment or a component thereof.

PEAK
PETROLEUM TESTING SERVICES, INC.

ISO/IEC 17025:2005

Department of Mechanical Engineering
Colorado State University
Campus Delivery 1374
Fort Collins, CO 80523-1374

Marc E Baumgardner

October 27, 2014
Job #:CSU102214
Page: 1 of 1

Laboratory Report

Sample ID: Used Oil
Matrix: Pegasus 40 Oil
Results:

Test	Method	Units	Value
Sulfur,	ASTM D4294	weight%	0.508
Zinc	ASTM D5185	ppm	451*
Phosphorus	ASTM D5185	ppm	359*

Sample ID: New Oil
Matrix: Pegasus 40 Oil
Results:

Test	Method	Units	Value
Sulfur	ASTM D4294	weight%	0.539
Zinc	ASTM D5185	ppm	443*
Phosphorus	ASTM D5185	ppm	358*

Discussion: * Performed By Titan Laboratories, Denver, Colorado

Shadley Patton
Analysis Performed by: Shadley Patton

Report Reviewed by: Josh Raaff

Phone 303.657.0007 7100 Broadway Suite 2Q, Denver, CO 80221 Fax 303.657.0003
www.peakpetrotesting.com

Figure B.2: PEAK Oil Contaminates Specification Sheet

Appendix C: XPS Raw Material Data

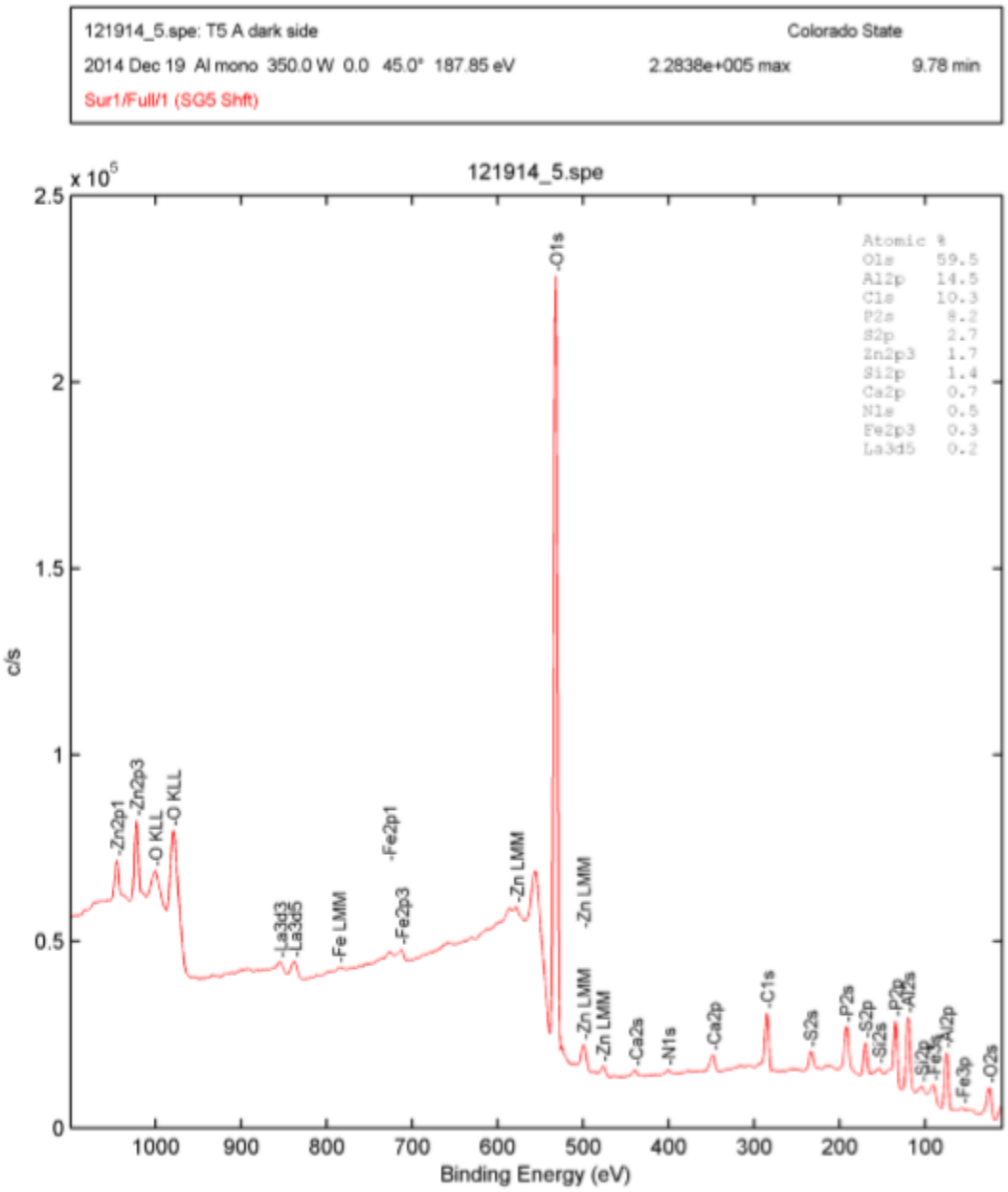

Figure C.1: Specimen A XPS Data for Test 5

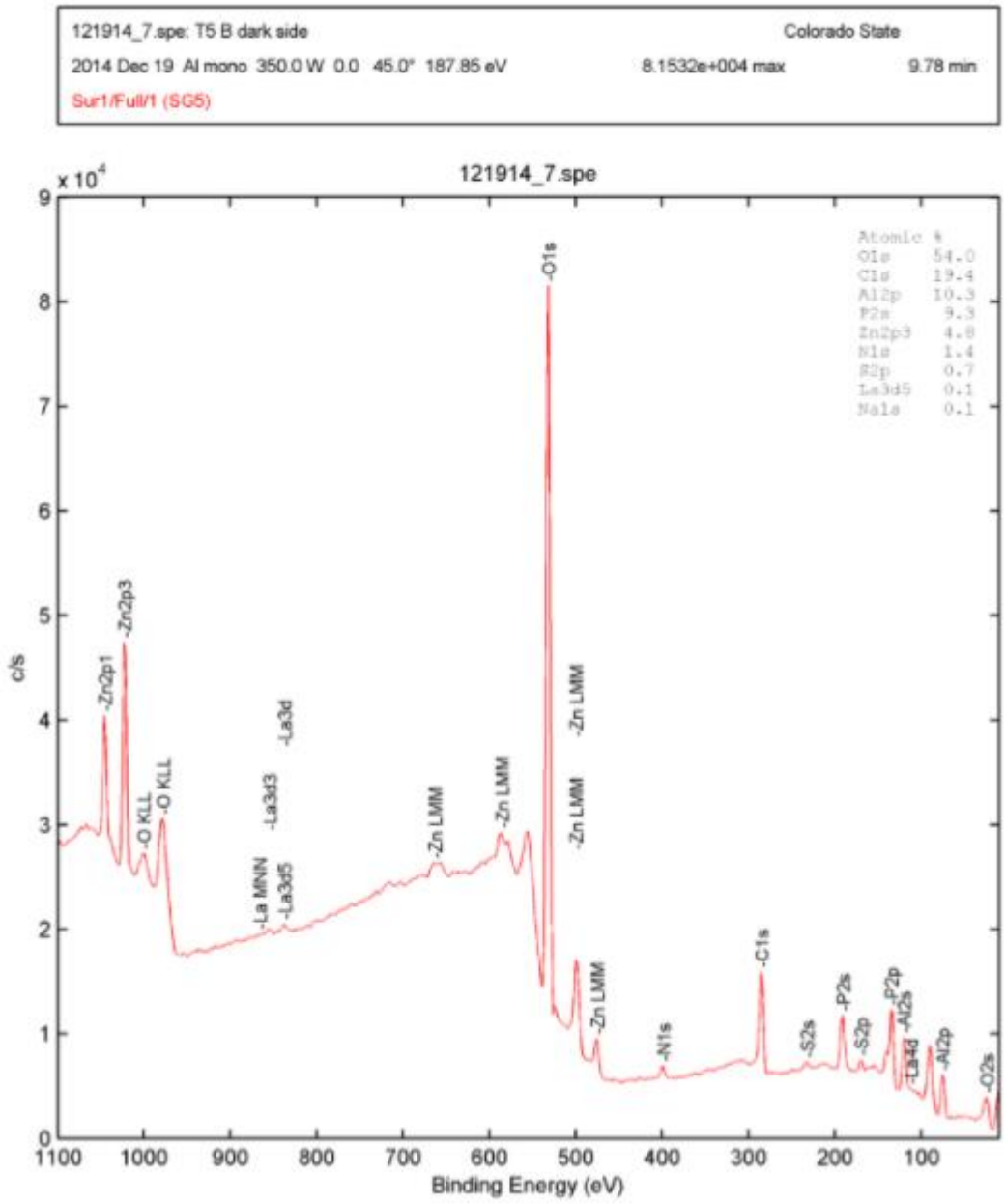

Figure C.2: Specimen B XPS Data for Test 5

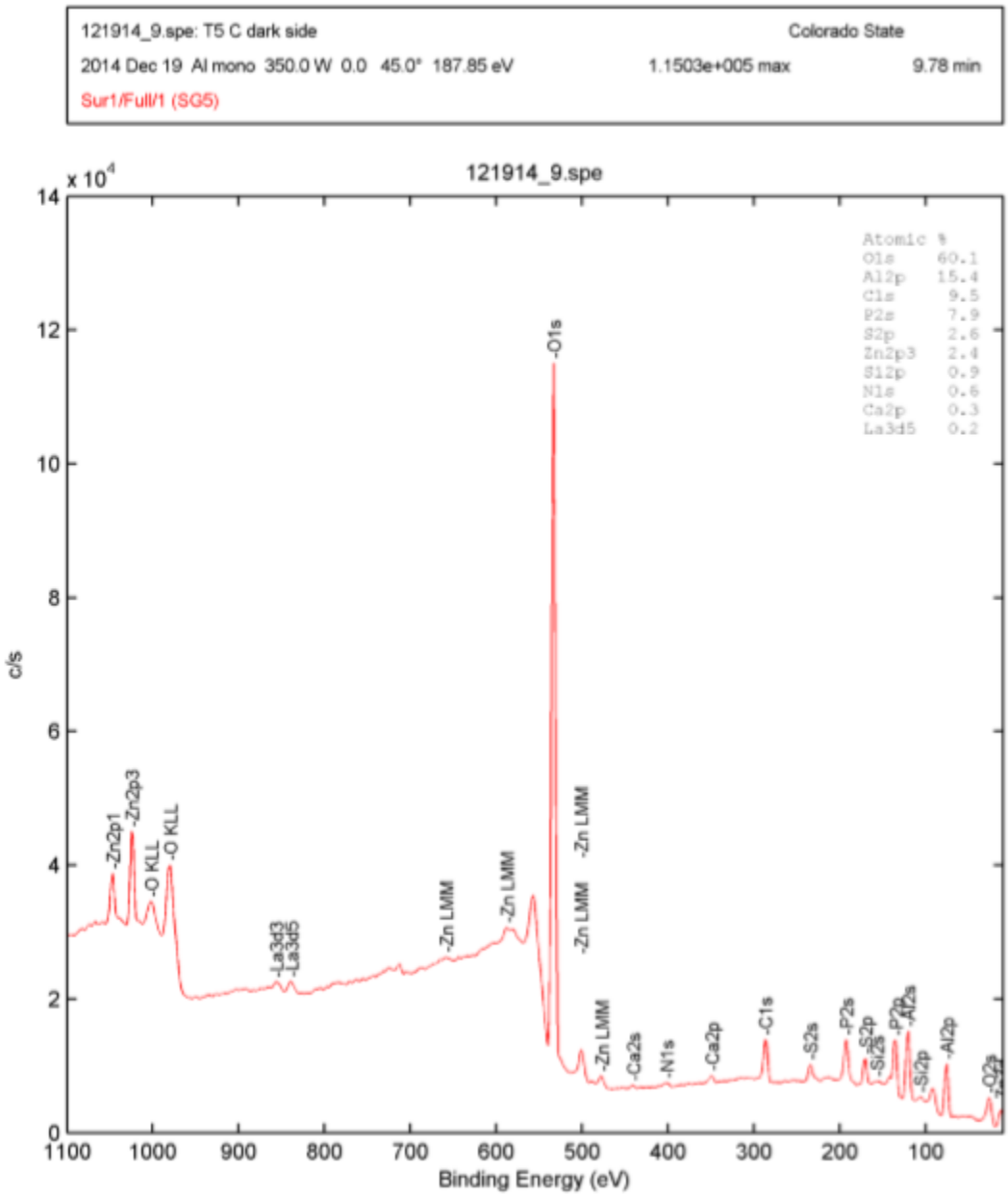

Figure C.3: Specimen C XPS Data for Test 5

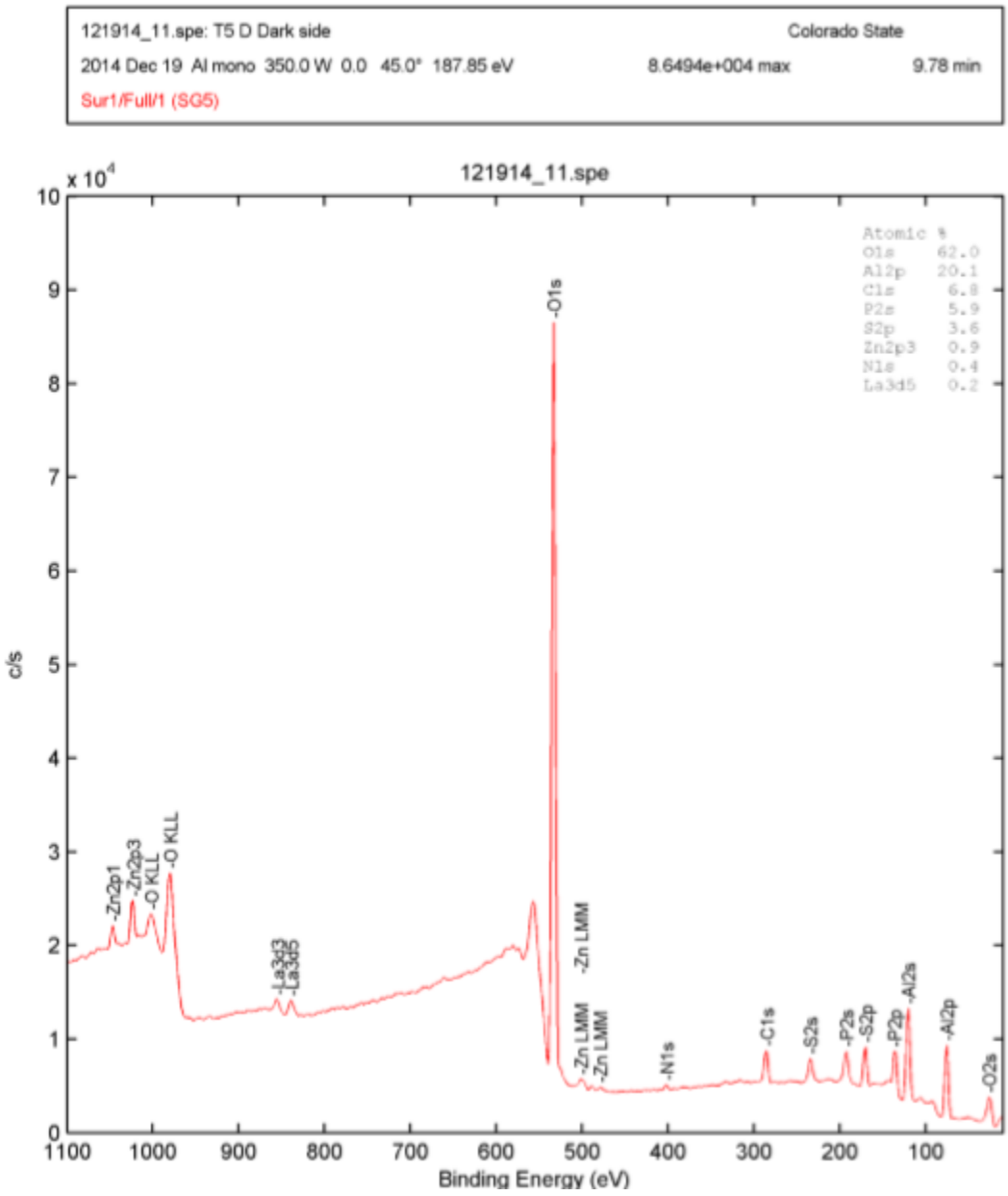

Figure C.4: Specimen D XPS Data for Test 5

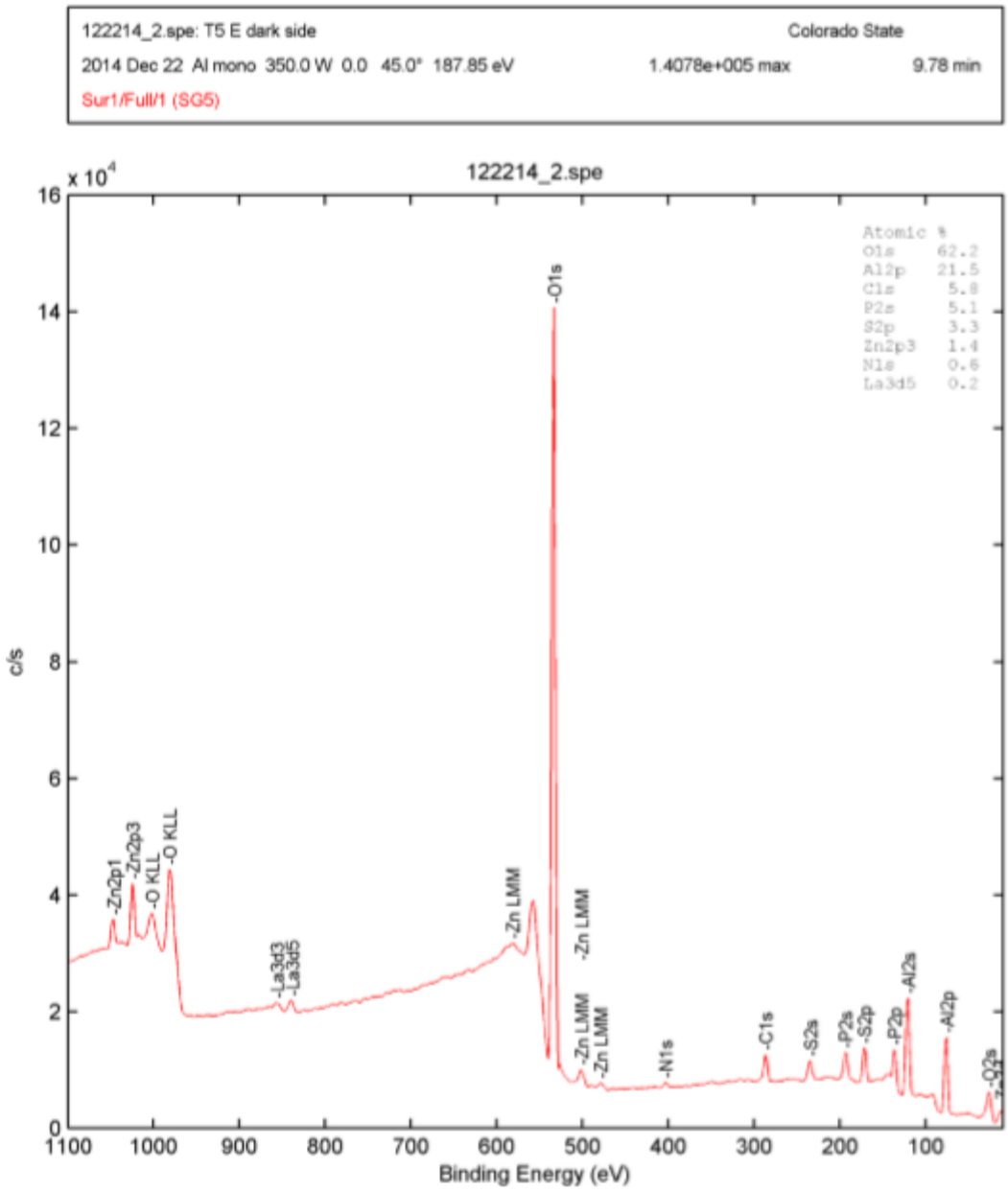

Figure C.5: Specimen E XPS Data for Test 5

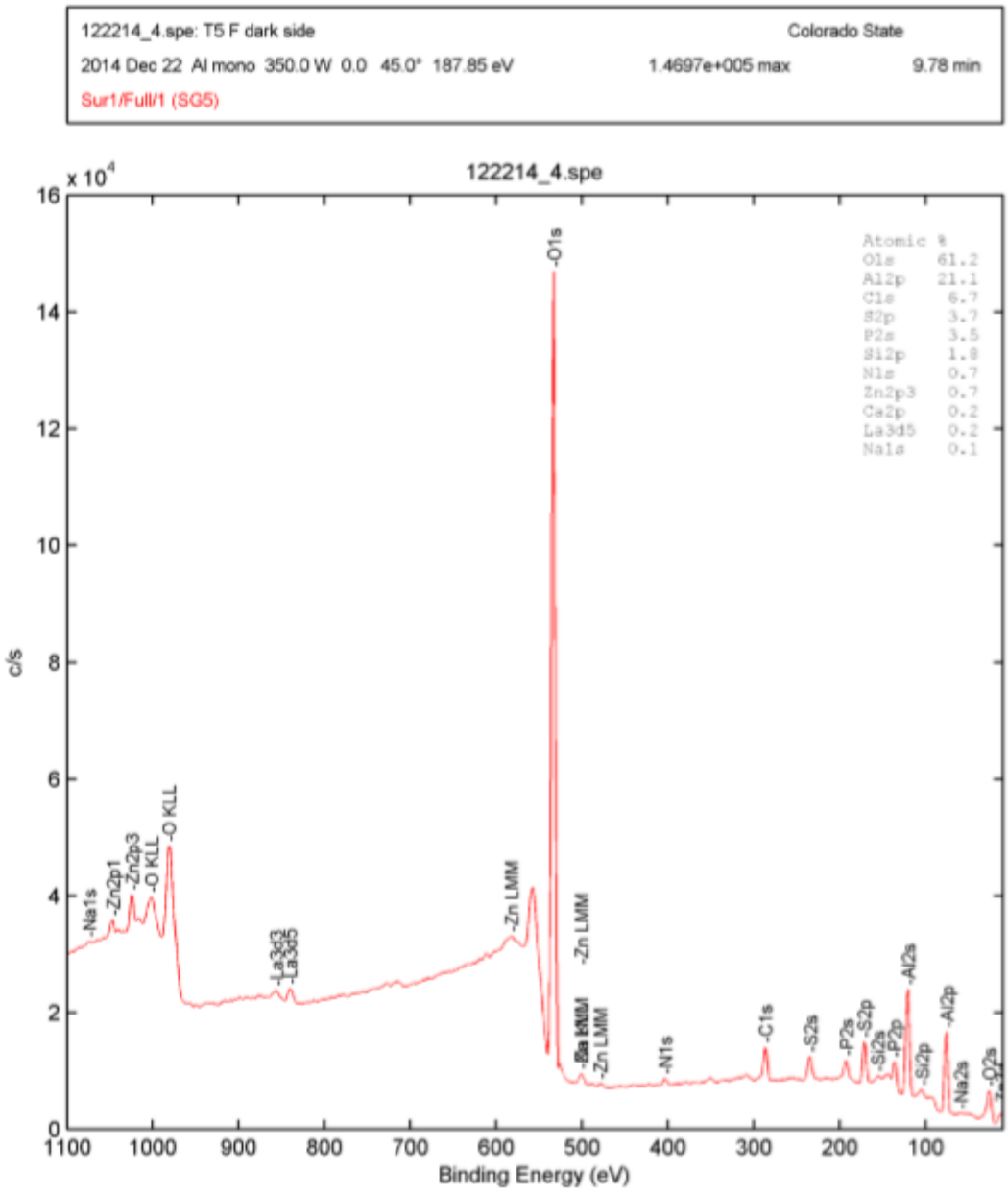

Figure C.6: Specimen F XPS Data for Test 5

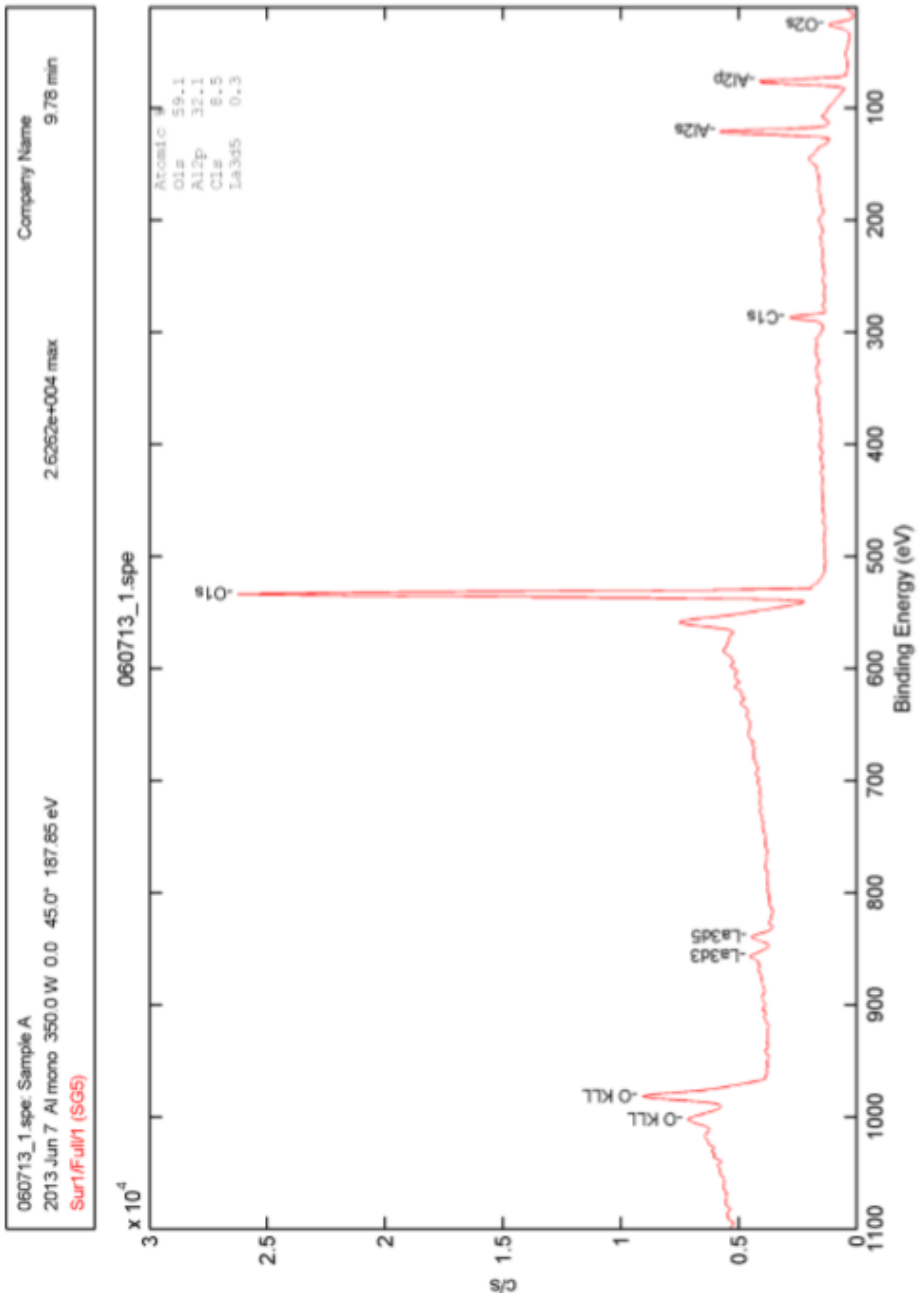

Figure C.7: Specimen A XPS Data for Baseline Test

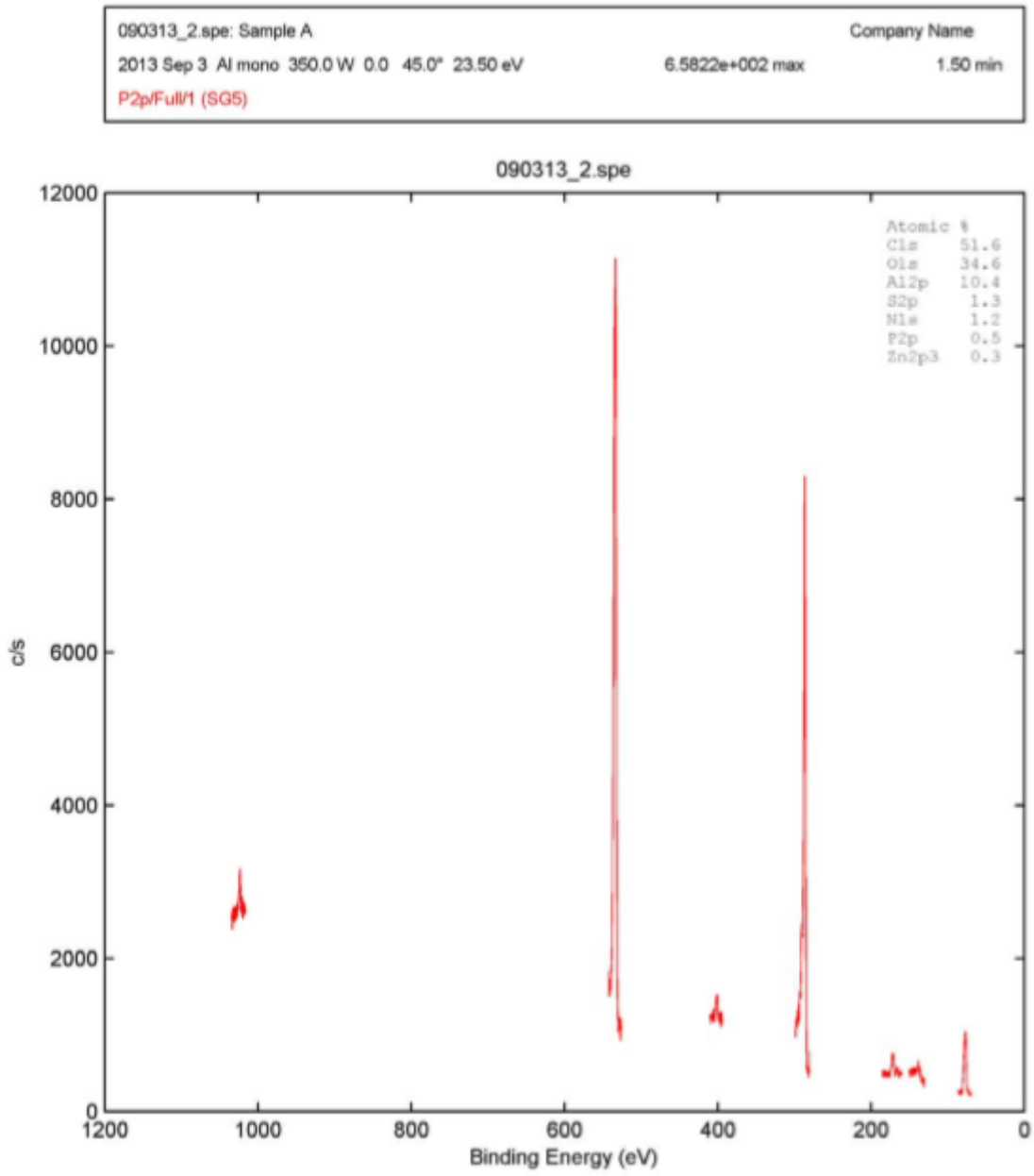

Figure C.8: Specimen A XPS Data for Test 1

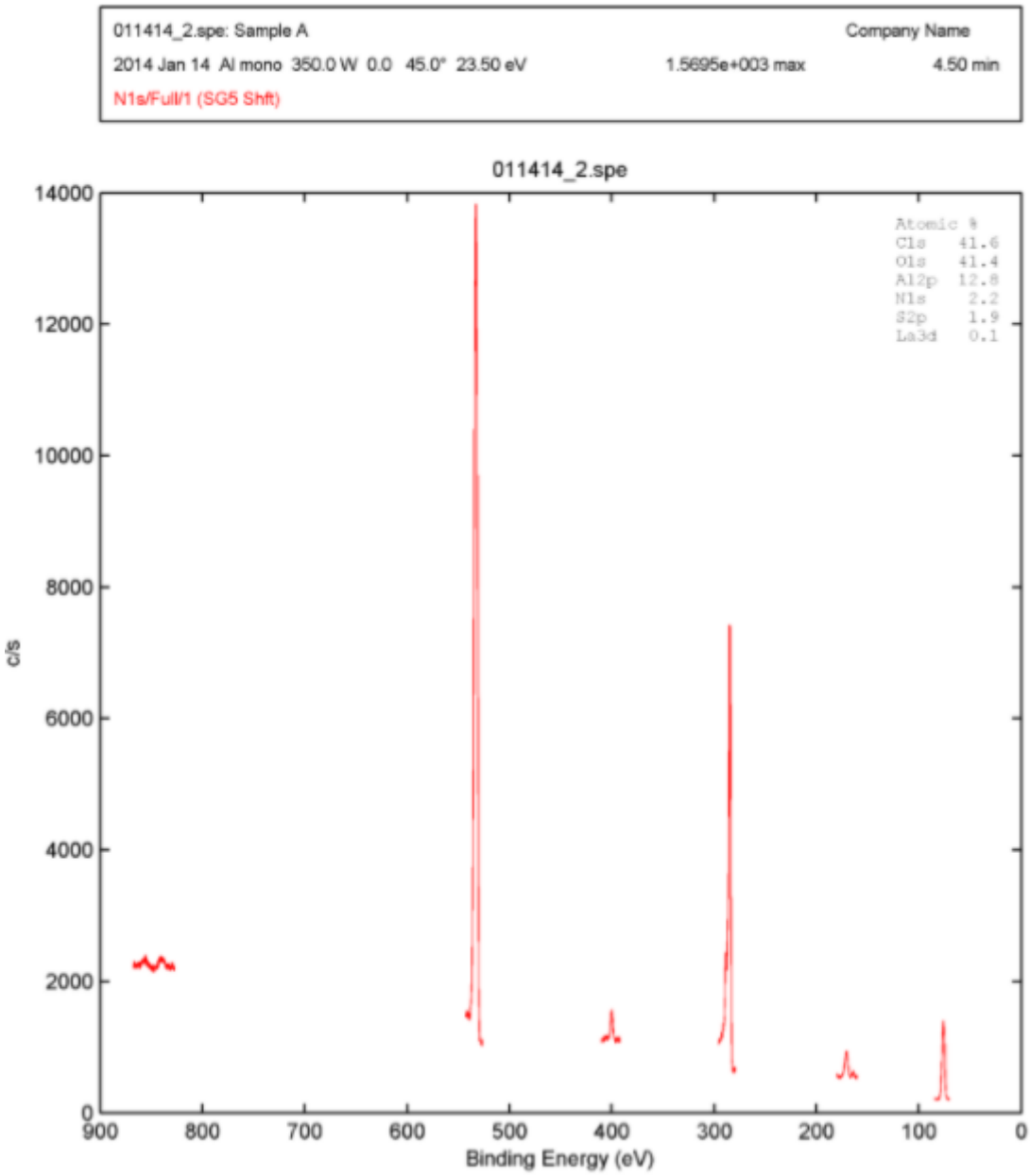

Figure C.9: Specimen A XPS Data for Test 2

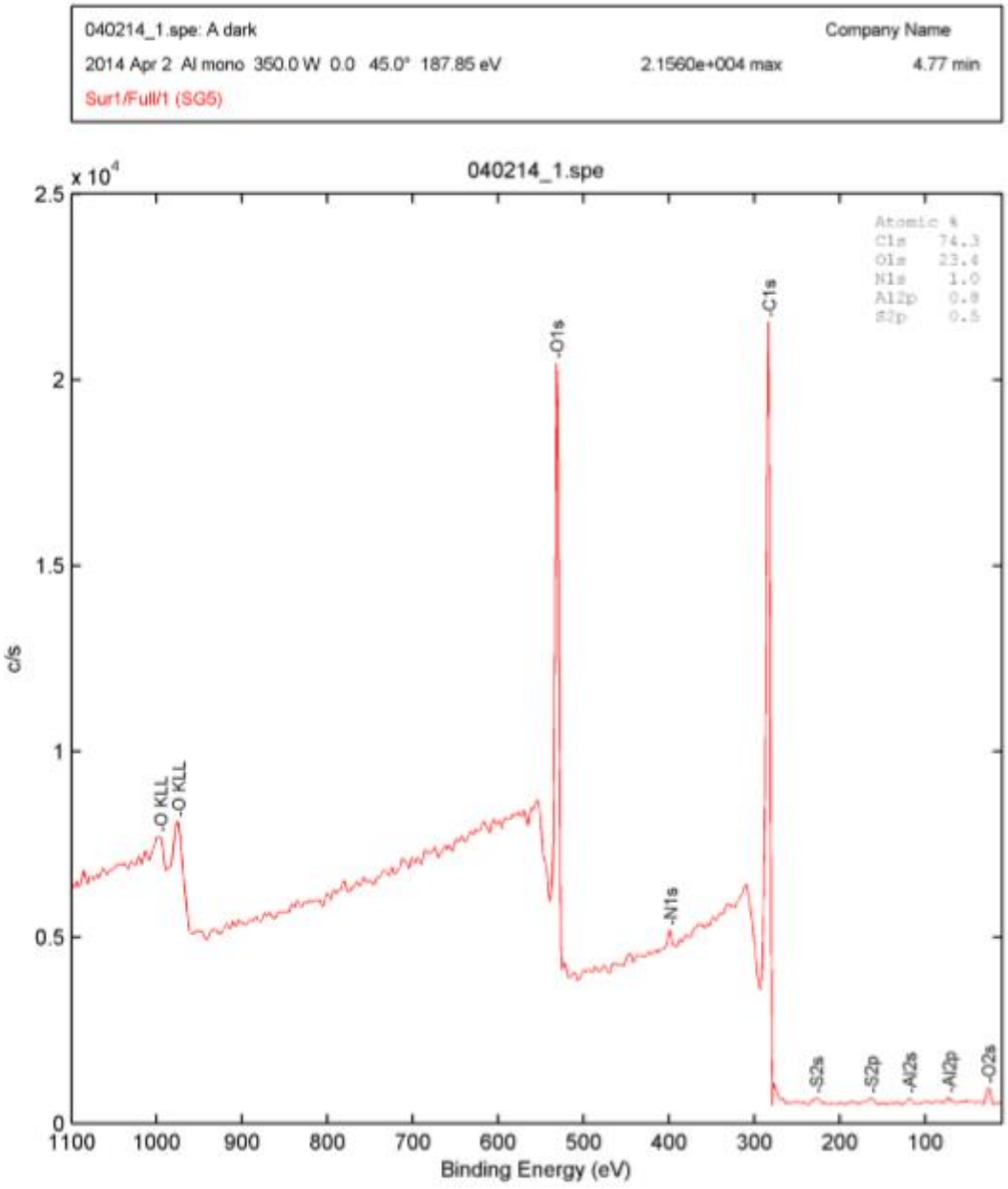

Figure C.10: Specimen A XPS Data for Test 3

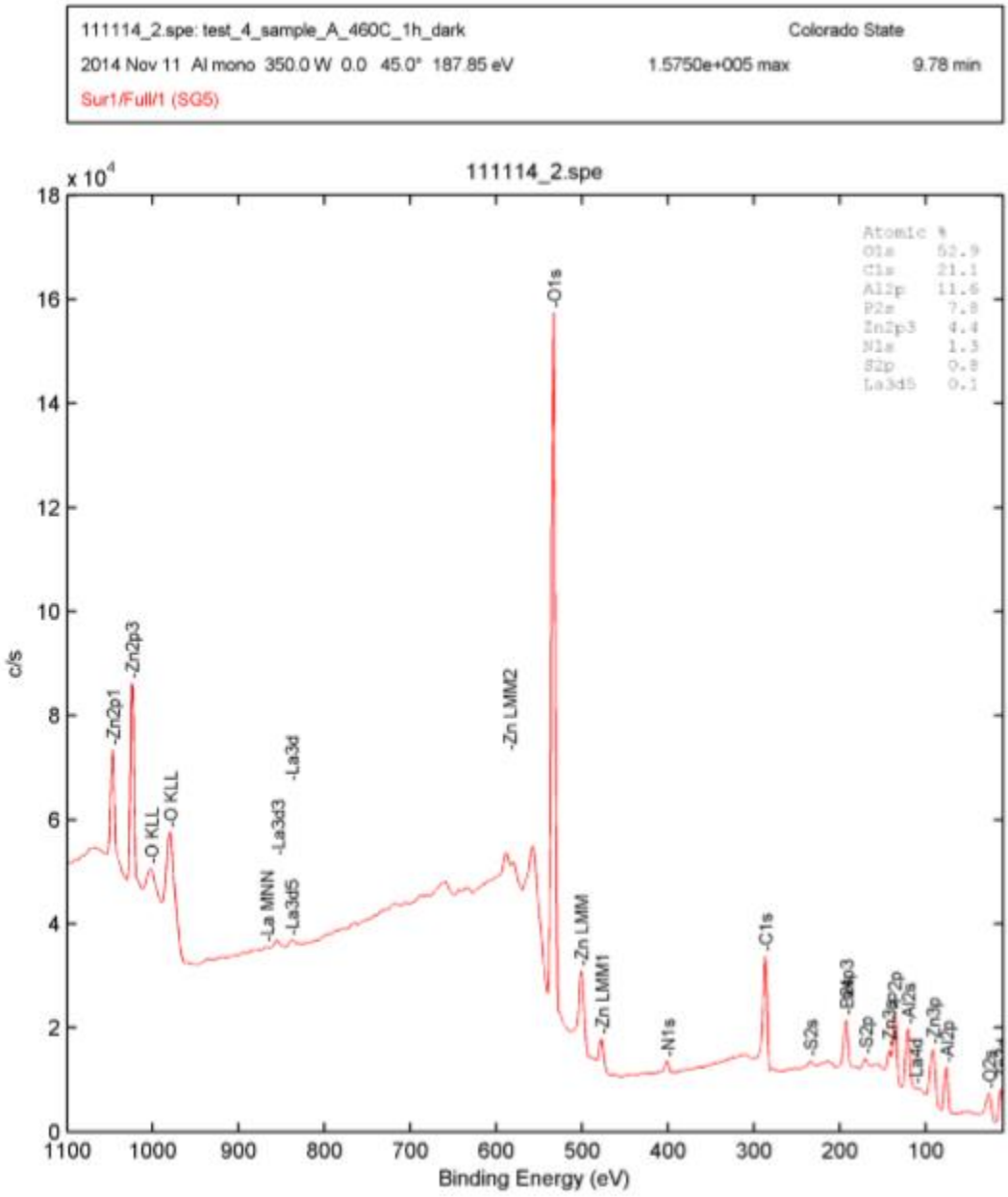

Figure C.11: Specimen A XPS Data for Test 4

Appendix D: Propane and Ethane Emissions Reduction

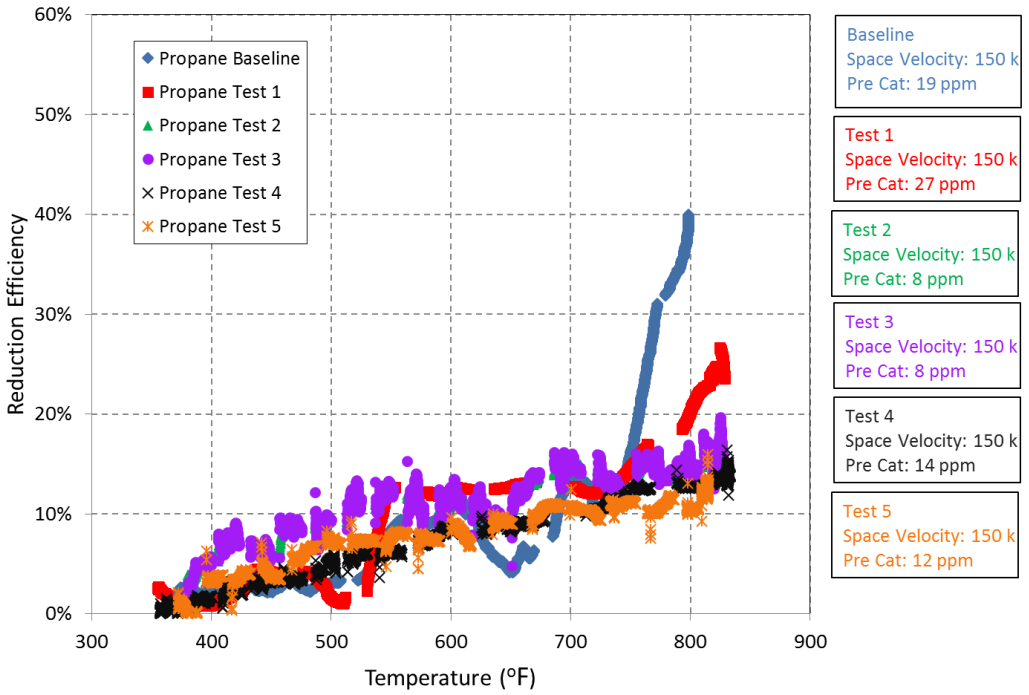

Figure D.1: Propane Temperature Sweeps

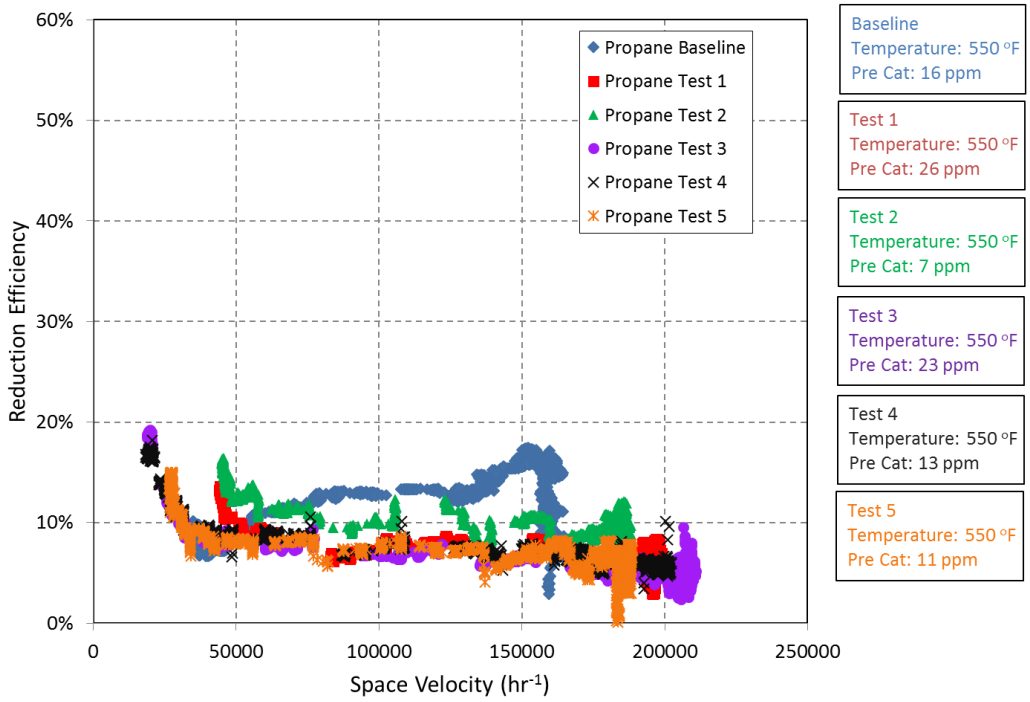

Figure D.2: Propane Space Velocity Sweeps

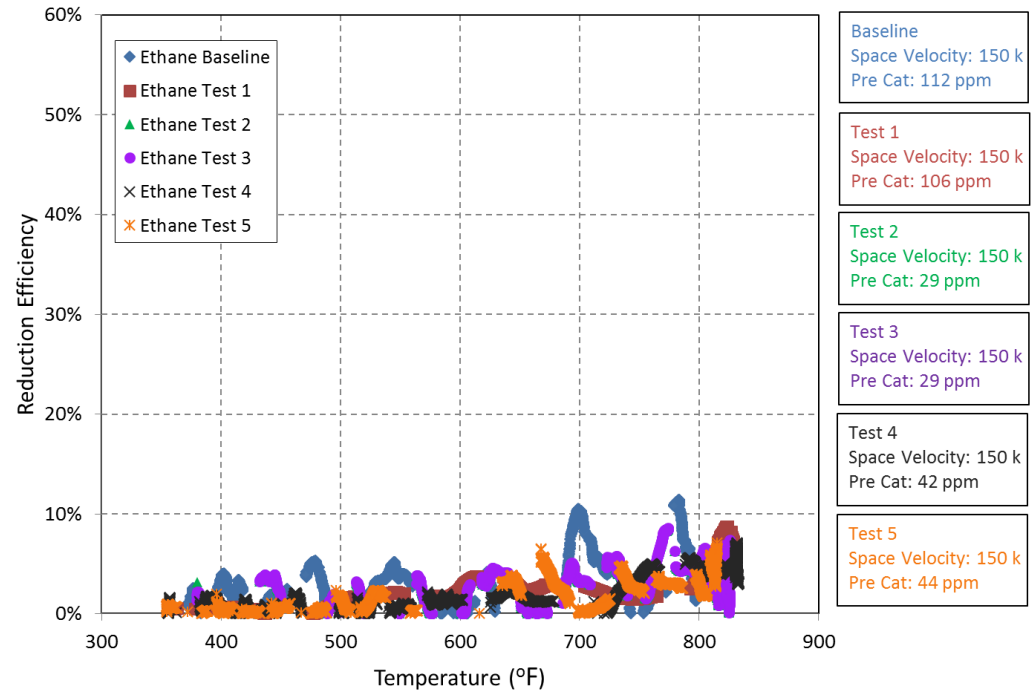

Figure D.3: Ethane Temperature Sweeps

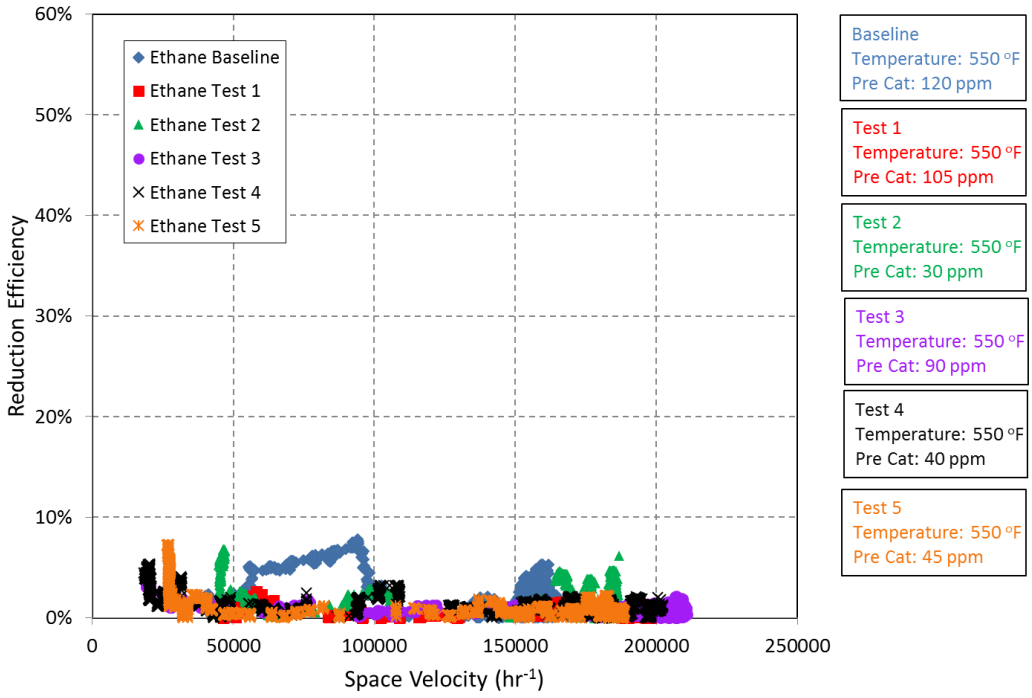

Figure D.4: Ethane Space Velocity Sweeps

Appendix E: Sample Field Engine Data Trends

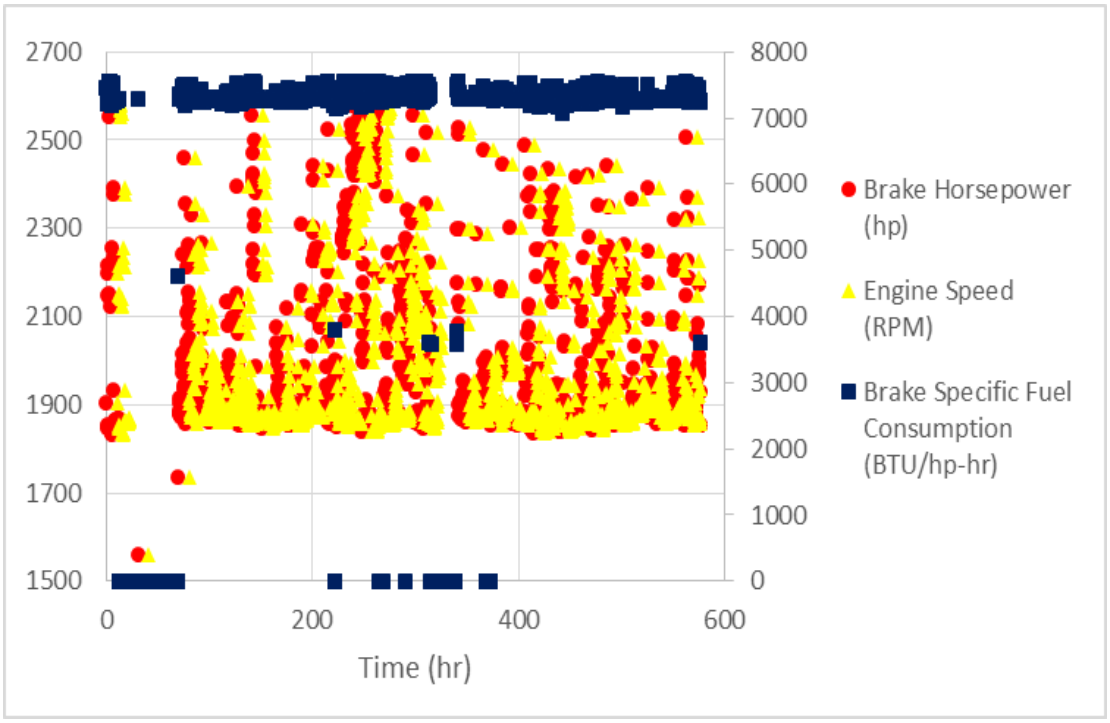

Figure E.1: Sample Field Engine Data

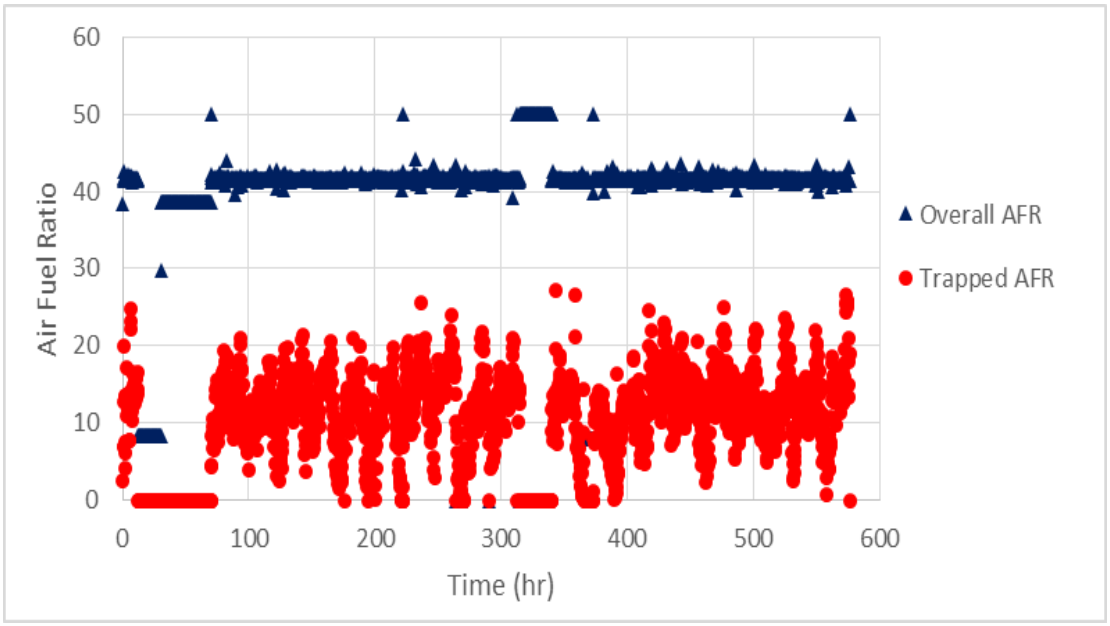

Figure E.2: Sample Field Air Fuel Ratio

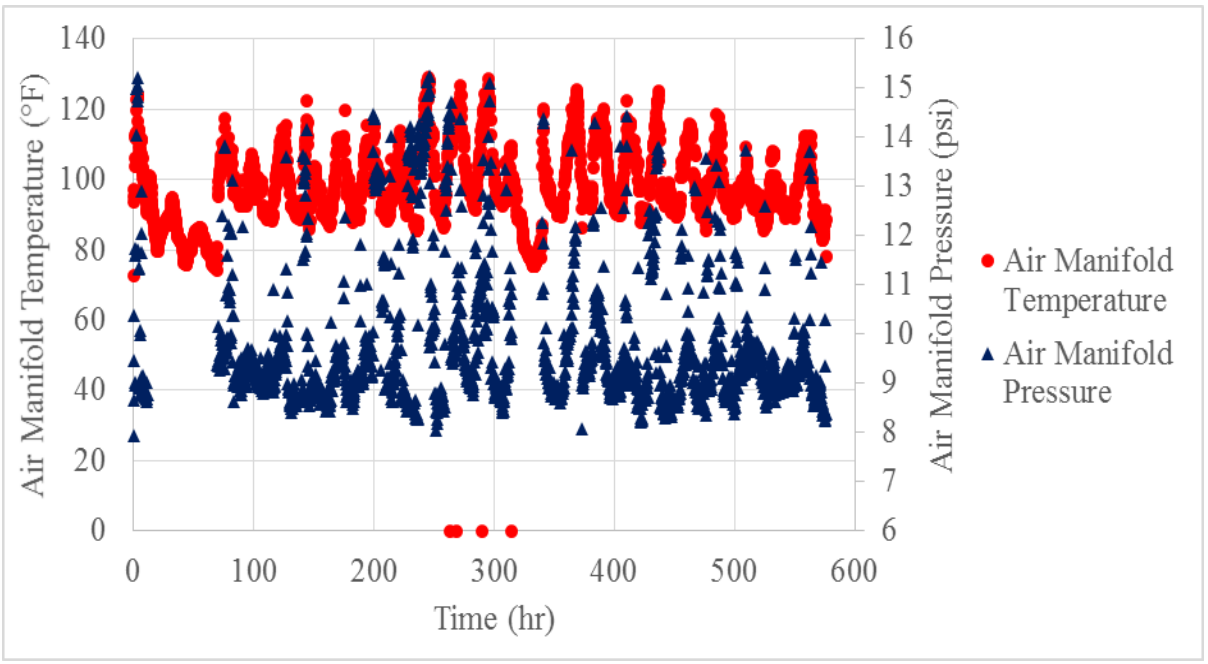

Figure E.3: Sample Field Engine Air Manifold Temperature and Pressure

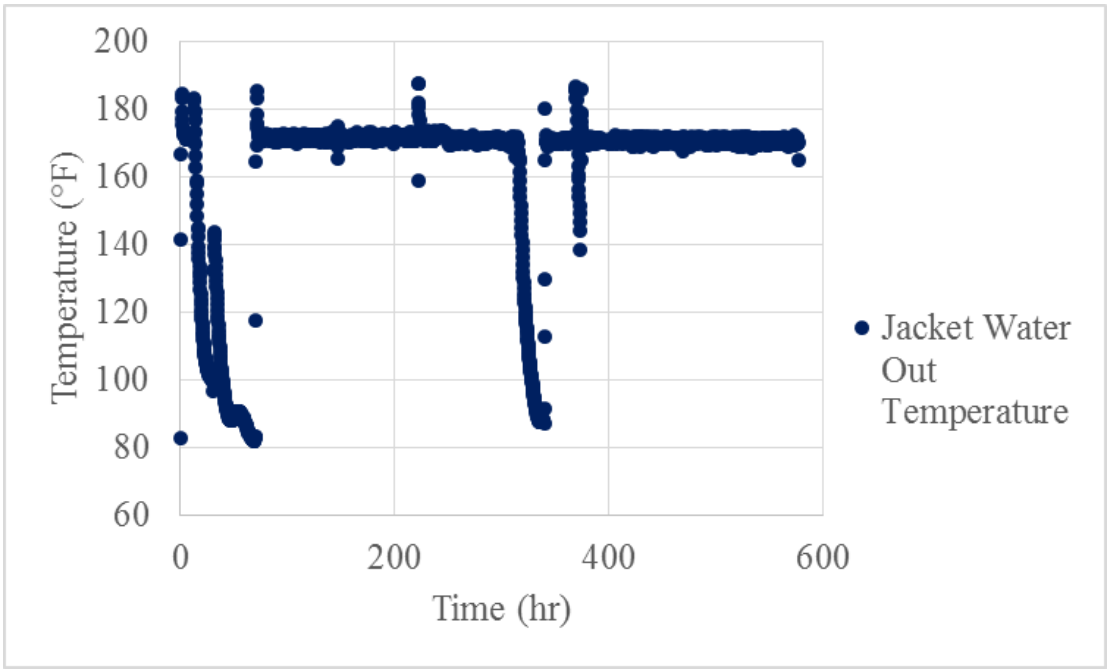

Figure E.4: Sample Field Engine Jacket Water Out Temperature

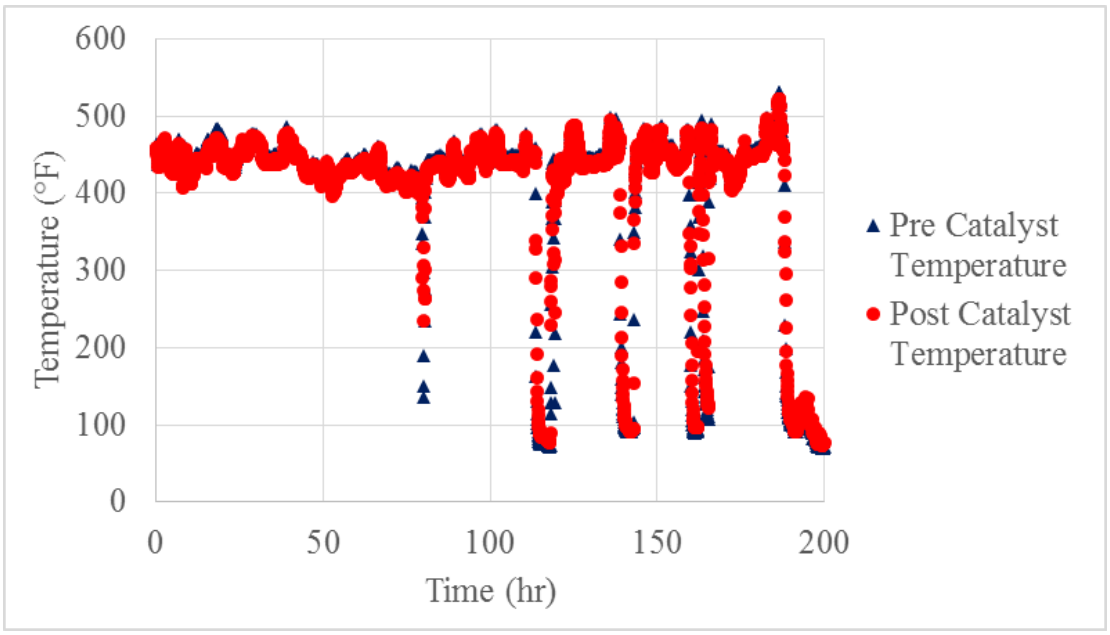

Figure E.5: Sample Field Pre and Post Catalyst Temperature

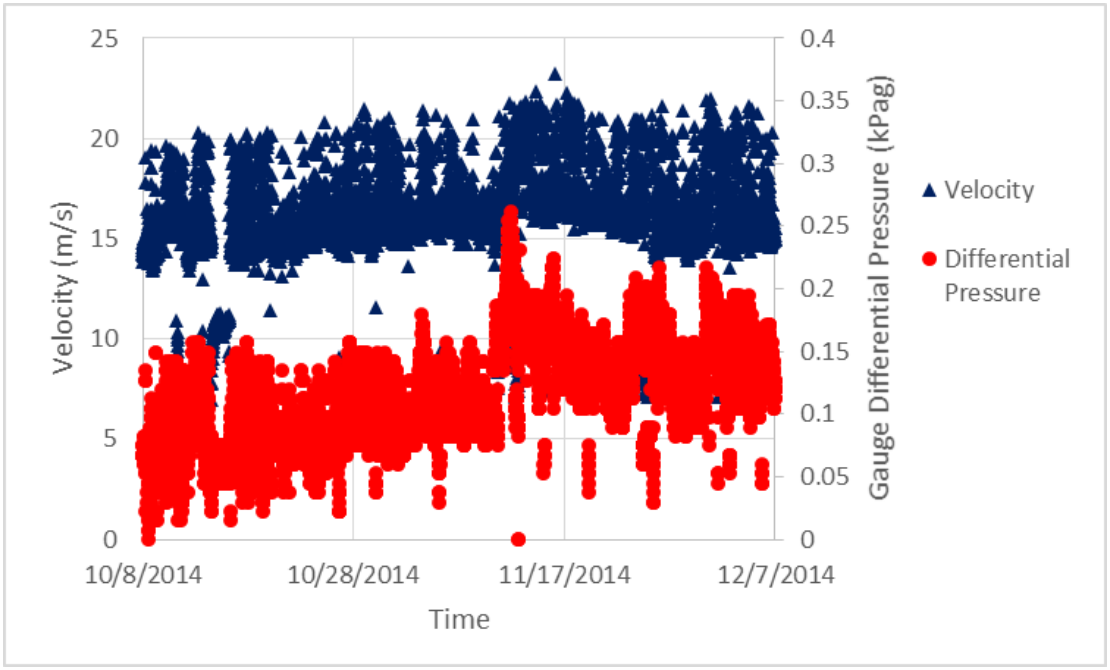

Figure E.6: Sample Field Exhaust Velocity and Differential Pressure through Slipstream

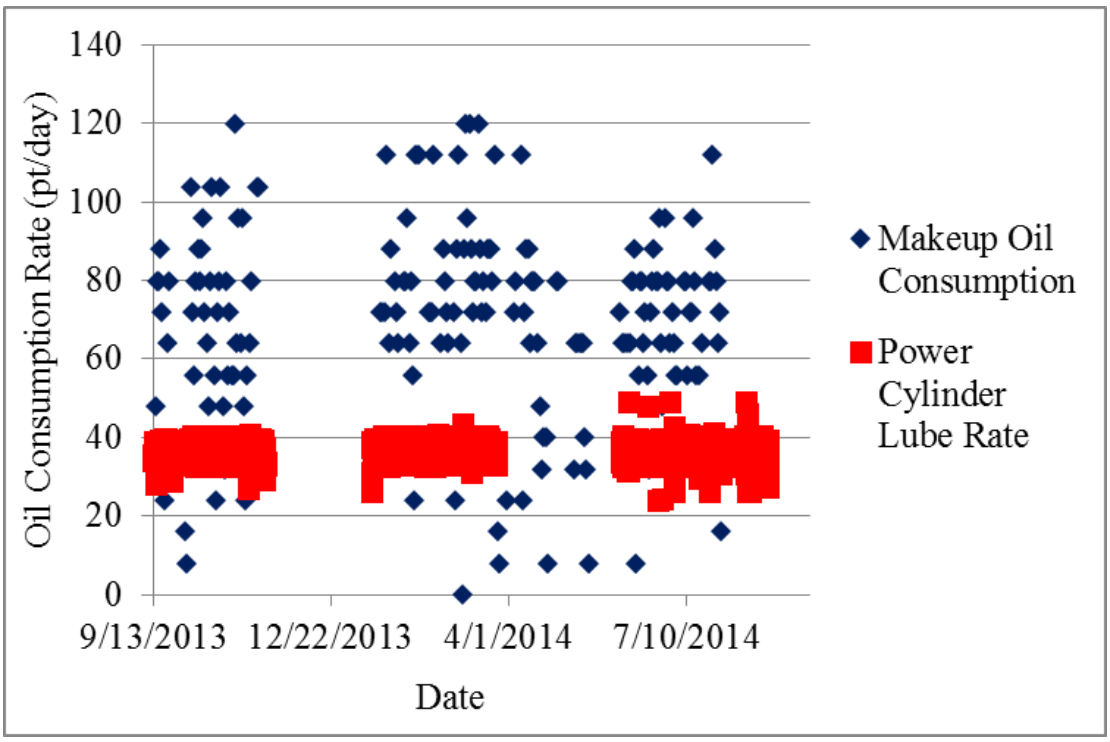

Figure E.7: Sample Field Lube Oil Consumption Rates